Geophys. J. R. astr. Soc. (1984) **77**, 185–264

Active tectonics of the Alpine–Himalayan Belt between western Turkey and Pakistan

James Jackson and Dan McKenzie *Bullard Laboratories, Madingley Rise, Madingley Road, Cambridge CB3 0EZ*

Received 1983 August 10; in original form 1983 January 5

Summary. Over 80 new fault plane solutions, combined with satellite imagery as well as both modern and historical observations of earthquake faulting, are used to investigate the active tectonics of the Middle East between western Turkey and Pakistan.

The deformation of the western part of this region is dominated by the movement of continental material laterally away from the Lake Van region in eastern Turkey. This movement helps to avoid crustal thickening in the Van region, and allows some of the shortening between Arabia and Eurasia to be taken up by the thrusting of continental material over oceanic-type basement in the southern Caspian, Mediterranean, Makran and Black Sea. Thus central Turkey, bounded by the North and East Anatolian strike-slip faults, is moving west from the Van region and overrides the eastern Mediterranean at two intermediate depth seismic zones: one extending between Antalya Bay and southern Cyprus, and the other further west in the Hellenic Trench. The motion of northern Iran eastwards from the Van region is achieved mainly by a conjugate system of strike-slip faults and leads to the low angle thrusting of Iran over the southern Caspian Sea. The seismicity of the Caucasus shows predominantly shortening perpendicular to the regional strike, but there is also some minor elongation along the strike of the belt as the Causcasus overrides the Caspian and Black Seas.

The deformation of the eastern part of this region is dominated by the shortening of Iran against the stable borders of Turkmenistan and Afghanistan. The north-east direction of compression seen in Zagros is also seen in north-east Iran and the Kopet Dag, where the shortening is taken up by a combination of strike-slip and thrust faulting. Large structural as well as palaeomagnetic rotations are likely to have occurred in NE Iran as a result of this style of deformation. North–south strike-slip faults in southern Iran allow some movement of material away from the collision zone in NE Iran towards the Makran subduction zone, where genuinely intermediate depth seismicity is seen.

Within this broad deforming belt large areas, such as central Turkey, NW Iran (Azerbaijan), central Iran and the southern Caspian, appear to be almost aseismic and therefore to behave as relatively rigid blocks surrounded by active belts 200–300 km wide. The motion of these blocks can usefully be

described by poles of rotation. The poles presented in this paper predict motions consistent with those observed and also predict the opening of the Gulf of Iskenderun NE of Cyprus, the change within the Zagros mountains from strike-slip faulting in the NW to intense thrusting in the SE, and the relatively feeble seismicity in SE Iran (Baluchistan). This description also explains why the north–south structures along the Iran–Afghanistan border do not cut the east–west ranges of the Makran.

Within the active belts surrounding the relatively aseismic blocks a continuum approach is needed for a description of the deformation, even though motions at the surface may be concentrated on faults. The evolution of fault systems within the active zones is controlled by geometric constraints, such as the requirement that simultaneously active faults do not, in general, intersect.

Many of the active processes discussed in this paper, particularly large-scale rotations and lateral movement along the regional strike, are likely to have caused substantial complexities in older mountain belts and should be accounted for in any reconstructions of them.

1 Introduction

This study uses recent and historical seismicity, fault plane solutions, and young structures visible on satellite images to investigate the active deformation of the Alpine–Himalayan Belt between the rift system of western Turkey and the fold belts of the Zhob and Loralai ranges in western Pakistan. Since this area was last investigated in detail by McKenzie (1972), who presented fault plane solutions up to 1969, much more information has become available and the motivations for such a study have changed. Early attention was focused on whether the successful plate tectonic description of oceanic kinematics could be applied in any useful way to the deformation occurring on the continents. McKenzie (1972, hereafter referred to as I) described the deformation in the Mediterranean region in terms of the motions of a few small plates, although the material at the boundaries between them does not deform in the same way as oceanic plate boundaries. The general motions proposed in I are confirmed by the much larger data set presented in this paper, and it is perhaps surprising in retrospect how few reliable fault plane solutions were needed to obtain a good general picture of the kinematics in this region.

Fig. 1 shows that the seismicity of the Middle East is not confined to a few faults but is dispersed over bands 100–300 km wide. This is not the result of location errors and the active deformation clearly visible on satellite images shows the same behaviour. Yet it is clear from Fig. 1, and especially from the locations of larger earthquakes (e.g. Figs 7, 13, 26 and 30) that large areas of central Turkey, the southern Caspian, central Iran and NW Iran have low levels of seismicity compared to those of the relatively narrow belts surrounding them. This same behaviour is strikingly confirmed by studies of historical seismicity (Ambraseys 1975; Ambraseys & Melville 1982). It is only possible for this pattern to exist for long periods if the deformation in the active zones is consistent with the effectively rigid motion of the regions in between. When several faults are active in each zone their combined motion must be controlled by the relative absence of deformation in the interior regions. It is in this sense that plate tectonics can, in places, form a useful framework in which to discuss the deformation of continental regions.

A different view, taken principally by those working further east in Asia (e.g. Molnar & Tapponnier 1975) was that the deformation is controlled by the regional stress field and not by kinematic constraints associated with finite deformation. One difficulty with this

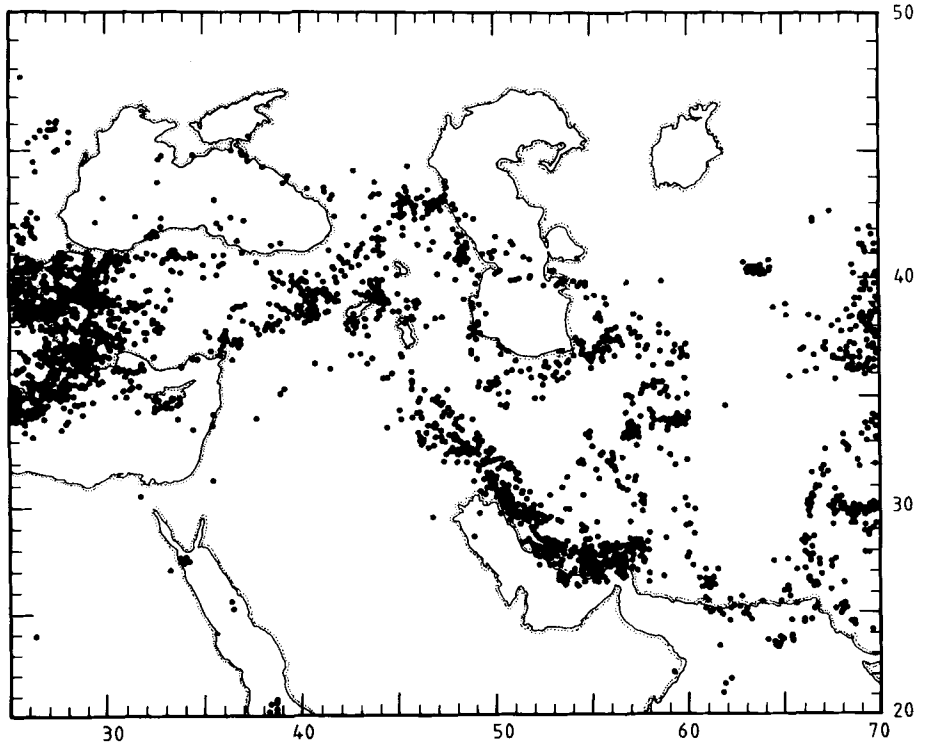

Figure 1. Epicentres between Turkey and Pakistan located shallower than 50 km by NOAA and its successors during the period 1961 January to 1980 December.

approach is that the stress field must now be very inhomogeneous because of the existence of major fault zones. Furthermore, finite slip along the curved planes of initial failure is only possible if the material behaves plastically. Under such conditions there will be no aseismic regions and strike-slip faults will not follow small circles. Nevertheless, in spite of the clearly discontinuous deformation implied by the movement of a single fault, the motions within intensely deforming active belts several hundred kilometres wide require some sort of continuum description. Such a description is the subject of a separate paper (McKenzie & Jackson 1983), though it is discussed briefly in a later section of this one. In both papers we argue that the strain rate and not the stress controls the deformation within these active belts.

Perhaps the major contribution of the earlier studies such as those of McKenzie (1972), Nowroozi (1972), Molnar & Tapponnier (1975, 1978) and Tapponier & Molnar (1977, 1979) was the discovery of general principles controlling the sort of processes that occur in continental tectonics. It is really in pursuit of the principles governing continental deformation, and not in testing plate tectonics on the continents, that studies such as this one are directed. One of the most universal of such principles appears to be that the subduction or thickening of continental crust is, if possible, avoided by moving continental material away from collision zones along strike slip faults sub-parallel to the regional trend. Thus Turkey moves westwards relative to Eurasia along the North and East Anatolian Faults, and the compression of Arabia against Eurasia between the Black Sea and the Caspian is, to some extent, taken up further SW by the subduction of Mediterranean seafloor in the Hellenic Trench. Because of its buoyancy, the subduction of continental crust into the upper mantle

is expected to be difficult, though it may be possible to remove limited amounts of continental material in this way (Molnar & Gray 1979). Moreover, it is probable that subducted continental crust is too hot to deform seismically (Chen & Molnar 1983) and so it will only be detected by sophisticated velocity analysis, as is claimed by Roecker (1982) in the Hindu Kush. Another fundamental principle, emphasized by many authors (e.g. Sykes 1978), is the susceptibility of old fault zones and lines of weakness to be reactivated, particularly in later orogenies.

In several areas the detailed investigation of active tectonics has led to the discovery of important deformation mechanisms that do not appear to occur in the oceans. In extensional regions dominated by normal faulting, such as the Aegean (McKenzie 1978a, b; Jackson, King & Vita-Finzi 1982b; Jackson & McKenzie 1983), stretching and thinning of the lithosphere may occur over a much wider area than is commonly seen at mid-ocean ridges. This process, which leads to regional subsidence and increased heat flow, appears to play an important role in the development of many continental sedimentary basins. In regions of compression, such as Iran, the re-thickening of previously stretched basement is probably an important mechanism and allows considerable shortening without creating abnormally thick crust (Helwig 1976). This shortening may well occur by the reactivation of old normal faults as high angle reverse faults (Jackson 1980a) as has been demonstrated in some of the inverted basins of NW Europe (e.g. Stoneley 1982). Stable cratons within and adjacent to deforming belts exert a strong influence on the location and style of faulting. Several Palaeozoic and Mesozoic orogenic belts in Asia have been reactivated by the collision with India and Arabia, while other shield areas like the Tarim Basin, and Arabia and India themselves, appear to have remained undeformed. Moreover, there is some indication that the intensity of deformation is greatest in the youngest reactivated belts, which, in general, have the highest observed heat flow (Molnar & Tapponnier 1981). This is an indication that lateral differences in rheological properties are important in the large-scale deformation of continents, because the creep strength of minerals is very dependent on temperature, and so the crust and mantle beneath hotter, younger belts should be much weaker than that beneath older belts. In particular, it is the temperature of olivine that appears to control the strength of the lithosphere as a whole (England 1983). Recent studies have also demonstrated that the stresses induced by topography are appreciable and can exert a profound influence on deformational processes (Dalmyrac & Molnar 1981; England & McKenzie 1982).

The bulk of this paper is concerned with the presentation of data. After describing the methods and approach to data reduction used here, the whole region is, for convenience, split into six areas, each of which is discussed separately. The active deformation of Iran, which spans five of the six areas discussed, is both complicated and illustrative, and is summarized to help the reader before a general discussion of the motions in the entire region. In order to investigate the connection between the deformation in Iran and that further east in Asia, this study was extended beyond that of I to 70°E.

2 Data reduction

The epicentres used in this study are those reported by the United States Coast and Geodetic Survey (USCGS), the National Ocean and Atmospheric Administration (NOAA) and the National Earthquake Information Service (NEIS). Since the publication of I and McKenzie (1978a) various developments have led to a better understanding of how to evaluate these locations. In general the accuracy of teleseismic locations increases with both magnitude and date, as it depends mainly on the number of stations reporting *P* arrival times. This is borne out by the studies of Ambraseys (1978) and Berberian (1979a) who compared

instrumentally determined epicentres in Iran with those estimated from macroseismic data. The epicentres of large ($m_b > 5.5$) shocks are generally accurate to within 10–20 km and are often better than this, though smaller ones ($m_b < 5.0$) may be in error by considerably more. Relative location techniques can improve the pattern of epicentres in a region and help to resolve the fault plane ambiguity in fault plane solutions (Jackson & Fitch 1979), but in the absence of a precisely determined absolute location for a reference shock, such patterns cannot be placed in geographical coordinates. However, where the absolute position of one of the epicentres in the pattern is accurately known (because, for example, it was an aftershock recorded by a locally installed network) the pattern can be placed geographically and may show a clear relation to surface faulting. This technique has been successfully applied in Greece and Algeria (Yielding *et al.* 1981; Soulfleris *et al.* 1982; Jackson *et al.* 1982b) but not yet in Iran and Turkey. Although the technique depends on having an accurate location for a reference shock, it can be used in retrospect by installing a local network long after a major earthquake sequence, thus improving the estimated epicentre for the mainshock and helping to relate its position to the surface deformation. The relative location method is effective because errors in the assumed earth velocity model are reduced if the ray paths from different events to a particular station are the same outside the epicentral region. This requirement is likely to be met if the source region is small, such as in an aftershock sequence, but may not be fulfilled if different events are separated by 100 km or more since lower crustal and mantle velocities are known to change on this scale (Asudeh 1981). For this reason, regional relative relocations such as those carried out by Dewey (1976) have not been attempted here. In this study two epicentral maps are shown for each region; one showing the larger earthquakes with m_b5.0 or greater or with at least 50 recording stations, and the other showing all instrumentally recorded seismicity. The latter is of interest because some areas have rather few large shocks and also because areas of genuinely low seismicity are convincingly revealed.

The quality of the hypocentral depth reported by the USCGS, NOAA and NEIS is generally much worse than the epicentre. *pP* is not used in these depth estimates, which are based on *P* arrival times alone. Several microearthquake surveys in Iran and Turkey have failed to find seismicity deeper than about 25 km in regions where teleseismic depths down to 100 km have been reported (Savage, Alt & Mohajer-Ashjai 1977; von Dollen *et al.* 1977; Niazi *et al.* 1978; Nowroozi *et al.* 1977; Ref'an Ateş, private communication). These reported intermediate depths are generally for small shocks recorded by few stations with poor azimuthal coverage. In such circumstances large depth errors may be expected (Jackson 1980b). The larger earthquakes generally have shallower reported depths in agreement with locally recorded activity. The most significant recent advance in the determination of focal depth has been the use of long-period body-wave modelling, employing a technique pioneered by Langston & Helmberger (1975). This technique has been widely used and is capable of estimating the depth of large ($m_b > 5.0$) shocks to within about ± 4 km. Jackson & Fitch (1981), using a slightly modified approach (see Appendix), applied it to several earthquakes in the Zagros mountains of Iran, and showed them to have crustal (< 20 km) rather than intermediate depths. An important result of this work is the realization that shallow thrust faulting events in the magnitude (m_b) range 5.5–6.2 often produce long-period waveforms that are very similar (usually an inverted 'W' shape at distance stations). These waveforms are easily recognizable and differ strongly from those produced by genuinely subcrustal events (Fig. 2). In Iran, where thrust faulting is predominant, the time-consuming process of constructing synthetic seismograms for all events of $m_b > 5.5$ can thus be avoided and only those whose waveforms are distinctly different need special attention.

Although many events with hypocentres deeper than 50 km have been reported from the

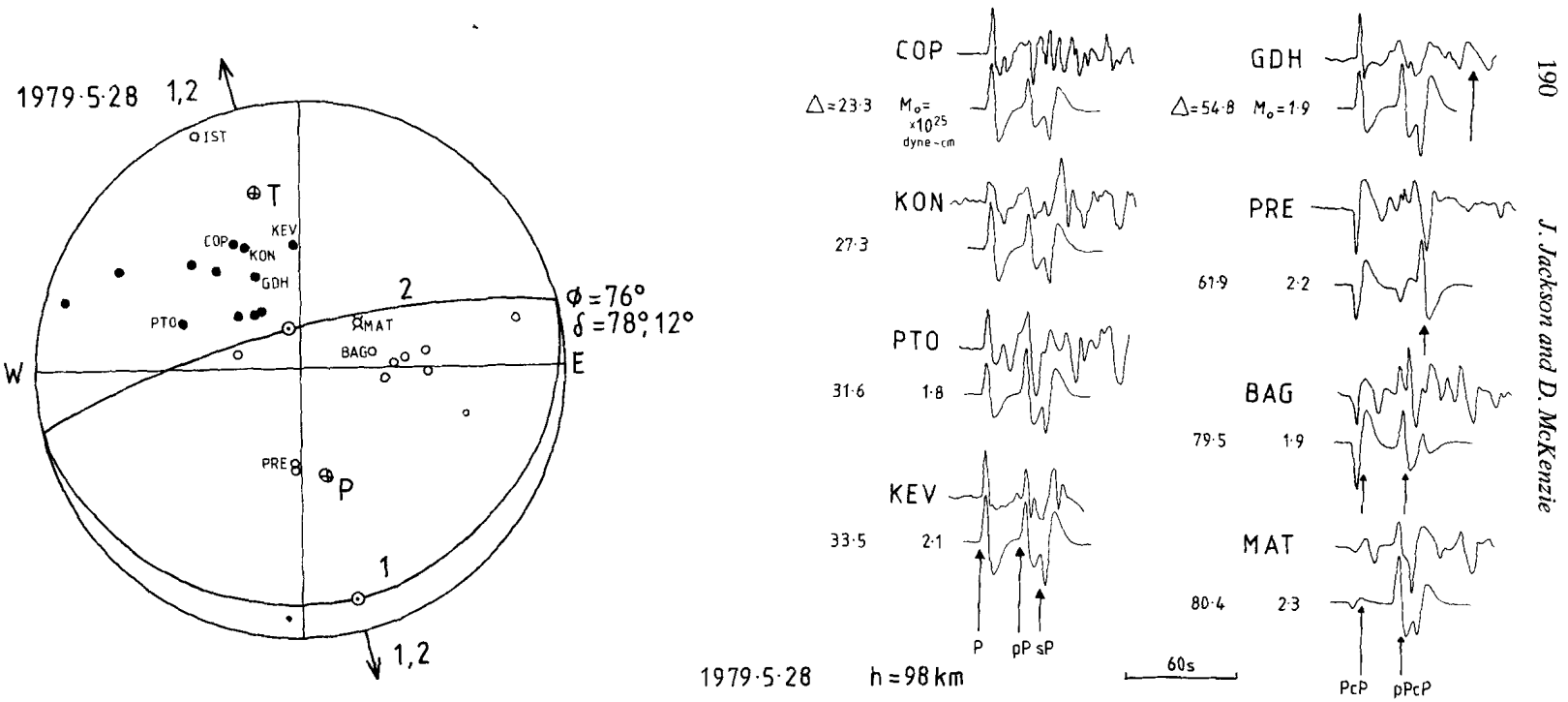

Figure 2. Fault plane solution for an earthquake on 1979.5.28 in Antalya Bay, SW Turkey, plotted with a mantle velocity of 8.1 km s^{-1} at the focus using an equal area lower hemisphere projection. Open symbols are dilatational first motions and closed are compressional. Nodal onsets are marked with crosses. All readings are from long-period WWSSN instruments. Where short-period onsets are used (as in Fig. 4) they are mentioned specifically in figure captions or text. First motions marked by smaller symbols are thought to be less reliable than those marked with large symbols. *P*- and *T*-axes are marked with larger crossed circles and slip vectors are shown as circles with dots on the nodal planes. Arrows mark the horizontal projections of slip vectors on the two numbered nodal planes. Also shown are observed (top) and synthetic (bottom) long-period waveforms on the vertical component WWSSN instruments. These are intended to demonstrate that the intermediate focal depth reported by NEIS and ISC is genuine. Synthetic waveforms containing only *P*, *pP* and *sP* were generated by the technique of Langston & Helmberger (1975), with a triangular time function of 4 s duration, a focal depth of 98 km, and a value for t^* of 1.0 s. Although this technique is not strictly valid at these depths because of the assumptions made about geometrical spreading, these synthetics are sufficient to confirm an intermediate focal depth. Stations to the north, such as KEV and KON (COP is really too close and included only for illustration), whose surface reflection points are on land (see Fig. 7), have very simple waveforms consisting of *P*, *pP* and *sP*. Those to the west and south (e.g. PTO and PRE), whose reflection points are in the sea, are complicated by reflections from the seabed as well as the sea surface. As the bathymetry is steeply sloping here, and as the effect of a dipping surface on reflected amplitudes is complex (see Butler 1982), further modelling of these records was not thought justified for our purposes, and water was not included in our velocity model above the source. At stations further than about 70° from the epicentre, *PcP* arrives before the reflected phases *pP* and *sP*. The predicted arrival times of *PcP* and *pPcP* are shown by arrows at BAG and MAT and correspond well with arrivals on the observed seismograms. Arrows at GDH and PRE mark the arrival times of *PcP*.

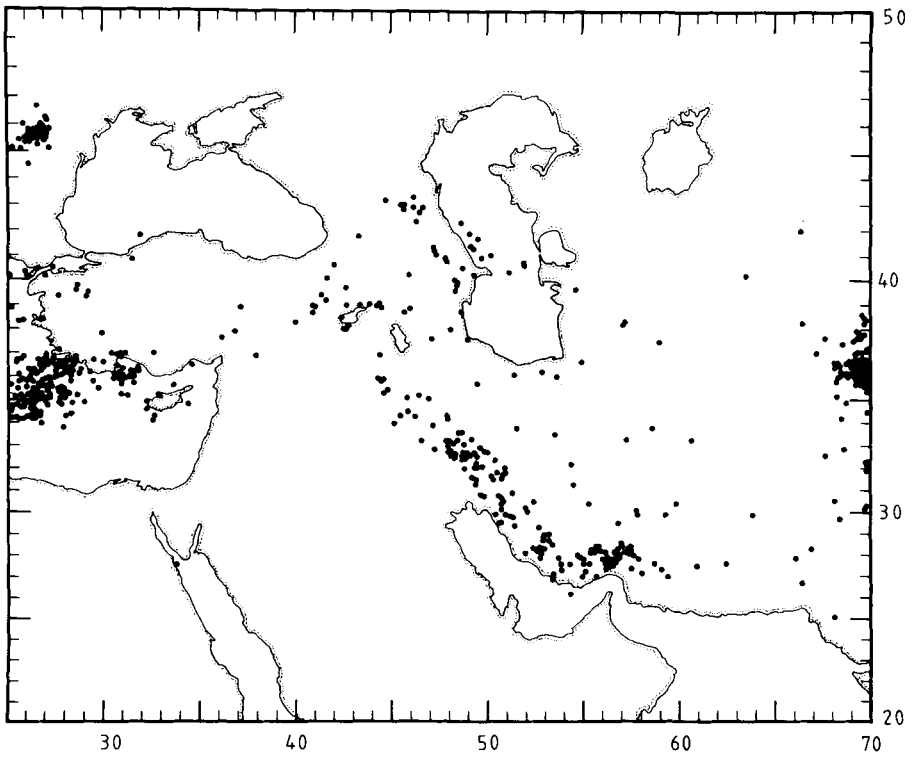

Figure 3. Epicentres of shocks reported deeper than 50 km by NOAA and its successors during the period 1961 January to 1980 December. Genuine focal depths greater than 50 km are known in Romania, the Hellenic Trench, SW Turkey, the Makran and the Hindu Kush. Most of the earthquakes in other places are likely to be mislocated crustal events that have been incorrectly assigned subcrustal focal depths (see text).

Zagros, the Caucasus and eastern Turkey (Fig. 3), they are small and poorly recorded and their depths cannot be believed without detailed investigations. Such shocks were also examined in the *ISC* (International Seismological Centre) *Bulletin*, which has considerably more reporting stations than the NEIS and also lists apparent *pP* arrivals. Convincingly consistent *pP–P* times for shocks reported deeper than 50 km could not be found. However, in both southern Iran and south-western Turkey genuine hypocentres deeper than 50 km have been confirmed by waveform modelling. In these two regions shocks with reported depths greater than 50 km have been marked on the seismicity maps (Figs 6, 7, 11, 29 and 30). In other regions all hypocentres have been assumed to be shallow, except for the occasional shock, such as the one in southern Afghanistan on 1979.1.31 at 1550 GMT (Fig. 30) which was given a depth of 183 km by the NEIS, 173 km by the ISC and was reported by 98 and 122 stations respectively. Such exceptions are discussed in the text.

The new focal mechanisms reported here are all based on WWSSN seismograms read by the authors. The approach used by McKenzie (1972, 1978a) was to plot the station positions on the focal sphere using a *P* velocity below the source of 7.8 km s^{-1} unless orthogonal nodal planes could not be fitted, in which case a crustal velocity of 6.8 km s^{-1} was used. Since it is now known that most of the shocks in this region have crustal depths, a source velocity of 6.8 km s^{-1} was used in this study unless the hypocentre was known to be in the mantle.

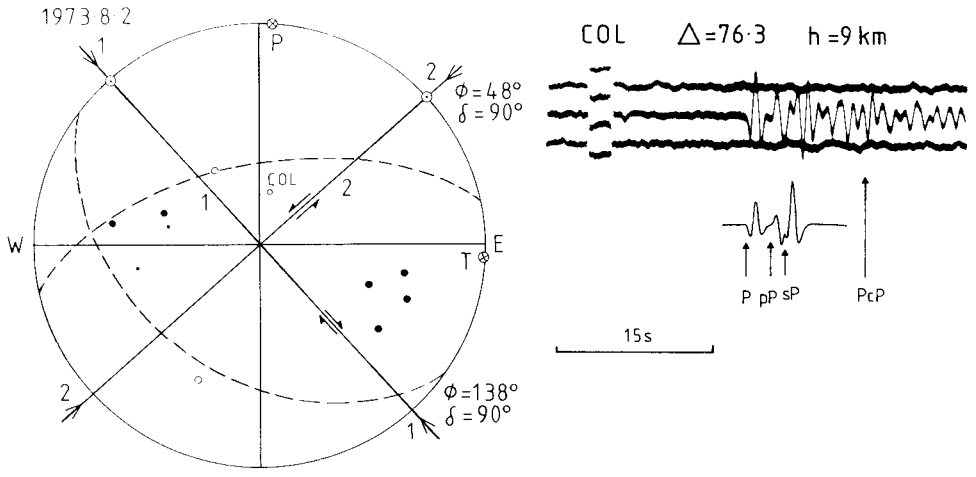

Figure 4. Fault plane solution for 1973.8.2 in NE Iran (see Fig. 26). The long-period polarity observations are compatible with both a thrusting (dashed lines) and a strike-slip (solid lines) solution. The short-period WWSSN record at COL, where the long-period onset is too small to be read, shows the dilatational instrument response and does not allow the thrust solution. A synthetic seismogram is also shown at COL for a source at 9 km depth with a triangular time function of 0.4 s duration. The compressional *pP* and dilatational *sP* predicted by the strike-slip solution matches the observed waveform quite well, although it is obviously not possible to constrain the mechanism with a single seismogram.

Although the long-period vertical WWSSN instrument was used for almost all the polarity observations, occasional use was made of the polarity on the short-period vertical instrument in cases where the long-period onset was too small or obscured and where the short-period onset was particularly clear and recognizable as the instrumental impulse response. In such cases an ambiguity in the type of fault plane solution could sometimes be resolved. An example is shown in Fig. 4 for the shock of 1973.8.2 (m_b 5.3) in NE Iran. The long-period polarities cannot distinguish between thrust (dashed lines) and strike-slip (solid lines) faulting. The short period onset at COL, where the long-period onset was too small to see, is clearly the instrumental response to a dilatational impulse (a 'W' shape on the short-period vertical instrument) and confirms the strike-slip solution. It is the recognition of the instrumental impulse response that gives confidence in the determination of this polarity as dilatational. Such an onset is common for small earthquakes where the far field time function is very simple and of short duration. It is rarely observed on short-period instruments for large earthquakes. In Fig. 4 synthetic seismogram at COL is also shown for the strike-slip solution at 8 km depth. Although it is obviously not possible to constrain the mechanism and depth from a single seismogram, the fit is not bad, and appears to indicate that the early part of this short-period seismogram is indeed simple and made up of the direct *P* and reflected *pP* and *sP* phases.

Occasionally a station showed reversed polarity on its vertical component instrument. This problem occurred notably at SHI after 1973 (Asudeh 1981) and at BUL after 1979. At these stations, if the polarities on both long-period horizontal components were not consistent with that of the vertical, the station was ignored.

Several other authors have reported fault plane solutions in this region. Both Shirokova (1967, 1977) and Chandra (1981) published diagrams of lower focal hemisphere projections for numerous earthquakes in Iran, but generally without showing individual polarity readings. Some of their solutions are consistent with ours while others are not. In the

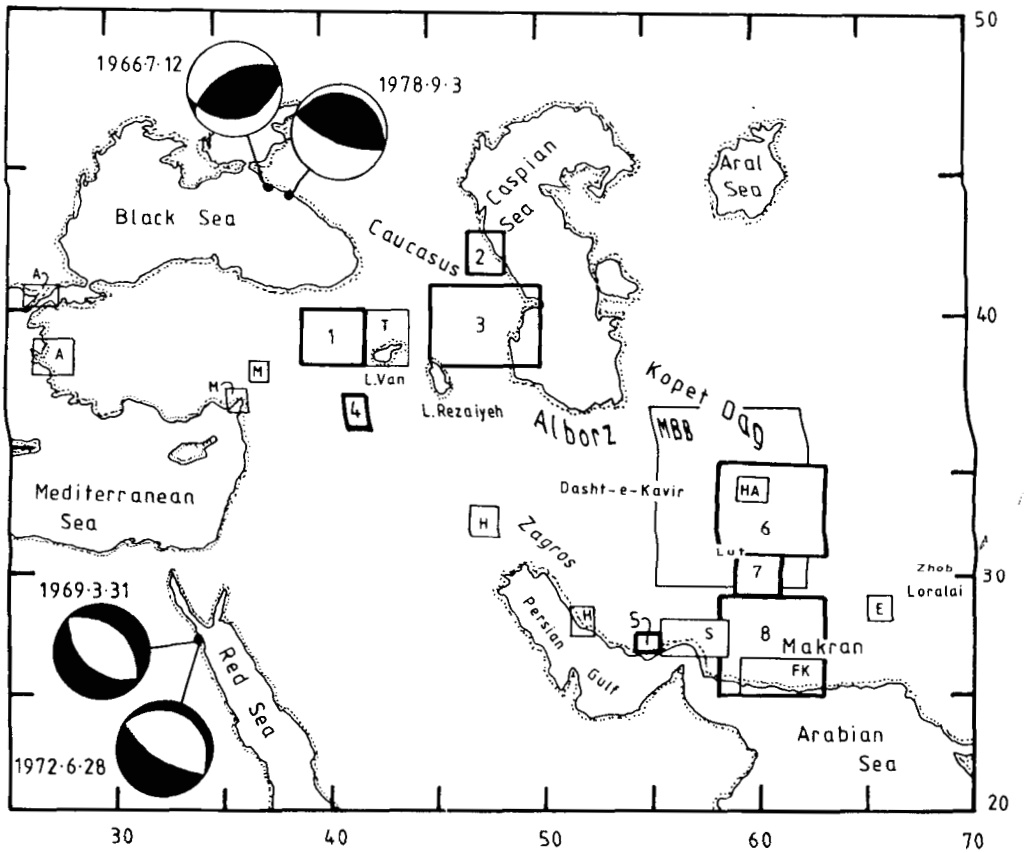

Figure 5. Location map showing the geographical names used as well as the areas in which satellite images are discussed. Boxes outlined in heavy ink are Plates 1 to 8, those in light ink are published in: Allen (1975) [A]; McKenzie (1976) [M]; Tchalenko (1977) [T]; Halbouty (1980) [H]; Sherman (1976) [S]; Fahoudi & Karig (1977) [FK]; Mohajer-Ashjai *et al.* (1975) [MBB] and EOS (1980) [E]. Also shown are lower hemisphere fault plane solutions for shocks in the Red Sea and the Black Sea, with compressional quadrants shaded. Polarity readings for these shocks are in Fig. 8 (see Table 1).

absence of polarity readings their solutions are difficult to check. In several cases, however, Chandra (1981) presents solutions for shocks whose onsets, in our opinion, were simply too small for polarities to be reliably read on either short- or long-period instruments. Inconsistencies in other solutions may be traced to incorrect polarities very close to nodal planes, where onsets must be read with particular care. Alptekin (1973) and Alptekin & Ezen (1978) give solutions for several shocks in south and west Turkey. These solutions contain many inconsistencies arising from the use of polarity data listed in bulletins, and we do not regard them as reliable.

The seismicity maps presented here were drawn to overlie the $1:10^6$ ONC topographic maps, with errors in latitude and longitude of about 0.2 km (see McKenzie 1978a). *Landsat* images were also useful and made into mosaics on a scale of $1:10^6$, though with a slightly different projection. Fig. 5 shows the geographical locations used in the text, as well as an index to the various satellite images presented in this and other reports. Hypocentral parameters of all the earthquakes with focal mechanisms discussed here are given in Table 1, where the numbers of the figures containing the polarities used in each individual fault plane solution are also given.

Table 1. Hypocentral parameters for shocks with fault plane solutions. Depths are those reported by NOAA, USCGS and NEIS, except where they are marked with an asterisk, which denotes that the focal depth is constrained by waveform observations. m after the depth indicates that a mantle source velocity was used in preparing the fault plane solution, otherwise a crustal velocity of 6.8 km s^{-1} was used. In the second column from the right the figure is indicated where the individual polarity readings may be found. Those not in this paper are marked: M72 (McKenzie 1972), Mpc (Molnar, private communication), J81 (Jackson & Fitch 1981), M78 (McKenzie 1978a), Q79 (Quittmeyer *et al.* 1979) M70 (McKenzie, Molnar & Davies 1970) and B82 (Berberian 1982).

Date	Time	Lat.	Long.	Dep.	Ms	mb	Fig.	Region
1938.4.19	10 59 17	39.50	33.80	0	6.6		8a	C. Turkey
1939.12.26	23 57 17	39.70	39.41	0m	8.0		M72	E. Turkey
1943.6.20	15 32 50	40.70	30.38	0m	6.3		M72	W. Turkey
1948.10.5	20 12 04	37.78	58.41	5m	7.3		M72	Kopet Dag
1951.8.13	18 33 30	40.95	32.57	0m	6.7		M72	N. Turkey
1956.2.20	20 31 38	39.86	30.49	9m	6.0		M72	W. Turkey
1957.5.26	06 33 32	40.66	30.89	0m	7.0		M72	W. Turkey
1957.7.2	00 42 23	36.14	52.70	10m	6.8	7.0	M72	N. Iran
1957.12.13	01 45 05	34.35	47.65	40m	6.7	6.5	M72	W. Iran
1962.9.1	19 20 40	35.63	49.87	27	7.2	6.9	M72	N.W. Iran
1963.3.24	12 44 00	34.30	47.80	10	5.8	5.5	22a	W. Iran
1963.7.16	18 27 18	43.10	41.50	33m		5.8	M72	Caucasus
1963.9.18	16 58 12	40.90	29.20	33	6.4	5.2	8b	W. Turkey
1964.6.14	12 15 31	38.00	38.50	8	5.9	5.5	M72	S.E. Turkey
1964.12.22	04 36 35	28.20	57.00	18*	6.1	5.5	M72	Zagros
1965.6.21	00 21 16	28.10	55.90	40m	5.4	6.0	M72	Zagros
1966.1.24	07 23 10	29.90	69.70	26		5.6	Mpc	Pakistan
1966.2.7a	04 26 11	29.90	69.70	10		6.0	Mpc	Pakistan
1966.2.7b	23 06 35	30.30	69.90	11		5.8	Mpc	Pakistan
1966.3.7	01 16 10	39.10	41.60	38	5.6	5.3	M72	E. Turkey
1966.4.20	16 42 06	41.70	48.20	36		5.4	M72	Caucasus
1966.7.12	18 53 10	44.60	37.30	46m		5.7	M72	Black Sea
1966.7.27	14 49 02	32.60	48.80	33		5.3	M72	Zagros
1966.8.1a	20 30 55	30.00	68.50	17		5.6	Mpc	Pakistan
1966.8.1b	21 02 59	30.10	68.60	33		6.0	Mpc	Pakistan
1966.8.19	12 22 11	39.20	41.60	33m	6.9	5.8	M72	E. Turkey
1966.8.20	11 59 09	39.40	40.90	12m		5.3	M72	E. Turkey
1966.9.18	20 43 54	27.90	54.30	18	5.4	5.9	M72	Zagros
1966.12.10	17 08 32	41.00	33.50	13		4.9	M72	N. Turkey
1967.1.11	11 20 46	34.10	45.70	34		5.6	M72	Zagros
1967.4.7	18 33 31	37.40	36.20	39	4.8	5.0	8c	S.E. Turkey
1967.7.22	16 56 53	40.70	30.80	4m	7.0	6.0	M72	W. Turkey
1967.7.26	18 53 01	39.50	40.40	33m	5.9	5.6	M72	E. Turkey
1967.7.30	01 31 02	40.70	30.40	16m		5.6	M72	W. Turkey
1968.4.29	17 01 58	39.20	44.30	34		5.3	M72	N.W. Iran
1968.6.23	09 16 19	29.81	51.16	8*	5.5	5.2	J81	Zagros
1968.8.2	13 30 23	27.51	60.92	62m		5.7	31a	S.Iran
1968.8.31	10 47 37	33.97	59.02	13m	7.3	6.0	M72	E. Iran
1968.9.1	07 27 30	34.04	58.22	15m	6.3	5.9	M72	E. Iran
1968.9.3	08 19 52	41.79	32.31	5	6.6	5.7	8d	N. Turkey
1968.9.4	23 24 47	33.99	58.24	15	5.2	5.4	M72	E. Iran
1968.9.14	13 48 31	28.44	53.11	33	5.6	5.8	M72	Zagros
1969.1.3	03 16 38	37.13	57.90	11	5.2	5.6	M72	N.E. Iran
1969.1.14	23 12 08	36.18	29.20	33m	6.0	5.5	M72	S.W. Turkey
1969.3.31	07 15 54	27.67	33.99	33	6.8	6.0	M70	Red Sea
1969.11.7	18 33 59	27.85	60.06	35m	6.7	6.1	31b	S. Iran
1970.2.23	11 22 26	27.82	54.53	20	5.6	5.5	22b	Zagros
1970.2.28	19 58 48	27.83	56.32	35		5.5	22c	Zagros
1970.3.14	01 51 44	38.59	44.71	23	4.8	5.3	14a	N.W. Iran
1970.3.28	21 02 23	39.18	29.49	20	7.1	6.0	M78	W. Turkey
1970.5.14a	09 20 22	43.01	47.08	17	5.5	5.6	14b	Caucasus
1970.5.14b	18 12 28	43.03	47.09	44m	6.5	5.6	14c	Caucasus
1970.7.30	00 52 19	37.82	55.88	19m	6.6	5.7	28a	N.E. Iran
1970.10.25	11 22 18	36.77	45.13	19	4.8	5.5	14d	N.W. Iran
1970.11.9	17 41 42	29.52	56.85	106m		5.5	31c	S. Iran
1971.2.14	16 27 36	36.56	55.63	39	5.3	5.2	28b	N.E. Iran
1971.4.6	06 49 52	29.80	51.89	10	5.1	5.2	22d	Zagros
1971.4.12	19 03 26	28.31	55.60	44	5.9	6.0	22e	Zagros
1971.5.12	06 25 13	37.59	29.76	23	5.9	5.5	M78	W. Turkey
1971.5.22	16 43 59	38.83	40.52	3	6.7	6.0	8e	E. Turkey
1971.5.26	02 41 46	35.51	58.22	26	5.4	5.4	28c	E. Iran
1971.11.8	03 06 36	27.05	54.48	36	5.9	5.6	22f	Zagros

Table 1 – *continued*

Date	Time	Lat.	Long.	Dep.	Ms	mb	Fig.	Region
1971.12.9	01 42 30	27.24	56.40	15	5.8	5.3	22g	Zagros
1971.12.20	01 41 05	41.14	48.39	33	5.2	5.2	14e	Caucasus
1972.4.10	02 06 53	28.43	52.83	12*	6.9	6.1	J81	Zagros
1972.6.12	13 34 01	33.11	46.32	33	5.0	5.4	22h	Zagros
1972.6.14	04 34 28	33.03	46.10	33		5.3	22i	Zagros
1972.6.28	09 49 35	27.65	33.76	15	5.5	5.6	8m	Red Sea
1972.7.2	12 56 07	30.10	50.85	31	5.3	5.4	22j	Zagros
1972.8.6	01 12 50	25.07	61.23	33		5.5	31d	Makran
1972.8.8	19 09 34	25.03	61.13	41	5.0	5.5	31e	Makran
1972.11.17	09 09 00	27.35	59.09	65m*		5.4	32	S. Iran
1972.12.1	11 39 04	35.42	57.91	33	5.2	5.4	28d	E. Iran
1973.1.20	12 34 20	29.28	68.57	17	5.6	5.3	Q79	Pakistan
1973.8.2	19 56 27	37.35	56.51	9*		5.3	4	N.E. Iran
1973.11.11	07 14 51	30.57	52.89	11	5.5	5.5	22k	Zagros
1974.3.7	11 36 02	37.60	55.83	21	5.0	5.1	J79	N.E. Iran
1974.8.4	15 06 17	42.34	45.93	33	5.0	5.4	14f	Caucasus
1974.10.4	22 24 33	26.29	66.54	33	5.9	5.8	31f	M. Makran
1974.11.17	15 05 48	32.81	55.07	43		5.2	28e	C. Iran
1974.12.2	09 05 44	27.99	55.82	36		5.4	22l	Zagros
1975.3.7	07 04 43	27.50	56.26	11*	6.1	5.8	22m	Zagros
1975.3.24	05 33 47	29.55	68.60	26	5.4	5.5	31g	Pakistan
1975.4.28	02 01 17	33.31	54.83	42		5.3	28f	C. Iran
1975.4.30	04 28 57	36.18	30.77	56m*		5.6	M78	S.W. Turkey
1975.9.6	09 20 11	38.47	40.72	10*	6.7	6.1	8f	E. Turkey
1975.10.3a	05 14 23	30.25	66.31	11	6.7	5.8	31h	Pakistan
1975.10.3b	17 31 36	30.41	66.35	33	6.4	5.7	31i	Pakistan
1975.12.24	11 48 57	27.01	55.54	33	5.5	5.5	22n	Zagros
1976.2.3	16 40 41	39.93	48.42	58		5.2	16	Caucasus
1976.3.16	07 28 58	27.31	55.06	33	5.2	5.4	22o	Zagros
1976.4.22	17 03 08	28.71	52.13	24	5.5	6.0	22p	Zagros
1976.7.28	20 17 42	43.17	45.60	21	6.1	5.4	14g	Caucasus
1976.11.7a	04 00 52	33.80	59.16	13	6.2	5.6	28g	E. Iran
1976.11.7b	11 07 57	33.24	47.96	51	4.8	5.5	22q	Zagros
1976.11.24	12 22 19	39.12	44.03	36	7.3	6.1	14h	E. Turkey
1977.3.21	21 18 54	27.61	56.39	12*	6.9	5.2	J81	Zagros
1977.3.22	11 57 31	27.58	56.47	15*	5.9	5.7	J81	Zagros
1977.3.23	23 51 16	27.62	56.59	9*	5.4	5.8	J81	Zagros
1977.3.24	04 42 24	27.62	56.63	32		5.3	22r	Zagros
1977.3.25	02 39 58	38.56	40.02	21	4.9	5.2	8g	E. Turkey
1977.4.1	13 36 25	27.54	56.32	12*	6.0	6.2	J81	Zagros
1977.4.6	13 36 37	31.98	50.68	41	5.9	5.5	22s	Zagros
1977.4.26	16 25 29	32.66	48.92	47	4.8	5.4	22t	Zagros
1977.5.25	11 01 45	34.89	52.06	26	4.3	5.4	28h	C. Iran
1977.5.26	01 35 14	38.93	44.38	37	5.4	5.2	14i	N.W. Iran
1977.6.1	12 54 49	36.24	31.34	67m		5.7	8h	S.W. Turkey
1977.6.5	04 45 08	32.64	48.09	12*	5.8	5.5	J81	Zagros
1977.10.5	05 34 47	40.96	33.41	33	5.8	5.3	8i	N. Turkey
1977.10.19	06 35 11	27.79	54.88	33	5.2	5.6	22n	Zagros
1977.11.28	02 59 11	36.05	27.76	85m		5.6	8j	S.E. Aegean
1977.12.19	22 34 34	30.95	56.47	31	5.8	5.4	28i	C. Iran
1978.1.2	06 31 28	41.54	44.24	10	5.1	5.3	14j	Caucasus
1978.2.11	21 40 13	28.21	55.42	50	4.6	5.2	22v	Zagros
1978.3.16	02 00 50	29.93	66.30	33	5.9	5.3	31j	Pakistan
1978.5.6	11 16 10	29.84	66.21	33	5.7	5.5	31k	Pakistan
1978.5.26	13 43 38	41.96	46.55	38	5.2	5.6	14k	Caucasus
1978.9.3	00 21 16	44.40	38.05	33	5.4	5.7	8k	Black Sea
1978.9.16	15 35 57	43.39	57.33	33	7.3	6.5	B82	E. Iran
1978.11.4	15 22 19	37.67	48.90	34	6.0	6.1	28j	N.W. Iran
1978.12.14	07 05 21	32.14	49.65	33	6.2	5.7	22w	Zagros
1979.1.10a	01 26 09	26.61	60.93	33	5.8	5.6	31l	Makran
1979.1.10b	15 05 48	26.52	61.01	33	5.9	5.6	31m	Makran
1979.1.16	09 50 10	33.90	59.47	33	6.7	5.9	28k	E. Iran
1979.2.13	10 36 17	33.32	57.43	33	4.8	5.5	B82	E. Iran
1979.5.28	09 27 32	36.41	31.75	98m*		5.9	2	S.W. Turkey
1979.11.14	02 21 22	33.92	59.74	33	6.6	6.0	28l	E. Iran
1979.11.27	17 10 33	33.96	59.73	10	7.1	6.1	28m	E. Iran
1979.12.7	09 24 00	34.03	59.82	31	6.0	5.8	28n	E Iran
1979.12.9	09 12 07	35.05	56.82	48	5.3	5.2	28o	E. Iran
1979.12.31	06 21 34	36.18	31.51	79m		5.3	81	S.W. Turkey
1980.1.12	15 31 42	33.49	57.19	33	5.9	5.4	B82	E. Iran
1980.4.28	07 04 02	27.49	64.46	34m	4.7	5.4	31n	S.W. Pakistan
1980.5.4	18 35 20	38.05	48.99	46	6.2	5.4	28p	N.W. Iran
1980.12.19	01 16 56	34.59	50.65	33	5.8	5.6	28q	N.W. Iran
1980.12.22	12 51 21	34.50	50.59	41	5.2	5.5	28r	N.W. Iran
1981.6.11	07 24 25	29.91	57.72	33	6.7	6.1	28s	C. Iran
1981.7.28	17 22 24	30.17	57.84	33	7.1	5.8	28t	C. Iran

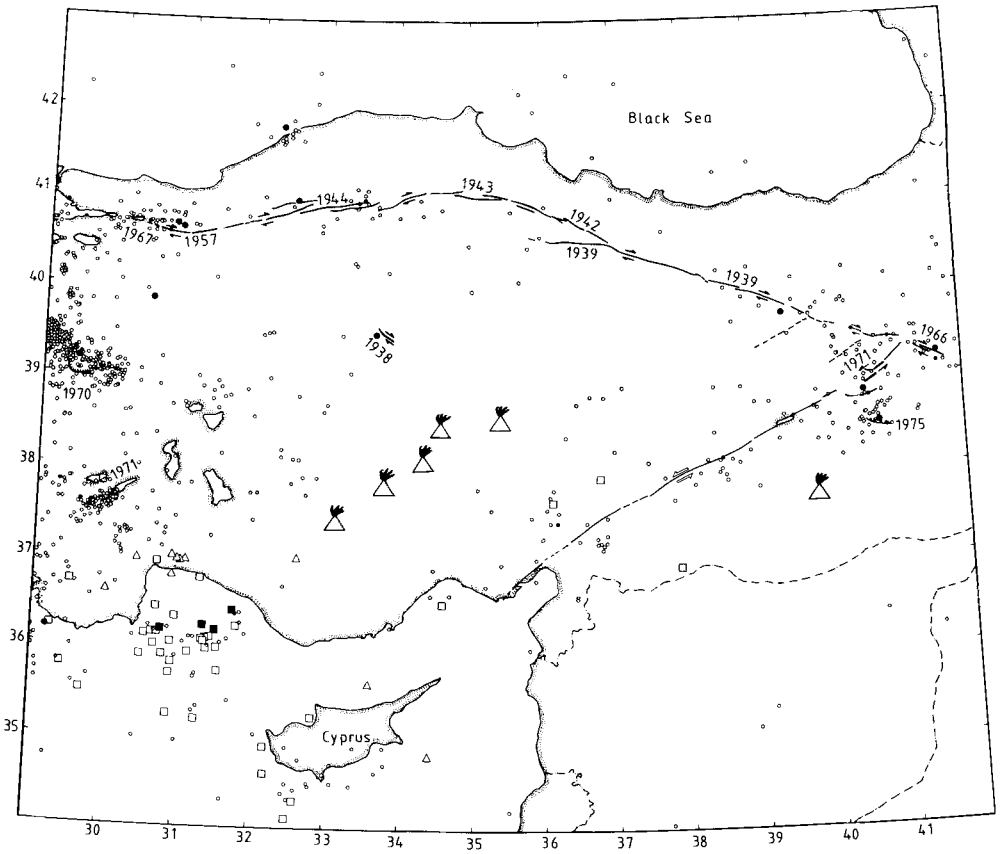

Figure 6. Epicentres reported by NOAA and its successors in Turkey during the period 1961 January to 1980 December. Open triangles are those with focal depths reported deeper than 100 km, squares are those between 50 and 100 km, and circles are those shallower than 50 km. Large symbols are events with magnitude (m_b or M_s) 6.0 or greater. The few shocks reported deeper than 50 km in eastern Turkey (Fig. 3) have been drawn as shallow, because there is no evidence that their depths are genuinely this great (see text). Filled symbols are shocks for which fault plane solutions are available in Fig. 7 (see also I and Table 1). Smoking triangles are Quaternary volcanoes, visible on satellite images and reported in Simkin *et al.* (1981). Faults known to be active are marked with continuous lines, with dates next to them where they were activated during specific earthquakes. Dashed lines are faults inferred from satellite images and field mapping.

3 Central and southern Turkey

3.1 THE NORTH ANATOLIAN FAULT ZONE

Except for the Mudurnu earthquake sequence in 1967, there has been little seismic activity on the North Anatolian Fault since 1961 (Figs 6 and 7), and only one additional fault plane solution since 1969. The new solution is for 1977.10.5 and shows the expected right lateral strike-slip motion. This shock occurred very close to a small earthquake of 1966.12.10 for which a poorly constrained solution (omitted in Fig. 7) is given in I. There is little to add to the remarks made by McKenzie in I. The curvature of the fault trace and the slip vectors of the earthquakes since 1939 suggest a rotation of Turkey relative to Europe about a pole at 14.6°N 34.0°E (see Section 10). For descriptions of the fault zone and surface breaks

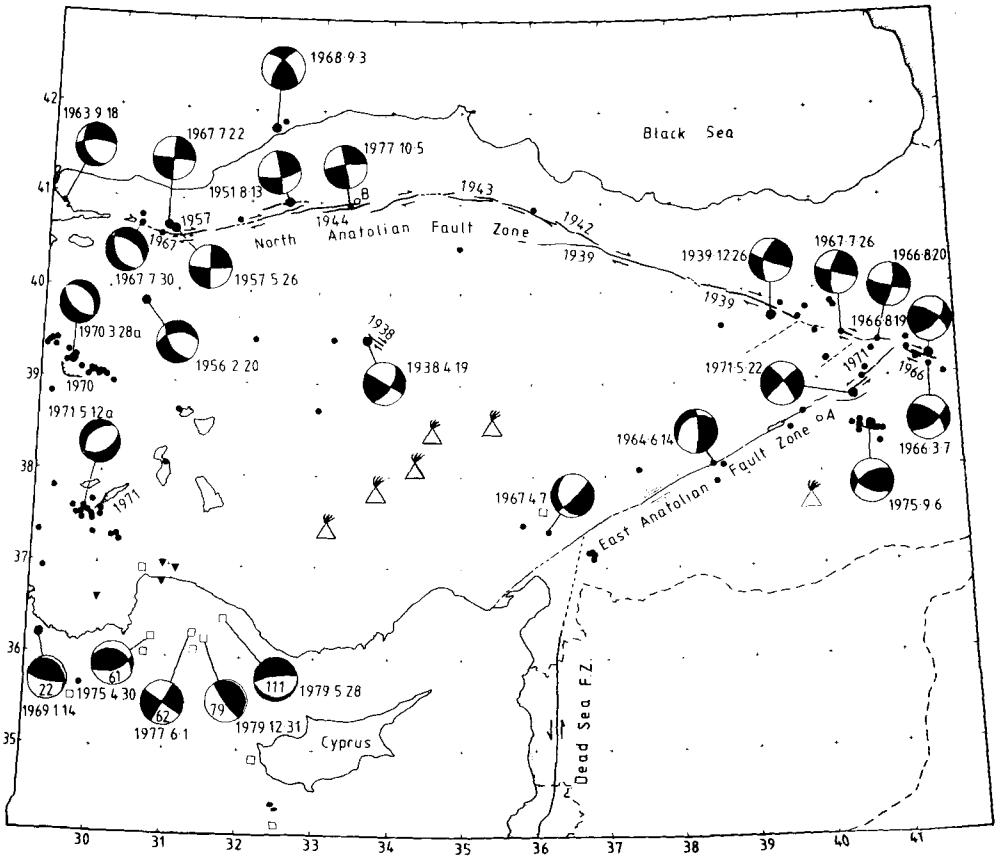

Figure 7. Epicentres of the larger shocks in Fig. 6, with m_b 5.0 or greater or with at least 50 recording stations. Large symbols are those of magnitude (m_b or M_S) 6.0 or greater. Volcanoes and faults as in Fig. 6. Fault plane solutions are those in I and Fig. 8 (see also Table 1). Numbers in the dilatational quadrants of the mechanisms in SW Turkey are the focal depths reported by the ISC. The epicentre marked A is that of the Palu earthquake (1977.3.25; Fig. 8g) and B is that of 1966.12.10, with a poor mechanism given in I.

during individual earthquakes the reader is referred to Ketin (1948), Allen (1965, 1969), Wallace (1968), Ambraseys & Zatopek (1968, 1969) and Ambraseys (1970). The present quiescence is not unusual in the history of this fault and there is some evidence that certain portions of it, such as that near Ismetpaşa on the 1944 surface break, are creeping, possibly as much as several centimetres per year (Ambraseys 1970). The morphology of the fault changes east of its junction with the East Anatolian Fault near Karliova (*c.* 41°E), and fault plane solutions show an increased component of thrusting associated with right lateral strike-slip (see Section 4). In the west the fault continues into the diffuse seismicity of western Turkey and the Aegean, but loses its distinct morphology as right lateral slip is distributed over a number of grabens with a large component of normal faulting (see McKenzie 1978a and Jackson *et al.* 1982a). This change in character appears to start at the western end of the 1967 Mudurnu surface breaks, where normal faulting is seen in the major aftershock of 1967.7.30 as well as in microearthquakes recorded in the region (see Fig. 9 and Evans *et al.* 1984). West of about 30.5°E the seismicity of Turkey is dominated by normal

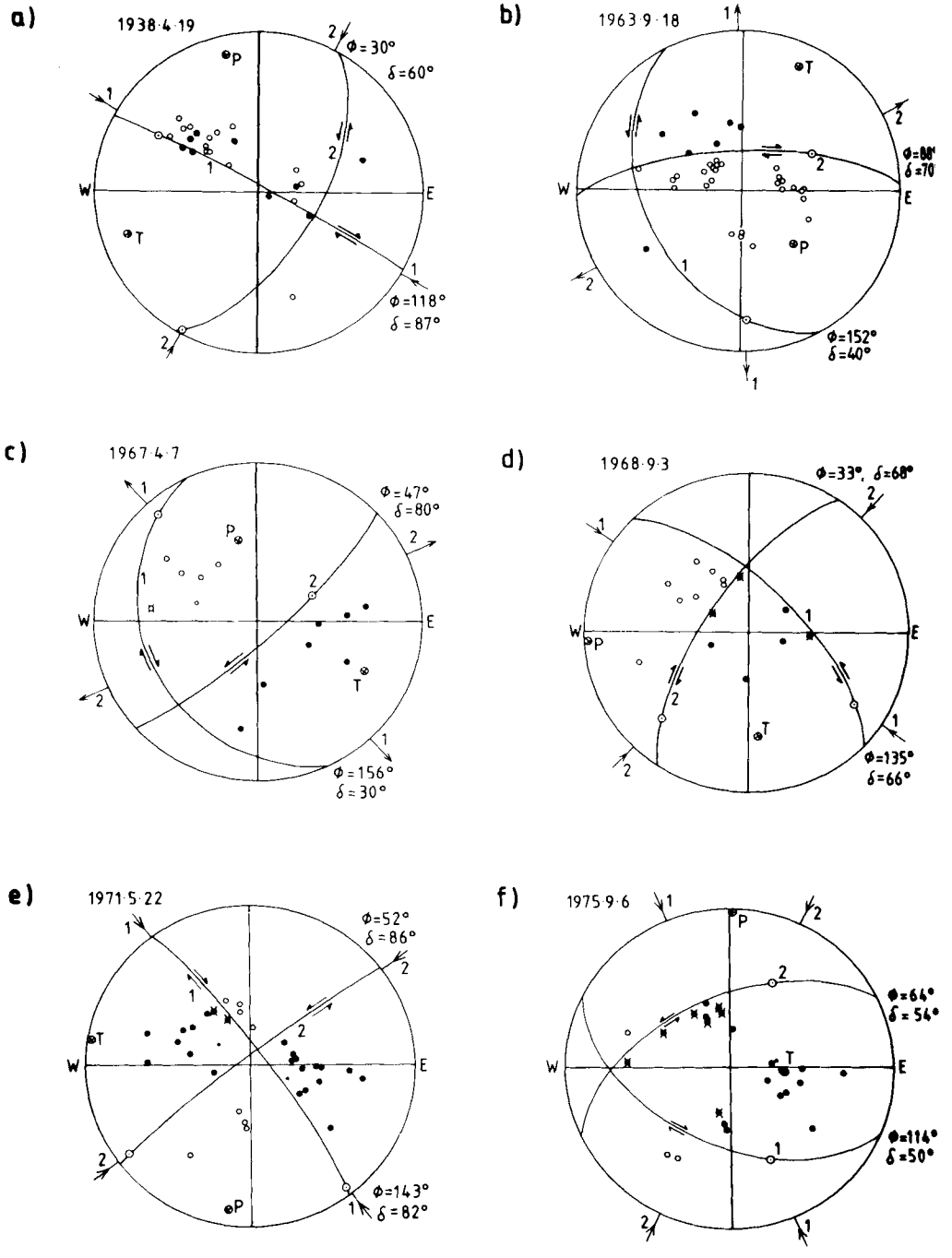

Figure 8. New fault plane solutions shown in Figs 5 and 7. Symbols as in Fig. 2. All except (h), (j) and (l) are plotted with a crustal velocity as the focus. Because of the reduction required, some of the smaller dilatational symbols (open circles) may look like compressons (filled circles). In this and subsequent similar figures *all* polarities are consistent with the nodal planes drawn unless specifically mentioned in the figure captions. In this case only (a) has some inconsistent polarities.

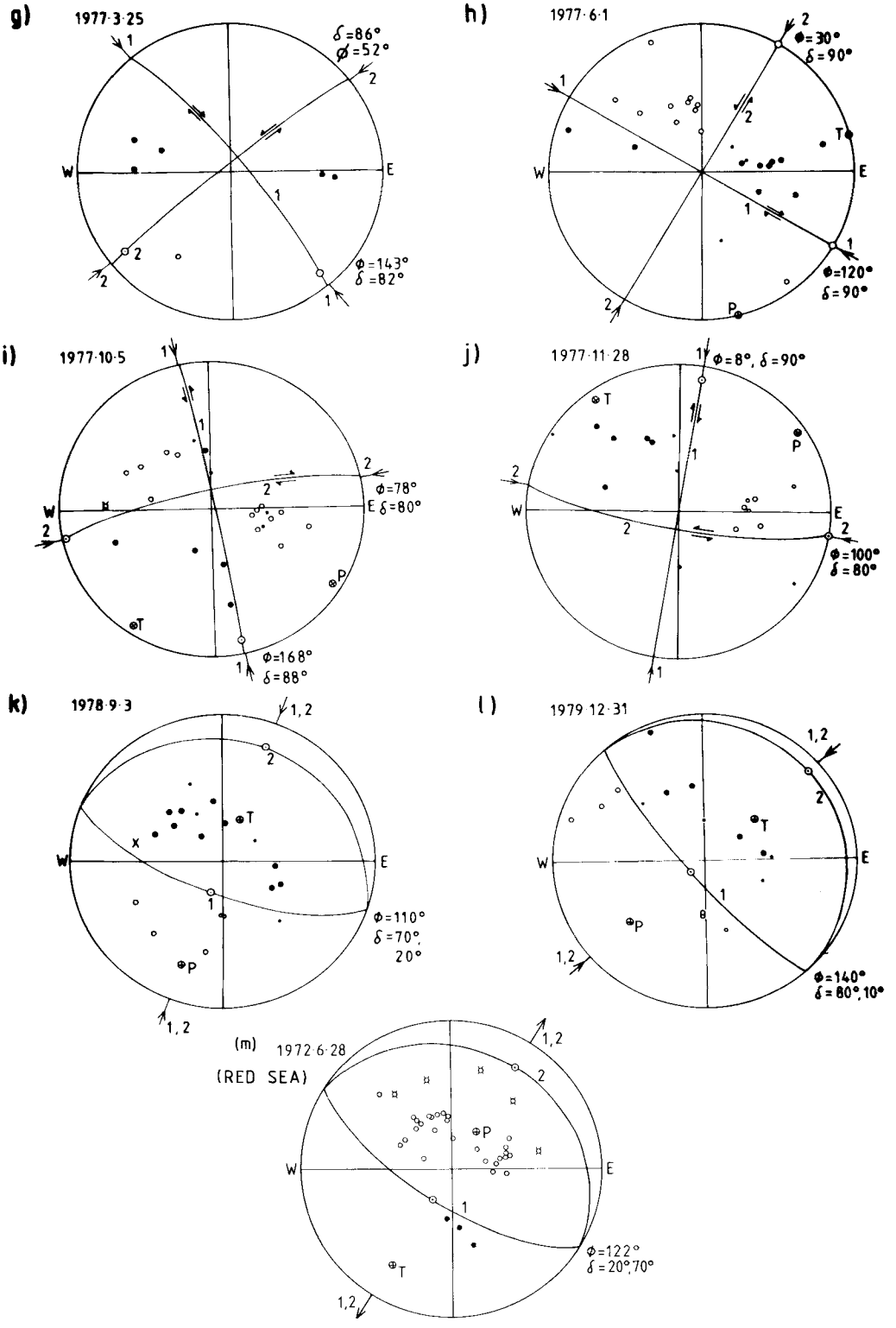

Figure 8 – *continued*

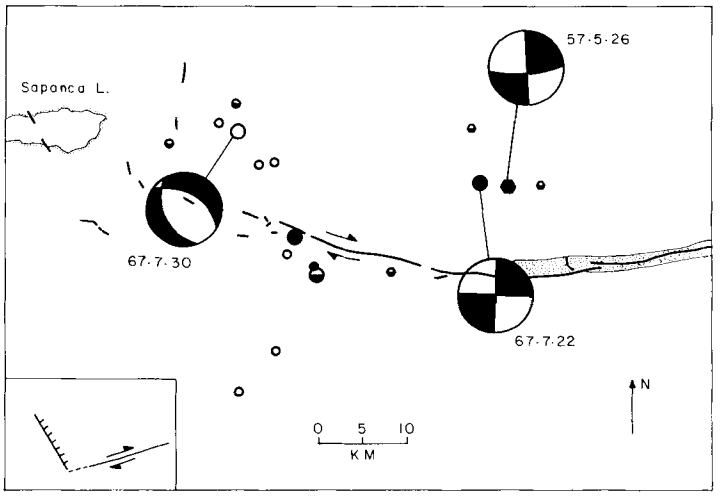

Figure 9. The aftershock sequence at Mudurnu relocated relative to 1967.7.30 by the technique of Jackson & Fitch (1979) and positioned in space using the ISC location for this shock (40.72°N 30.52°E). Large symbols are shocks with more than 50 arrival times in their relocation, small have more than 20. Errors are about 5 km for the larger shocks. Hexagons are the 1957 and circles the 1967 sequence. Filled symbols are shocks showing dilatations on the long-period WWSSN records at IST (Istanbul, azimuth 288°). Open symbols showed compressions and half-filled symbols could not be reliably read at IST. Fault breaks for the 1967 (solid lines) and 1957 (stippled) earthquakes are from Ambraseys & Zatopek (1969). Inset shows a cartoon description of the faulting.

faulting, which continues into the Aegean. This normal faulting has led to substantial north–south crustal extension and subsidence, which is discussed elsewhere (see McKenzie 1978a; Le Pichon & Angelier 1979; Jackson 1982b). Ambraseys & Tchalenko (1972) and Erinç *et al.* (1971) describe the surface breaks of 1970.3.28a and 1971.5.12a, shown in Figs 6 and 7.

3.2 THE EAST ANATOLIAN FAULT ZONE

The activity of the East Anatolian Fault since 1961 has been comparable to that of the North Anatolian Fault, although historically it too has been very active (Ambraseys 1971). The Bingol earthquake of 1971.5.22, with both fault plane solution and surface faulting showing left lateral motion (Arpat & Şaroğlu 1972; Seymin & Aydin 1972), has confirmed the sense of motion postulated in I, at least in the NE near its junction with the North Anatolian Fault. Dewey (1976) also gives a fault plane solution for 1971.5.22, which is in excellent agreement with ours. The earthquake of m_b 4.9 on 1977.3.25 (marked A in Fig. 7) had a macroseismic epicentre 20 km NW of its NEIS location, placing it near Palu on the East Anatolian Fault (Ateş & Bayulki 1977). Although the available first motions for this shock are consistent with left lateral motion on the East Anatolian Fault (Fig. 8g), there are not enough readings to constrain the fault plane solution satisfactorily. The fault plane solutions of two shocks on 1964.6.14 and 1967.4.7, which were presented in I, have been redrawn in Fig. 7 using a crustal source velocity. That of 1967.4.7 had a macroseismic epicentre near Bahçe, on the East Anatolian Fault 20 km SE of its NOAA location (Ambraseys & Jackson 1982). These two solutions are not well constrained, and though it

is possible to draw nodal planes with left lateral slip on a NE striking plane, this component of motion is small and faulting must have predominantly involved some other mechanism. Both these shocks were small and may not be representative of the major movement on the East Anatolian Fault. Detailed studies of the focal mechanisms of small shocks in aftershock sequences show that small earthquakes can have a complicated relationship to major shocks and probably reflect a geometrically required internal deformation of the blocks either side of large faults (see, e.g. Jackson *et al.* 1982b). The east Anatolian Fault has been mapped by Arpart & Şaroğlu (1972, 1975) who trace it southwards to its connection with the Dead Sea Fault system (see also Muehlberger 1981). The velocity triangle for the motions of Turkey, Eurasia and Arabia at the junction of the North and East Anatolian Faults (see I) suggests that the rate of motion on the East Anatolian Fault considerably exceeds estimates for the Dead Sea Fault, on which recent seismic activity has also been low (see, e.g. Ben-Menahem, Nur & Vered 1976; Garfunkel, Zak & Freund 1981). Moreover, if motion on the East Anatolian Fault is really strike-slip with an azimuth of about 60°E, it is different from that of about 5°E on the Dead Sea Rift. These arguments suggest that the East Anatolian Fault continues SW into the Gulf of Iskenderun and towards Cyprus. Such an extension is confirmed on land by satellite images (McKenzie 1976), on which a fault zone is seen bordering the Misis mountains on the NW side of the Gulf of Iskenderun. According to Pinar (1953) this part of the fault zone was associated with an earthquake of M_S 5.5 in 1952, but neither a focal mechanism nor reliable reports of surface faulting are available for this shock.

3.3 CENTRAL ANATOLIA

Significant activity does occur away from the North and East Anatolian Faults. The Bartin earthquake of 1968.9.3 on the Black Sea coast has a mechanism (redrawn from I with a crustal source velocity) with a substantial thrusting component, consistent with the recent as well as contemporaneous uplift of raised beaches on the shore (Ketin & Abdüsselamoğlu 1970; Aytun 1971; Şengör, Büyükaşikoğlu & Canitez 1983). This thrusting may represent a reactivation of the thrust faults observed in seismic reflection profiles offshore (Letouzey *et al.* 1977). The scattered epicentres in central Anatolia are probably not mislocations as damaging earthquakes are known to have occurred there historically. Particularly interesting is the Kirşehir shock of 1938.4.19, which was associated with a surface fault break 15 km long showing about 60 cm of right lateral motion trending NW (Arni 1938; Parejas & Pamir 1939; Richter 1958). Such motion is consistent with a fault plane solution for this shock based on polarities from the ISS and Wickens & Hodgson (1967), which, considering the unreliability of the data, is surprisingly good (Fig. 8a). Another sequence in 1940, with a mainshock of magnitude 6.1, was located 130 km east of Kirşehir at 39.8°N 35.3°E by Dewey (1976), but is not marked on Figs 6 and 7. Other earthquakes in central Anatolia are known from historical sources (Ambraseys, private communication).

Several SW-trending faults branching off the North Anatolian Fault occur west of its junction with the East Anatolian Fault. Some, marked with dashes in Figs 6 and 7, are visible on the satellite images (Plate 1), and one was activated at the western end of the 1939.12.26 surface break. Others are marked on the geological map of Turkey as linear Quaternary depressions (MTA 1962). It is difficult to relate any recent seismicity to these splay faults. An unconfirmed report in Tchalenko (1977) attributes a small NE-trending surface break passing through Kigi, on the easternmost dashed splay in Figs 6 and 7, to a small earthquake of m_b 5.1 on 1968.9.24. This was too small to obtain a reliable fault plane solution. Şaroğlu (private communication) considers several more splays to be active and has mapped a system of faults parallel to the East Anatolian Fault that penetrate central

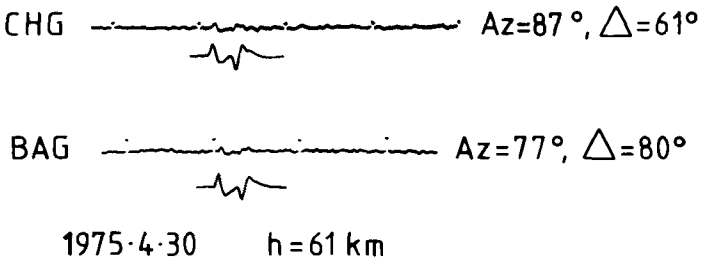

Figure 10. Observed and synthetic long-period waveforms from the earthquake in SW Turkey of 1975.4.30. Synthetic waveforms were calculated using the mechanism in Fig. 7 and a triangular time function of 4.0 s duration. The amplitudes of the synthetic seismograms have been exaggerated to show their shape more clearly. Although small, the waveforms do not resemble those of shallow earthquakes, and the later arrivals correspond well in relative amplitude and timing to those of the surface reflections predicted by the ISC depth of 61 km.

Anatolia, as well as additional NW-striking faults, such as that of 1938.4.19. A possible explanation for these north-easterly splays is that they record older positions of the East Anatolian Fault, which may have progressively jumped eastwards, thereby changing the motion on east–west faults from thrusting to strike-slip and lengthening the North Anatolian Fault. Although such a migration of the East Anatolian Fault eastwards would help prevent crustal thickening, there is no obvious way in which it releases gravitational energy and can be driven by topography. Another possibility is that some of the westward motion of Turkey relative to Eurasia is taken up on these splays in central Anatolia, which may account for the apparent decrease in displacement on the North Anatolian Fault towards the west (e.g. Şengör, Burke & Dewey 1982). None of these splay faults have morphologies as well developed as the North and East Anatolian Faults and displacements on them are probably not as large. Nevertheless, their presence, combined with the known occurrence of significant earthquakes in 1938 and 1940, questions whether central Anatolia can really be considered a rigid block. Historical studies such as those of Ambraseys & Melville (1982) may help resolve this matter.

3.4 SOUTHERN TURKEY, CYPRUS AND THE DEAD SEA RIFT

In southern Turkey it is now clear that some shocks in Antalya Bay have hypocentres genuinely deeper than 50 km. Three new fault plane solutions are shown, and clear surface reflections seen in the body waves for two shocks, of 1975.4.30 and 1979.5.28, constrain their depths to be about 61 and 98 km (Figs 2 and 10). The large number of recording stations, small surface waves, and epicentral positions of 1977.6.1 and 1979.12.31 make it likely that the depths of 62 and 79 km reported for these shocks by the ISC are reasonably accurate. They are also consistent with phases reported as *pP* and *sP* in the *ISC Bulletin.* Similar arguments make it probable that many of the hypocentral depths for the larger shocks in the Antalya Bay area reported as deeper than 50 km, are real (Jackson 1980b). It thus appears that there is a genuine zone of intermediate depth seismicity dipping north or NE in Antalya Bay (Figs 6 and 7; Rotstein & Kafka 1982). Its link with a similar zone in the Hellenic Arc remains enigmatic. Fig. 11 shows the seismicity reported as deeper than 50 km in this region. Also shown are the projected *P*, *T* and null axes from the available fault plane solutions of shocks deeper than 50 km near Antalya and Rhodes. (Note that one of the shocks near Rhodes, on 1961.5.23, was misplotted in the centre of western Turkey

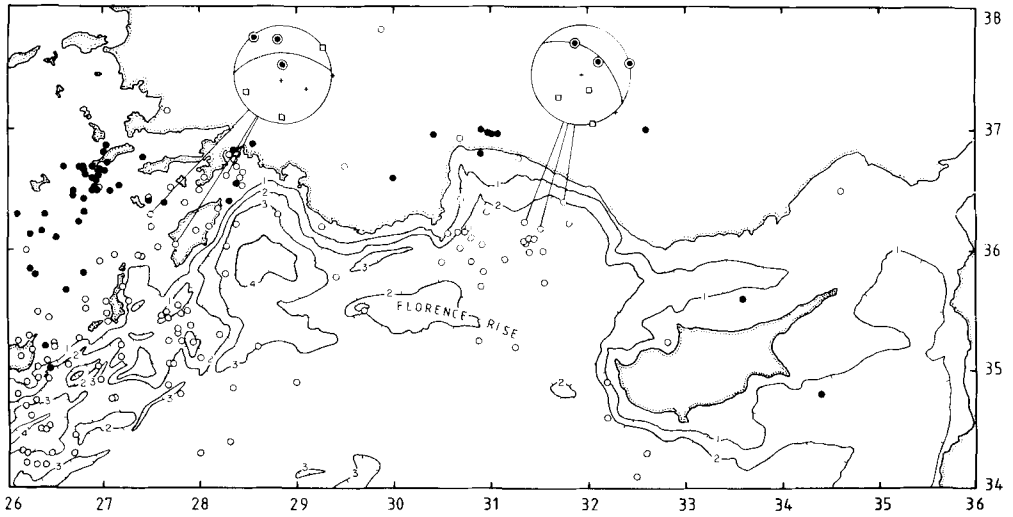

Figure 11. Epicentres reported deeper than 50 km (open circles) and deeper than 100 km (filled circles) in SW Turkey during the period 1961 January to 1980 December. Bathymetry in kilometre intervals is from Morelli, Pisani & Gantar (1975). Also shown are the projections of the *P*-axes (squares), *T*-axes (bull's-eyes) and null axes (crosses) of the subcrustal shocks near Rhodes and Antalya Bay, with the approximate dip and strike of the inclined seismic zone in each case. Those shown in Antalya Bay are 1977.6.1, 1979.5.28 and 1979.12.31 (Figs 2, 7 and 8). Those near Rhodes are 1961.5.23 and 1965.11.28 (see I) and 1977.11.28 (Fig. 8j). 1961.5.23 was misplotted in western Turkey in I and McKenzie (1978a).

in both fig. 22 of I and fig. 5 of McKenzie 1978a.) Fig. 11 should be viewed together with Fig. 7 (which shows the better located events) and Fig. 6.

The lack of reliably located seismicity to the west and SE of Antalya Bay makes any connection of this intermediate depth zone with Cyprus or Rhodes conjectural at best. The motion at the eastern end of the Hellenic Trench system is predominantly strike-slip (see McKenzie 1978a), accounting perhaps for the lack of intermediate depth seismicity further NE on land. East of Rhodes, shallow thrusting is seen both seismically (1969.1.14) and in reflection profiles (Jongsma & Mascle 1981). Seismic reflection profiles across the Florence Rise (Woodside 1977) show fold and diapiric structures similar to those on the Mediterranean Ridge (Tanner 1983) and it is possible that both structures represent shortening in sediments decoupled from their underlying basement, which is being subducted. The connection with Cyprus is also obscure. There are not many earthquakes large enough to view their locations with confidence and we were not able to verify the depths of the few isolated apparently intermediate depth shocks. In a general way the seismicity and bathymetry follows the southern coast of Cyprus (see also Fig. 1) which is known historically to be the most active part of the island (Ambraseys 1965; Mercier, Vergeley & Delibassis 1973). Cominiakis & Papazachos (1972) give two focal mechanisms for earthquakes south of Cyprus. Both show thrusting, which is indeed likely, but both shocks are small and these are poor quality solutions.

The almost total absence of seismicity between Cyprus, the Gulf of Iskenderun and the Levant coast makes any association between the East Anatolian Fault, the Dead Sea Rift and the Antalya–Cyprus system speculative. The Kyrenia mountains in northern Cyprus continue NE towards the Gulf of Iskenderun as a submarine morphological feature visible on reflection profiles (Evans *et al.* 1978). Ben-Menahem *et al.* (1976) offer fault plane solutions for several earthquakes in the Dead Sea Rift system showing the expected north–south

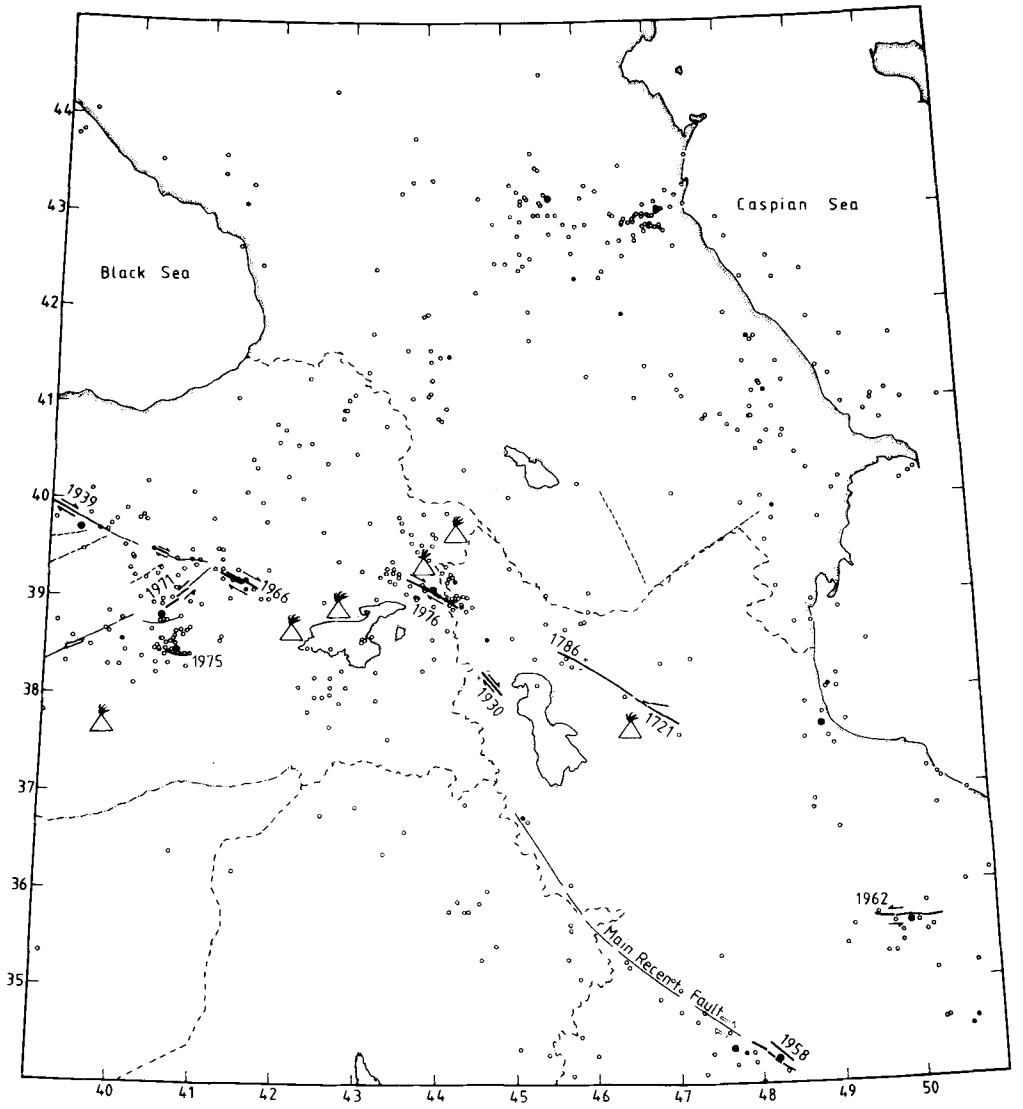

Figure 12. Epicentres of all shocks reported in eastern Turkey, NW Iran and the Caucasus during the period 1961 January to 1980 December. Symbols as in Fig. 6.

strike-slip solutions with east–west striking thrust faults in the Palmyra transverse fold belt. However, all these events are smaller than m_b 5.0 and their mechanisms rely on a small number of first motions combined with surface-wave analysis. These solutions are not of the same quality as the rest in Fig. 7, and so we have not included them, even though their mechanisms are not surprising and show the left lateral motion on the Dead Sea Rift known geologically and demonstrated to be related to opening in the Red Sea (see, e.g. Freund 1965). At present it is probably reasonable to assume an extension of the East Anatolian Fault system SW towards Cyprus, though it could involve strike-slip, thrusting or both. There is little modern seismicity to illuminate the connection between the East Anatolian and Dead Sea Faults, presumed from the work of Arpat & Şaroğlu (1975) to be near

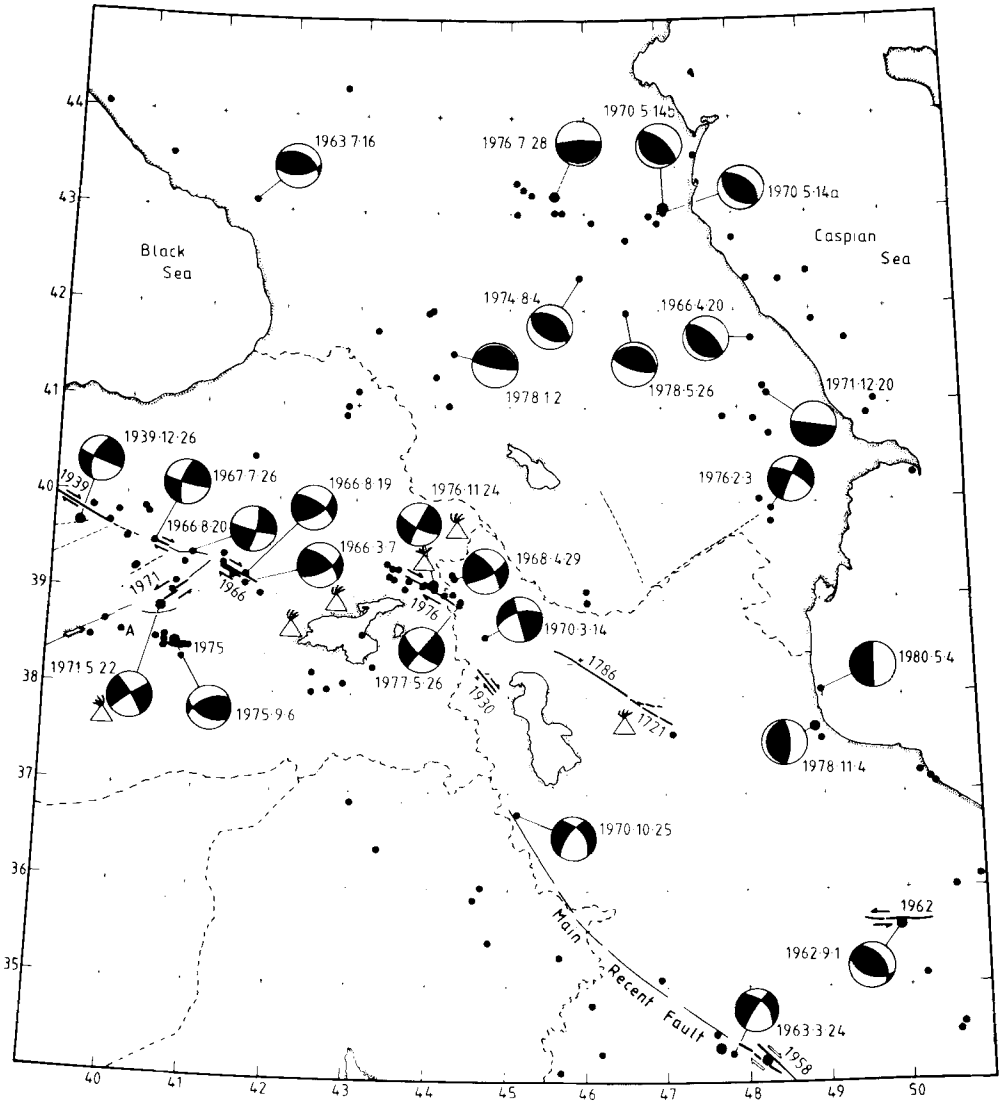

Figure 13. Epicentres of the larger shocks from Fig. 12. Symbols as in Fig. 7. New fault plane solutions are shown in Fig. 14 (see Table 1).

Kahramanmaraş (37.5°N, 36.8°E). In 1756 large earthquakes on the Dead Sea Fault Zone were associated with about 100 km of surface faulting in the Bekaa–Zebadani valleys, extending as far north as about 36.4°N (Ambraseys, private communication).

Offshore reflection profiling north and NE of Cyprus (Woodside 1977; Evans *et al.* 1978) reveals two asymmetric basins, the Cilician and Antalyan Basins, with very thick sedimentation on their northern sides coupled with general northwards tilting. The resolution of these profiles was not good enough to distinguish faulting and it is not yet possible to assess whether the Antalya and Cilician Basins are tectonically controlled; perhaps subsiding as a result of normal faulting and stretching as their south-western boundaries override the eastern Mediterranean seafloor by thrusting, in a manner similar to

that now occurring in the Aegean. If this is so, the rates of motion involved are presumably smaller than in the Aegean and Hellenic Trench, where the seismicity is greater and the morphology better developed.

Several young volcanoes in Cappadoccia and the Konya Basin are very prominent on satellite images and are shown in Fig. 6. Some, such as Hasan Dağ (the third from the SW) are known from archaeological evidence to have been active in Neolithic times (Melaart 1967). Little is known about these volcanoes, though Brinkmann (1976) refers to a temporal migration from SW (beginning in the Miocene) to NE (Quaternary). They are evidently calc-alkaline in nature (Innocenti *et al.* 1975; Keller *et al.* 1977; Schleicher & Schwarz 1977) but are a long way from the present intermediate depth seismicity of Antalya Bay. Their relation to events further south is discussed in Section 10.

4 Eastern Turkey, the Caucasus and NW Iran

4.1 EASTERN TURKEY AND NW IRAN

Immediately east of the junction of the North and East Anatolian Faults, fault plane solutions show a significant degree of thrusting as well as right lateral strike-slip (Figs 12 and 13). This change in mechanism is accompanied by an abrupt change in fault morphology (Allen 1969) from a single straight fault to shorter discontinuous segments, the change occurring between the Varto mainshock of 1966.8.19 and its major aftershock of 1966.8.20 (see also Ambraseys & Zatopek 1968; Wallace 1968). South of the projected continuation of the North Anatolian Fault thrust faulting is seen, such as in the Lice earthquake of 1975.9.6, where motion occurred on a north-dipping thrust about 20 km long (Arpat 1977a). Such faulting agrees well with the fault plane solution in Fig. 8(f). Long-period body waves of this shock have been studied by Eyidoğan (1980) and Nabelek (private communication) who found a shallow focal depth of about 10 km and a moment of 7.9×10^{25} dyne cm. South of the Lice earthquake is a young fold system striking east–west, which looks very similar to the Zagros folds on satellite images, and on which is scattered seismicity (Figs 12 and 13 and Plate 4). It is probable that, as in the Zagros, these folds cover active thrusts at depth. The north–south shortening involved in this folding and thrusting is representative of the expected direction of convergence between Arabia and Eurasia (see I).

The Chaldiran earthquake of 1976.11.24, with a fault break 55 km long (Arpat 1977b; Toksöz, Arpat & Saroğlu 1977), demonstrates that right lateral strike-slip continues east of the junction of the North and East Anatolian Faults into Iran. Our fault plane solution for this earthquake agrees well with that of Toksöz, Nabelek & Arpat (1978) as well as with the observed surface faulting. The body waves for this complicated event have been studied by Stewart & Kanamori (1982), who confirm its shallow focal depth. A smaller shock with a very similar mechanism occurred on 1977.5.26 at the eastern end of the Chaldiran fault zone. Berberian (1977) has shown that the young faults in the epicentral region of 1968.4.29 trend NW, and it is likely that this shock also involved right lateral strike-slip on a north-westerly fault. Further south, the Salmas earthquake of 1930.5.6 has been investigated in some detail (Tchalenko & Berberian 1974; Ambraseys & Melville 1982) and is known to have involved right lateral strike-slip with a normal faulting component downthrown to the NE. This is of considerable interest because such a mechanism is identical to that of the two available fault plane solutions of 1970.10.25 and 1963.3.24 further south on the Main Recent Fault, a structure on which, according to Tchalenko & Braud (1974), recent motion has been predominantly right lateral. It is thus probable that plane 1 was the fault plane in each case (Figs 14d and 22a). No epicentral data are available for 1970.3.14, a small shock which does not have a well-controlled solution. The two catastrophic earth-

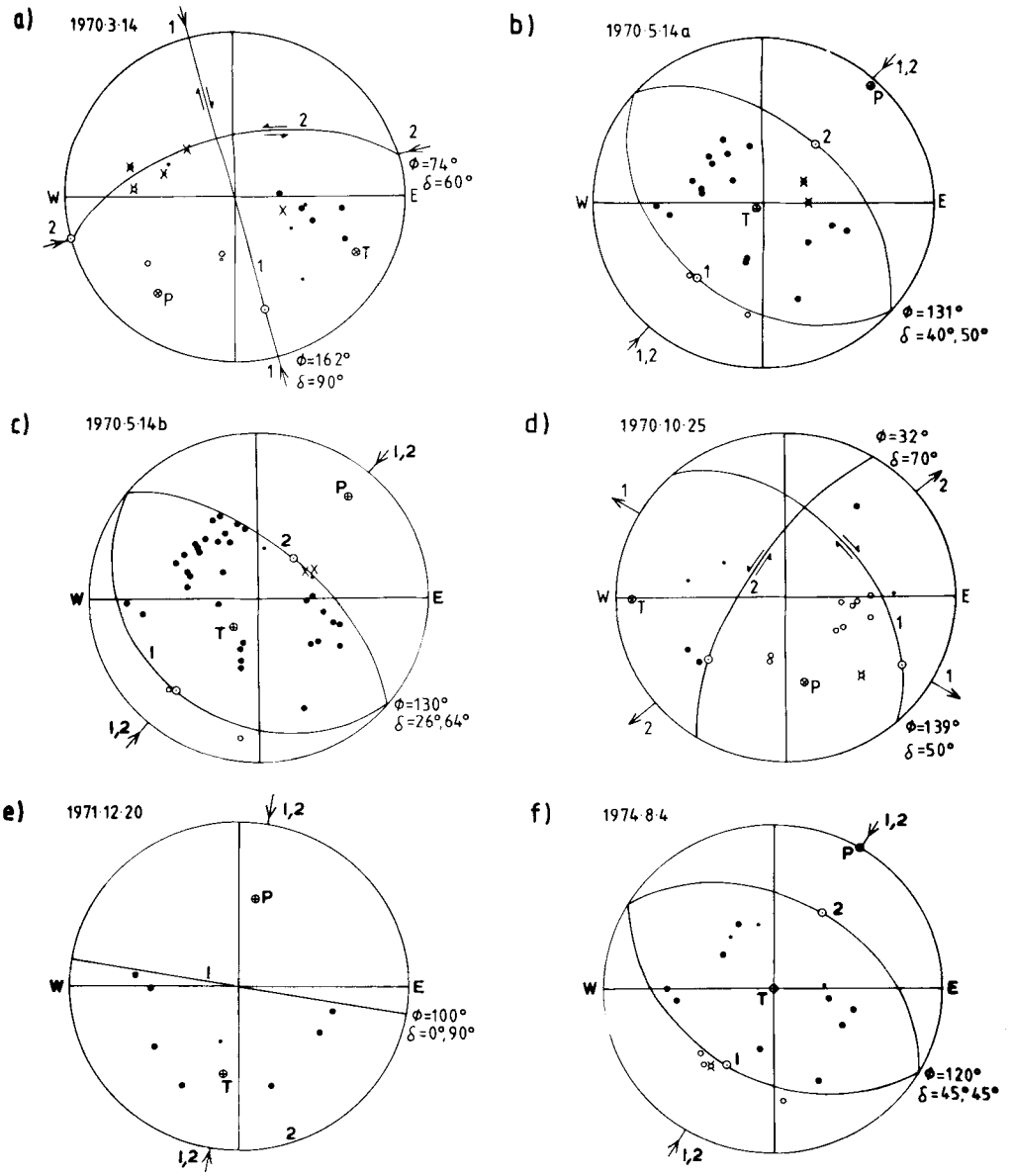

Figure 14. New fault plane solutions in eastern Turkey and the Caucasus, shown in Fig. 13. Symbols as in Fig. 2. All except (c) were plotted with a crustal velocity at the focus. All polarities are consistent with the nodal planes drawn.

quakes of 1721 and 1786, responsible for the destruction of Tabriz, involved substantial motion on a fault trending NW for about 150 km. These earthquakes have been studied by Berberian & Arshadi (1976) and Ambraseys & Melville (1982), who agree that the SW side of this fault was downthrown, but disagree on whether it was accompanied by right lateral strike-slip motion; which Ambraseys & Melville (1982) regard as doubtful. Tchalenko (1977) refers to stream diversions visible on aerial photographs that suggest young right lateral offsets on this fault, but these offsets were not verified on the ground.

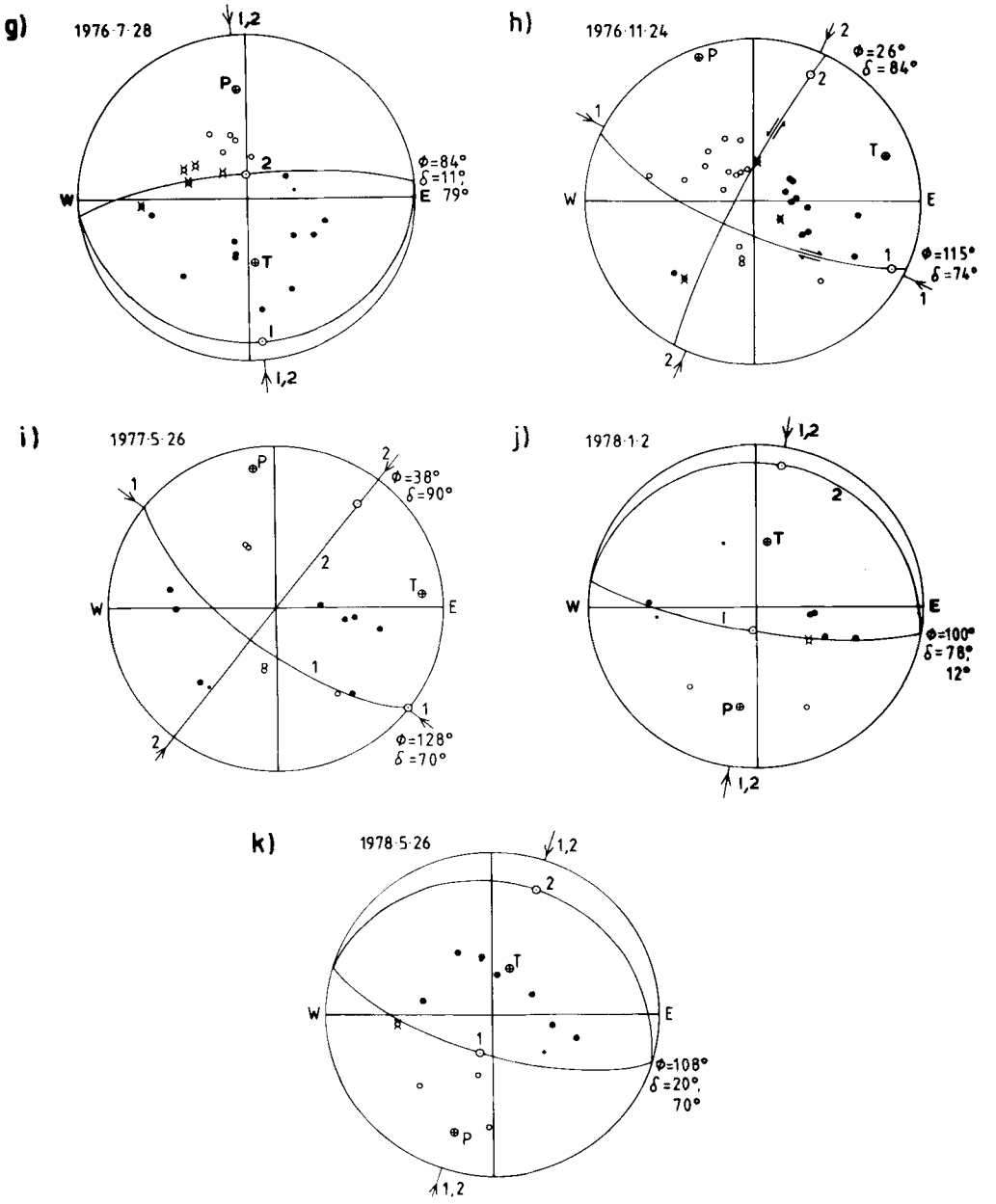

Figure 14 – *continued*

This evidence suggests that the right lateral motion of the North Anatolian Fault extends into Iran, but as discontinuous segments rather than a single fault. There is also a large change in strike of the slip vector, from ESE west of Karliova to SSE further east. This change appears to be accompanied by the development of a normal faulting component, seen in the mechanisms of 1970.10.25, 1963.3.24, the surface faulting at Salmas in 1930, and possibly the Tabriz earthquakes of 1721 and 1780 as well. In the Van region, Tchalenko (1977) refers to minor faults and lineations trending NE which are visible on

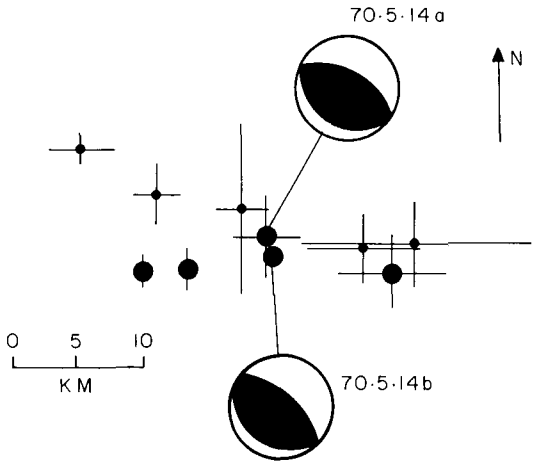

Figure 15. The Dagestan sequence relocated relative to 1970.5.14b (ISC location: 43.090°N 47.070°E) using the technique of Jackson & Fitch (1979). Error bars are shown. Large symbols have at least 55 arrival times used in their relocations, small have at least 33.

satellite images. Whether these lineations reflect any component of normal faulting and east–west extension in the Van region itself is uncertain. The major faults visible in the bathymetry of Lake Van appear to trend east–west (Wong & Finckh 1978). Little is known about the remarkable NE lineation of volcanoes in the Van area, though Innocenti *et al.* (1976) report a change from calc-alkaline to alkaline activity about 6 Ma ago. Except for the volcanoes and the rather uncertain evidence from minor faults with unknown senses of movement, there is no direct evidence for east–west extension in the Van region. The lack of geophysical data, particularly pertaining to crustal thickness, makes any such inference no more than plausible at the moment.

One of the most obvious features of Figs 12 and 13 is the lack of seismicity in the region between Rezayieh and the Buyin Zara earthquake of 1962.9.1. We refer to this region later as the Azerbaijan Block. It contains few obvious lineations visible on satellite images or on the ground and appears to have had low levels of historical seismicity. It may be one of the few relatively aseismic areas in Iran, and is discussed in Section 10.

4.2 THE CAUCASUS

In the northern Caucases several new fault plane solutions have become available since 1969, though mostly in the eastern part. With the exception of 1974.8.4 all solutions in the eastern Caucasus have one well-controlled steeply dipping nodal plane. If this is the auxiliary plane in each case, it would imply that the high Caucasus involves shallow underthrusting dipping towards the highest mountains on each side. This notion is in good agreement with the topography, the highest peaks being in a line trending NW between the epicentres of 1966.4.20 and 1978.5.26. There are no reliable reports of surface faulting of definite tectonic origin in the Caucasus, though there are several references to ground cracks and fissures of an unspecified nature, which may be attributable to landslides (Kirillova *et al.* 1960; Sadovski 1981). Trifonov (1978) describes several examples where Holocene reverse faulting and thrusting can be seen in outcrop, particularly in the southern Caucasus. The thrusting apparently follows the east–west trend of the fold axes in the region and is occasionally accompanied

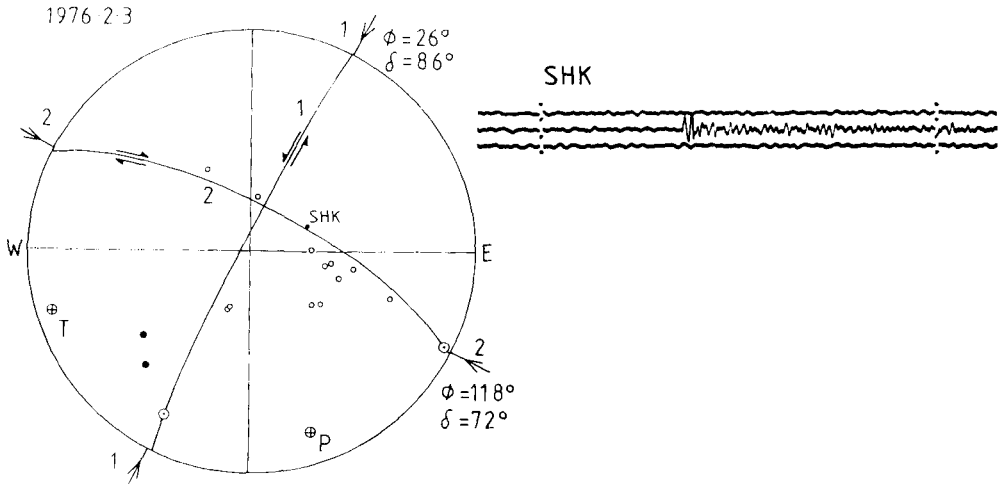

Figure 16. Fault plane solution for 1976.2.3 in the southern Caucasus. The long-period polarities allow both normal and strike-slip solutions to be drawn. However, at SHK, where the long-period onset was too small to be read, the impulsive short-period onset, whose arrival time agrees with that predicted by the J–B tables, favours the strike-slip solution.

by a SE dextral or NE sinistral strike-slip component. In the region of 1970.5.14a and b abrupt changes in alluvial slope can be seen on satellite images (Plate 2) and may be caused by thrusting dipping south. There is abundant evidence of vertical movement on the Caspian shore; such as a caravanserai built 800 years ago which was submerged in Baku Bay and is now uplifted (Kirillova *et al.* 1960), but these cannot be distinguished from possible sea-level variations. The large earthquake in Dagestan on 1970.5.14b was preceded by a foreshock (1970.5.14a) with a moment an order of magnitude lower (North 1977). Although the two shocks have similar body-wave magnitudes (about 5.6) their surface-wave magnitudes differ (5.5 and 6.5; North 1977), reflecting the difference in long-period radiation and moment. The fault plane solutions for both shocks are similar (Fig. 14b, c), though 1970.5.14b is drawn with a mantle source velocity to put the two nodal readings in the NE near a nodal plane. The solution for 1970.5.14a is drawn with a crustal velocity at the focus, though, because of the uncertainty in actual source velocity, we do not regard the difference between these two solutions as well constrained. The locations of these two events could not be distinguished with teleseismic arrival time data using the relative location techniques of Jackson & Fith (1979) which constrain the foreshock to be within about 5 km of the mainshock, perhaps on the same fault. The aftershocks of these events extended in a roughly WNW direction (Fig. 15). This sequence is discussed by Shteynberg *et al.* (1974) who make no reference to surface faulting. However, Sadovski (1981) mentions deep surface fissures and motion 'of the top of one of the mountains on the right side of the River Sulak by about 200 (sic) metres'. Further west the activity continues along the northern shore of the Black Sea, possibly with the shallow nodal plane dipping north in 1978.9.3 as the fault plane (Figs 8k and 5). To the east the seismicity crosses the central Caspian (Fig. 1) but no fault plane solutions are available in this zone.

In the SE Caucasus Chandra (1981) reported a normal faulting solution for a small (m_b 5.2) shock on 1976.2.3, but gave no individual polarity readings. The long-period WWSSN polarities for this shock (Fig. 16) are also compatible with strike-slip faulting, which is confirmed by the short-period polarity at SHK. This small event is at the NE end of a

dramatic lineament trending NE, followed by the Araxes river (Plate 3). If plane 1 is the fault plane in Fig. 16, the NE slip direction would be similar to that observed in the northern Caucasus and implies left lateral motion on the Araxes lineament. The combination of right lateral faulting extending from the North Anatolian Fault system and left lateral faulting on the Iran–USSR border would cause an easterly expulsion of NW Iran away from the collision zone in the Van region. This in turn may be responsible for the shallow overthrusting of the Caspian Sea by NW Iran, seen in the focal mechanisms of 1978.11.4 and 1980.5.4 (Fig. 13). Another prominent lineament, followed by the Akera river, extends NW towards Lake Sevan from the south-western end of the Araxes lineament. There has, however, been no recent seismicity to reveal its nature.

Although many earthquakes have been reported with hypocentres deeper than 50 km in eastern Turkey, the Caucasus and NW Iran (Fig. 3), on examination these are all found to be small and recorded by poor station distributions. All the larger shocks are given shallow focal depths, and there is not yet any convincing evidence of significant subcrustal activity. An aftershock survey using local stations in the southern Caucasus found all activity shallower than 10 km (Rustanovich 1974).

5 The Alborz and Kopet Dag

The seismicity of the Caucasus extends SE across the Caspian Sea into the Kopet Dag (Figs 17 and 18). None of the earthquakes in the Caspian have been large enough to obtain a reliable fault plane solution, but the thrusting in the Caucasus and Kopet Dag as well as the folds observed by offshore reflection profiling in the sediments (Shikalibeily & Grigoriants 1980) make it likely that this seismic belt crossing the Caspian also involves a large component of thrusting.

Another belt of seismicity follows the southern edge of the Caspian Sea and also joins the Kopet Dag in the east. This belt coincides with the Alborz mountains, and, although relatively quiet during the last 20 years, has been responsible for many catastrophic earthquakes in the past (see, e.g. Ambraseys & Melville 1982). Fault plane solutions indicate predominantly thrust faulting in the Alborz, with some strike-slip mechanisms in the east. The lack of unambiguous surface faulting following most of the shocks means that only in a few solutions can the fault plane be distinguished. The 85 km length of east–west surface faulting in the 1962.9.1 Buyin Zara earthquake showed predominantly thrust faulting dipping south with a left lateral strike-slip component (Ambraseys 1963), agreeing very well with the fault plane solution given in I, and implying a NE slip vector. Although Ambraseys, Moinfar & Tchalenko (1971) were unable to recognize surface faulting caused by the Karnaveh earthquake of 1970.7.30, relative relocations of the aftershocks of this event defined an elongated pattern trending NNE (Jackson & Fitch 1979), approximately parallel to the strike of one of the nodal planes in the fault plane solution. Moreover, the position of a later shock (1974.3.7) lies within this aftershock zone and its fault plane solution shows almost pure strike-slip faulting, with left lateral motion on the plane parallel to the elongated aftershock zone. These observations suggest that the activity was on a NE-trending fault with left lateral strike-slip motion, though the 1970.7.30 shock also involved a large normal faulting component. Reports of ground deformations following other events in the Alborz, such as 1957.7.2 (Tchalenko 1973a) and the Torud earthquake of 1953.2.12 (Ambraseys & Moinfar 1977a), for which a fault plane solution showing thrusting is given by Shirokova (1962; see I), are ambiguous and the fissuring they describe may well have been by landslides.

Faulting has been reported for two earthquakes this century in the Kopet Dag. The Ashkhabad earthquake of 1948.10.5 produced a series of enigmatic tensional fissures

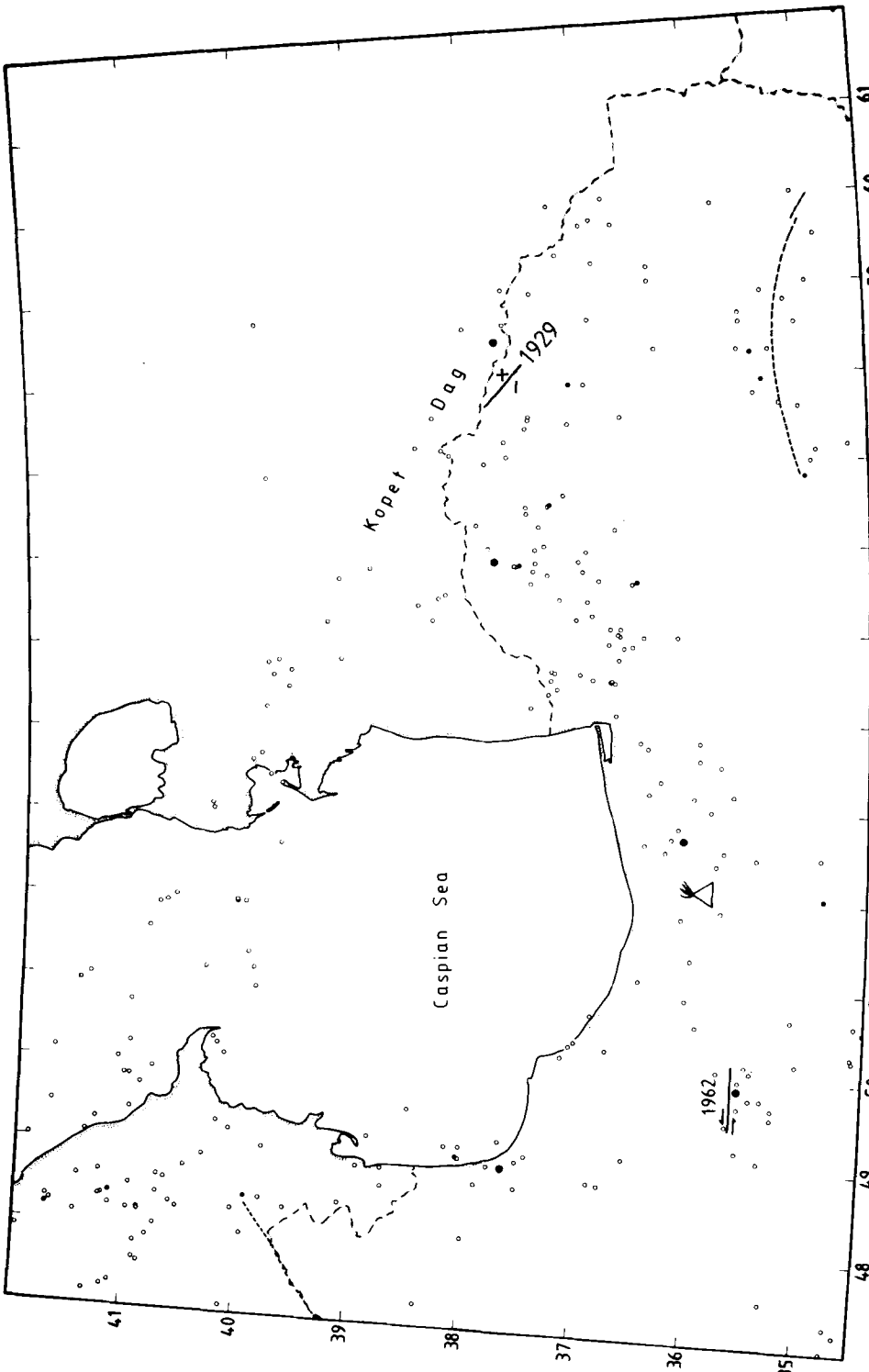

Figure 17. All epicentres reported in the Caspian, Alborz and Kopet Dag during the period 1961 January to 1980 December. Symbols as in Fig. 6.

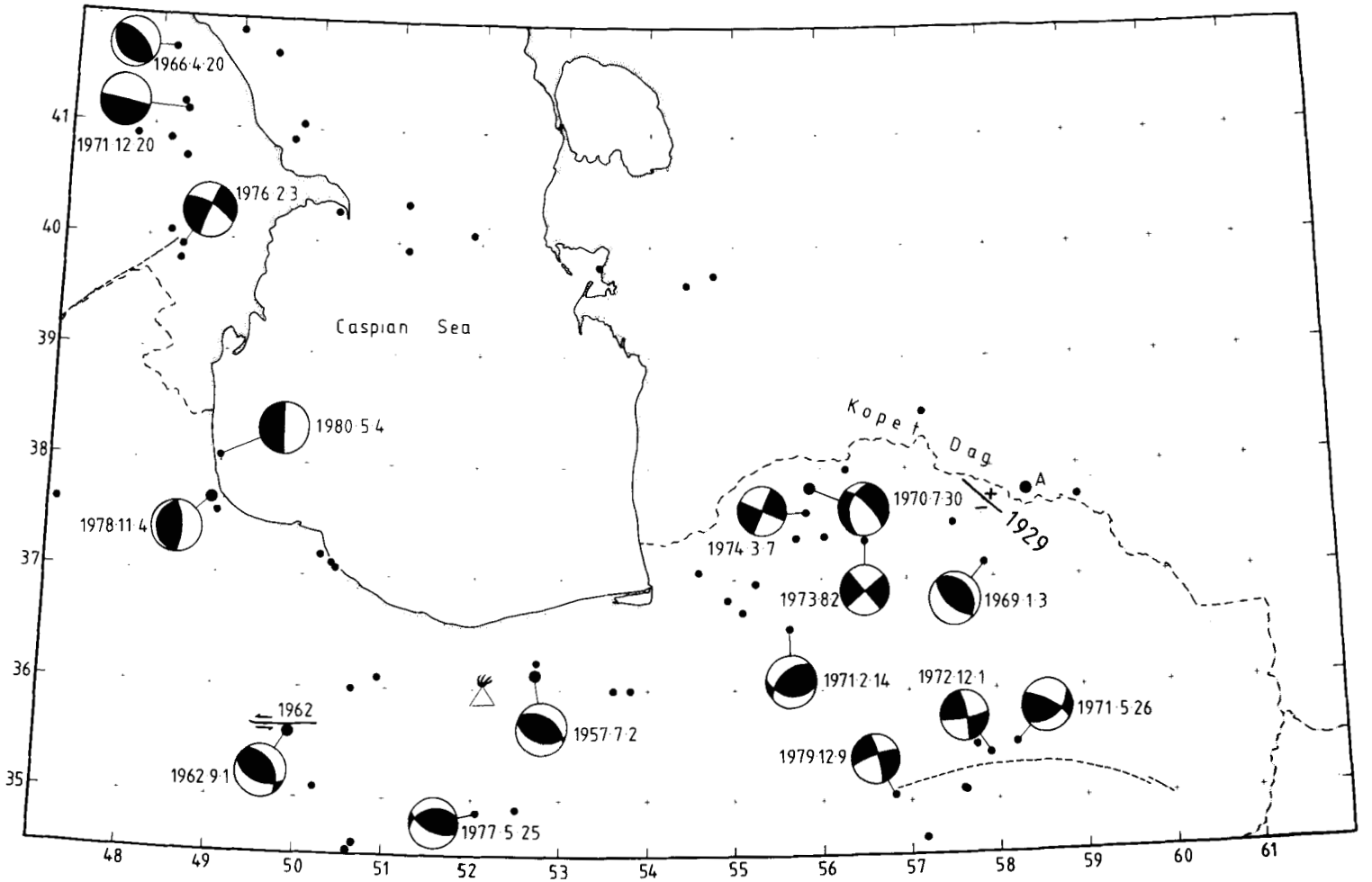

Figure 18. Epicentres of the larger shocks in Fig. 17. Symbols as in Fig. 7. New fault plane solutions are shown in Fig. 28 (see Table 1). The epicentre marked A is that of the Ashkhabad earthquake of 1948.10.5, for which a fault plane solution is shown in I.

striking NE (sic) (see Kopp *et al.* 1964 in Tchalenko 1975). A fault plane solution for this shock was presented in I and showed a thrust mechanism with an almost vertical nodal plane striking ESE and a shallow plane dipping SW. This mechanism agreed with that of Rustanovich & Shirokova (1964), who combined this solution with the results of levelling lines to show that the shallow plane dipping SW was the fault plane. None the less, the fault plane solution in I is badly constrained and has been omitted from Fig. 18, on which its epicentre is marked A. An earlier catastrophic earthquake on 1929.5.1 (Ms 7.3) occurred 50 km SW of 1948.10.5 and was associated with about 70 km of faulting with a strike of about 140°E (Tchalenko 1975; Ambraseys & Melville 1982). Motion on this fault involved uplift of about 2 m on the NE side but it is not known whether strike-slip motion also occurred.

Tchalenko (1975) gives an account of the structure and faulting observed in the Kopet Dag, based on field studies as well as *Landsat* images and aerial photographs. According to him, the structures of the Kopet Dag are separated from the stable Turan (Turkmenistan) shield on their NE border by a fault zone he calles the 'Main Fault Zone', which follows the seismicity NW to the Caspian. Measurement of sheared underground irrigation tunnels (quanats) on this Main Fault Zone apparently indicates right lateral displacement, in some places at rates of about 3–8 mm yr^{-1} (Trifonov 1971, 1978). In the eastern Kopet Dag, near the 1929 and 1948 earthquakes, Tchalenko (1975) describes SSE faults that splay off the Main Fault Zone, possibly with a right lateral component of motion. In the western Kopet Dag many NE-trending faults, which do not cross the Main Fault Zone but continue SW into Iran and the eastern Alborz, are visible on aerial photographs. Tchalenko (1975) and Sborshchikov, Savostin & Zonenshain (1981) suggest that left lateral motion occurs on these NE-striking faults, and this is supported by the mechanisms and aftershock locations of 1970.7.30 and 1974.3.7.

Most of the fault plane solutions in the Alborz and Kopet Dag shown in Fig. 18 have one nodal plane striking NW. If this is the auxiliary plane in each case, as it is in 1962.9.1 and 1970.7.30, the slip vectors in the Alborz and Kopet Dag are all directed NE (Fig. 19). This would imply a small component of left lateral motion across the Alborz mountains (as suggested in I and by Wellman 1966) and a slight right lateral component of slip in the eastern Kopet Dag, where the Main Fault Zone of Tchalenko (1975) is not exactly perpendicular to this NE compression or parallel to the Kopet Dag fold axes. The abrupt cut-off of seismicity NE of the Kopet Dag, combined with the slip vectors in Fig. 19, indicates that considerable crustal shortening must be taking place in the Kopet Dag, as Iran is compressed against the Turan shield. This shortening involves thrust faulting, left lateral strike-slip in the west, and probably right lateral strike-slip in the east. The slip vectors in Fig. 19 have a significantly greater component of easterly motion than that predicted for the overall motion between Arabia and Eurasia (see fig. 4 in I). This region of northern Iran is therefore moving in a more easterly direction relative to Eurasia than Arabia, apparently overthrusting the southern Caspian Sea and eventually shortening against the Turan shield. The overthrusting indicated by the mechanisms of 1980.5.4 and 1978.11.4 may also be responsible for the north–south zone of folding seen in the sediments off the west coast of the Caspian to the south of the Baku (Apscheron) peninsular (Shikalibeily & Grigoriants 1980).

The very great thickness (more than 25 km in places) of sediments in the southern Caspian has effectively obscured any direct information about the nature of its basement. Underneath the sediments is apparently a thick basement with P velocities of about 6.6 km s^{-1}, taken by Neprochnov (1968) and Rezanov & Chano (1969), among others, to indicate basaltic composition. The efficient propagation of S_n and poor propagation of L_g waves across the southern Caspian is cited as possible evidence for an oceanic basement by Kadinsky-Cade *et al.* (1981). In the Hellenic Trench (Tanner 1983), Makran (Section 8) and

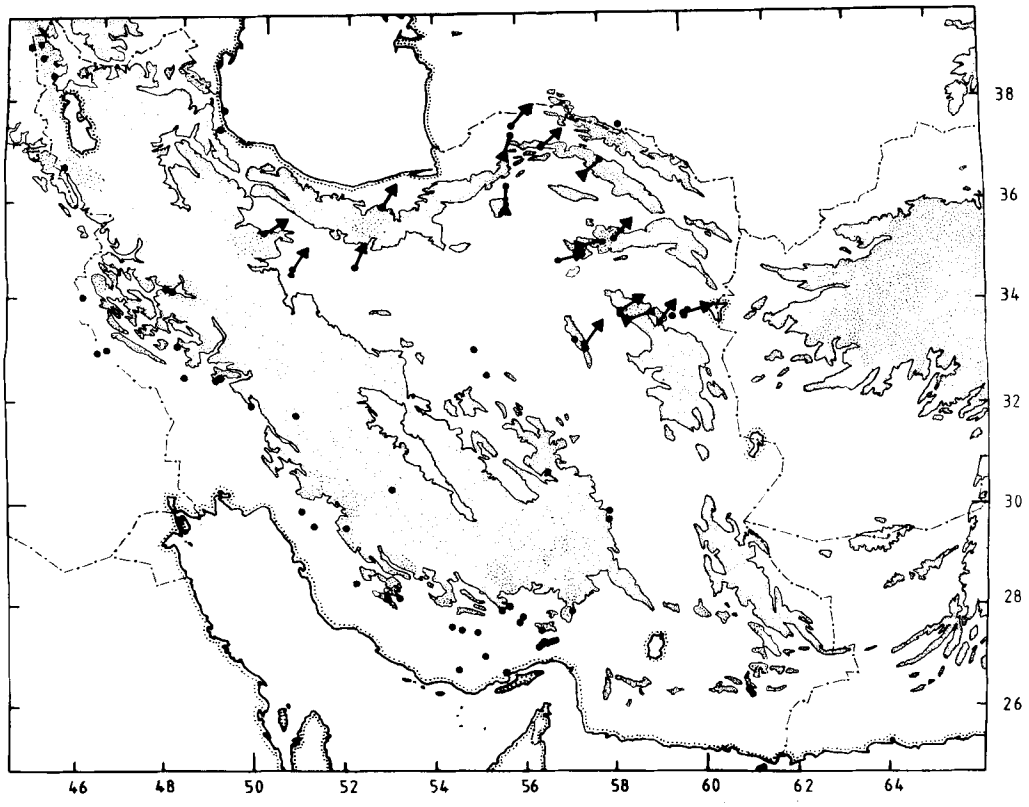

Figure 19. Topography of Iran, taken from the *Times Atlas* (1967 edition). Area above 1500 m is shaded. Filled circles are epicentres of earthquakes for which fault plane solutions are available. Arrows mark the probable slip vectors in northern Iran.

Bay of Antalya (Section 3), folding of thick marine sediments and associated shallow seismicity are seen several tens of kilometres offshore from landward-dipping intermediate depth seismic zones. Thus in places where thick sediments are being overthrust, shortening of the basement may not occur in the same place as shortening in the sediments. The scattered seismicity and folding off the south-western shore of the Caspian may be indicative of a similar process, though in this case there is no reliable evidence of accompanying intermediate depth seismicity in either the Alborz or the Kopet Dag. A local network installed in the epicentral region of the Ashkhabad earthquake and operated in 1949 and 1953 found most activity in the basement at 10–12 km depth (see Rustanovich 1957 in Tchalenko 1975). Teleseismic long-period body-wave modelling of 1978.11.4 indicates a focal depth of about 20 km (Berberian, private communication) and the short-period records of 1973.8.2 also indicate a shallow crustal depth (Fig. 4). The isolated and prominent volcano of Damavand (36°N, 52°E), with its alkaline activity continuing into Holocene times (see, e.g. Berberian & King 1981), seems not to be related to the motions occurring in the Alborz in any obvious way.

6 The Zagros mountains

The most striking feature of the seismicity following the Zagros mountains SE from the Van region is the abrupt cut-off of activity NE of the Main Zagros Reverse Fault (the 'Zagros

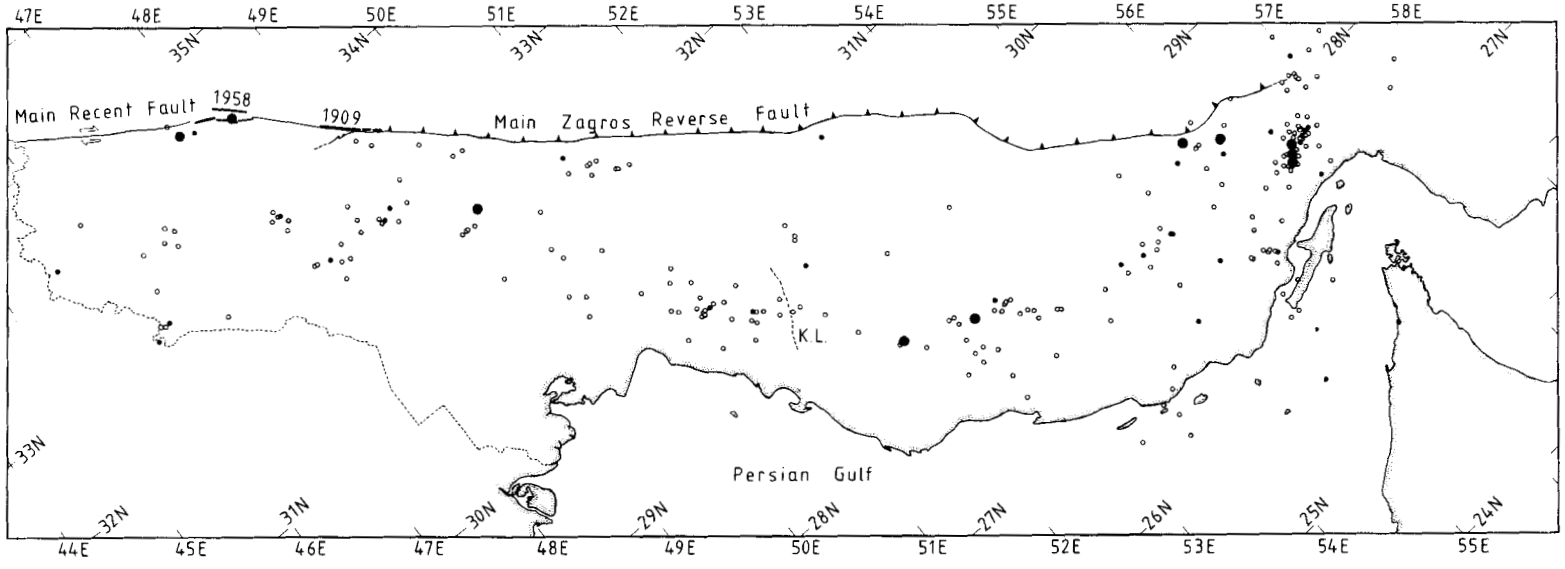

Figure 20. Epicentres of the larger earthquakes in the Zagros, with m_b 5.0 or greater or with at least 50 recording stations. For the general seismicity see Fig. 1. Large symbols are those with magnitude (m_b or Ms) 6.0 or greater. Filled symbols are those for which fault plane solutions are available in I and Fig. 21. The dashed line marked K.L. is the Kazerun Line. The Main Zagros Reverse Fault is shown by a toothed line and marks the north-eastern extent of the Zagros structures, though it is probably not active itself.

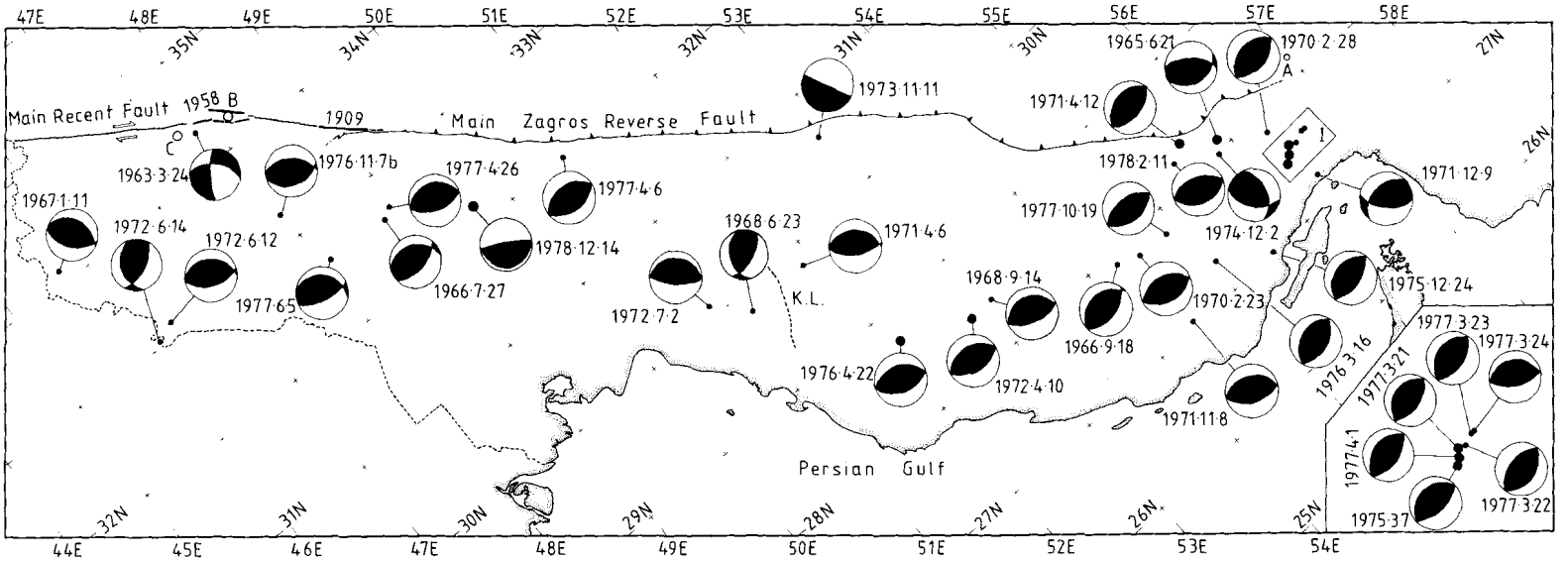

Figure 21. Fault plane solutions in the Zagros. New ones are shown in Fig. 22. Symbols as in Fig. 20. The area marked I is shown as an inset in the lower right corner. Epicentres marked A, B, C are those of 1964.12.22, 1958.8.14 and 1957.12.13 for which mechanisms are given in I and Shirkova 1967 (see Berberian 1981).

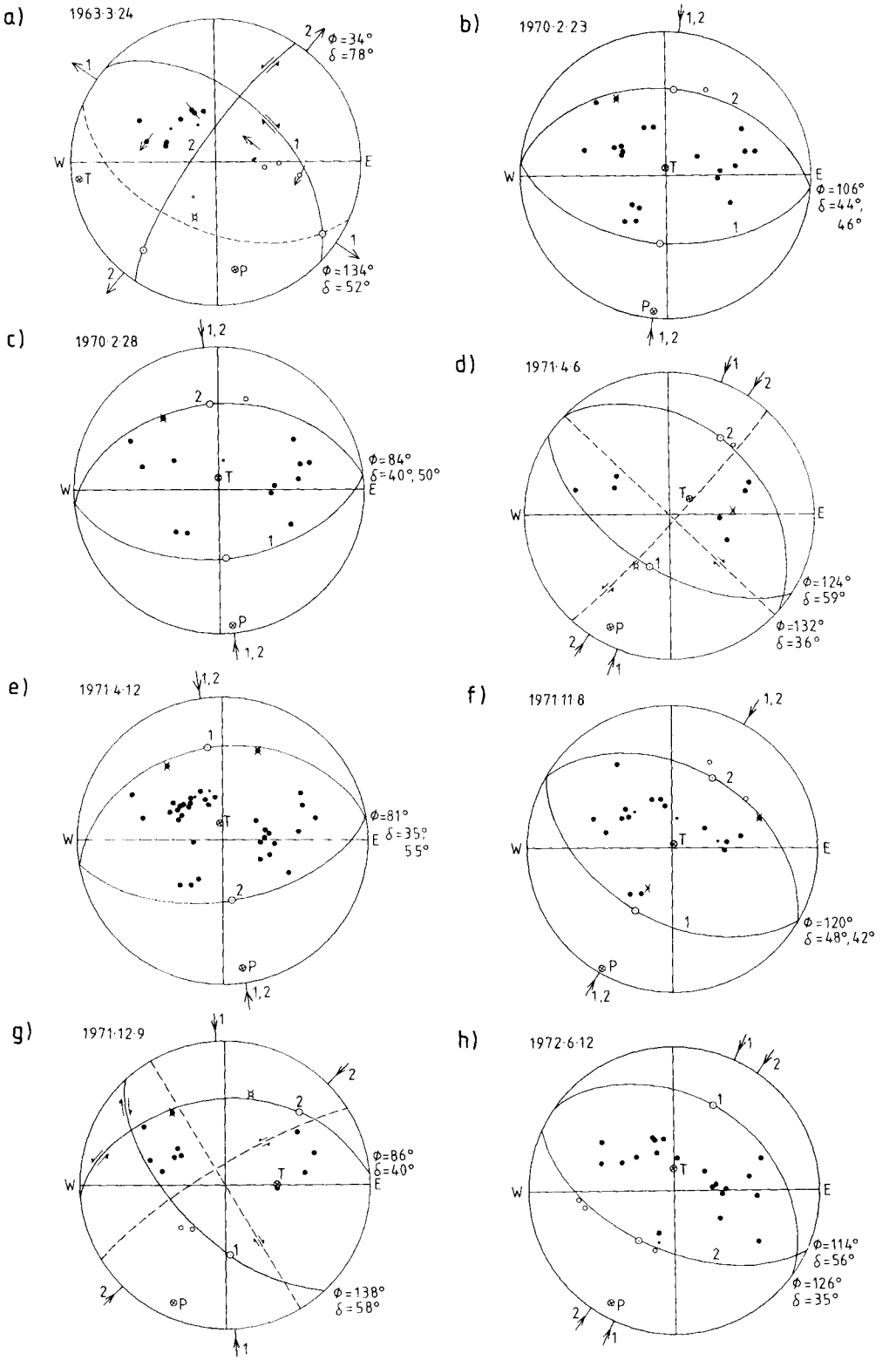

Figure 22. New fault plane solutions in the Zagros, shown in Fig. 21. Symbols as in Fig. 2. All are plotted with a crustal velocity at the focus. All polarities are consistent with the nodal planes drawn. Arrows in (a) mark the direction of first motion of *S*-waves.

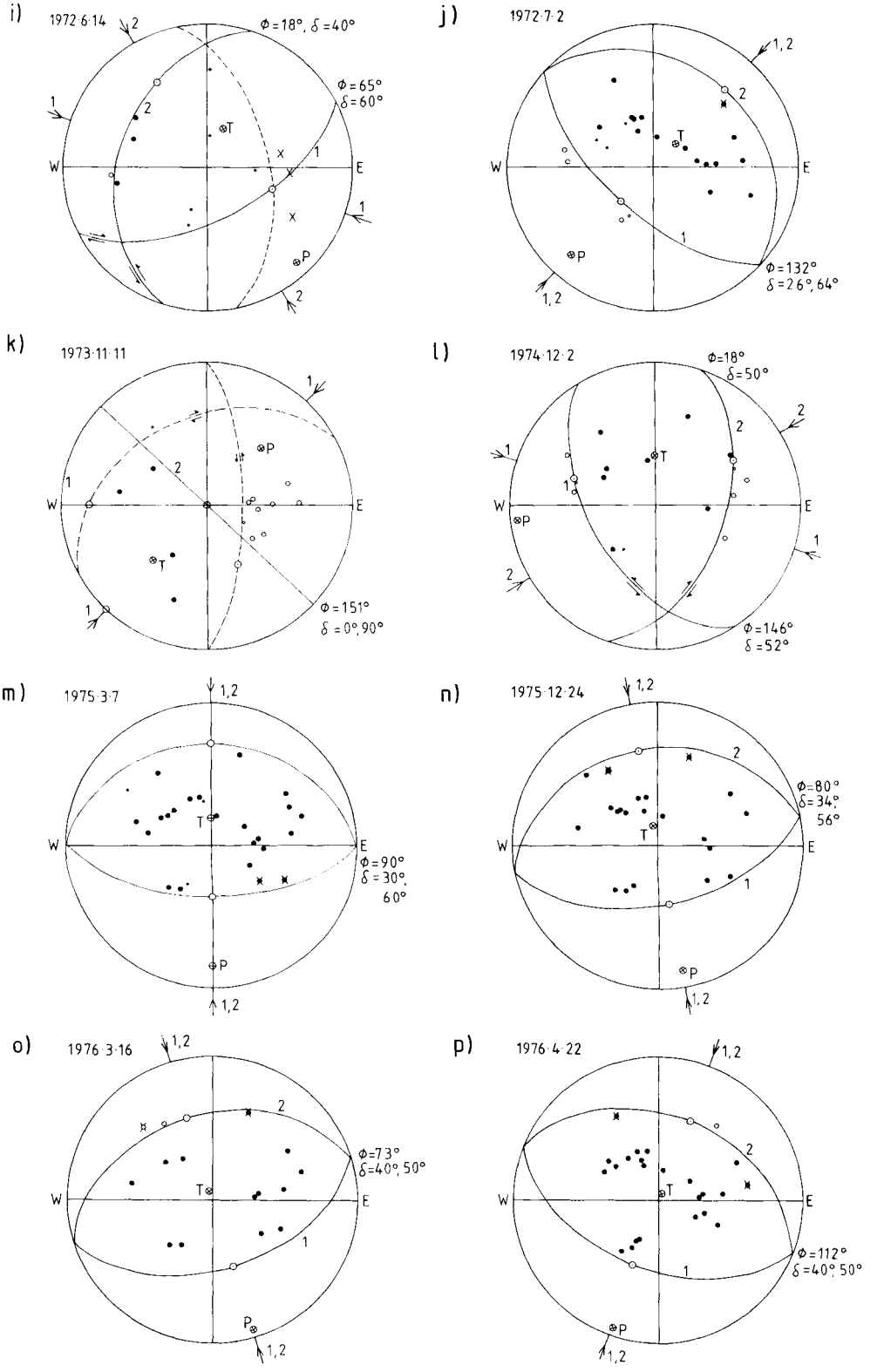

Figure 22 – *continued*

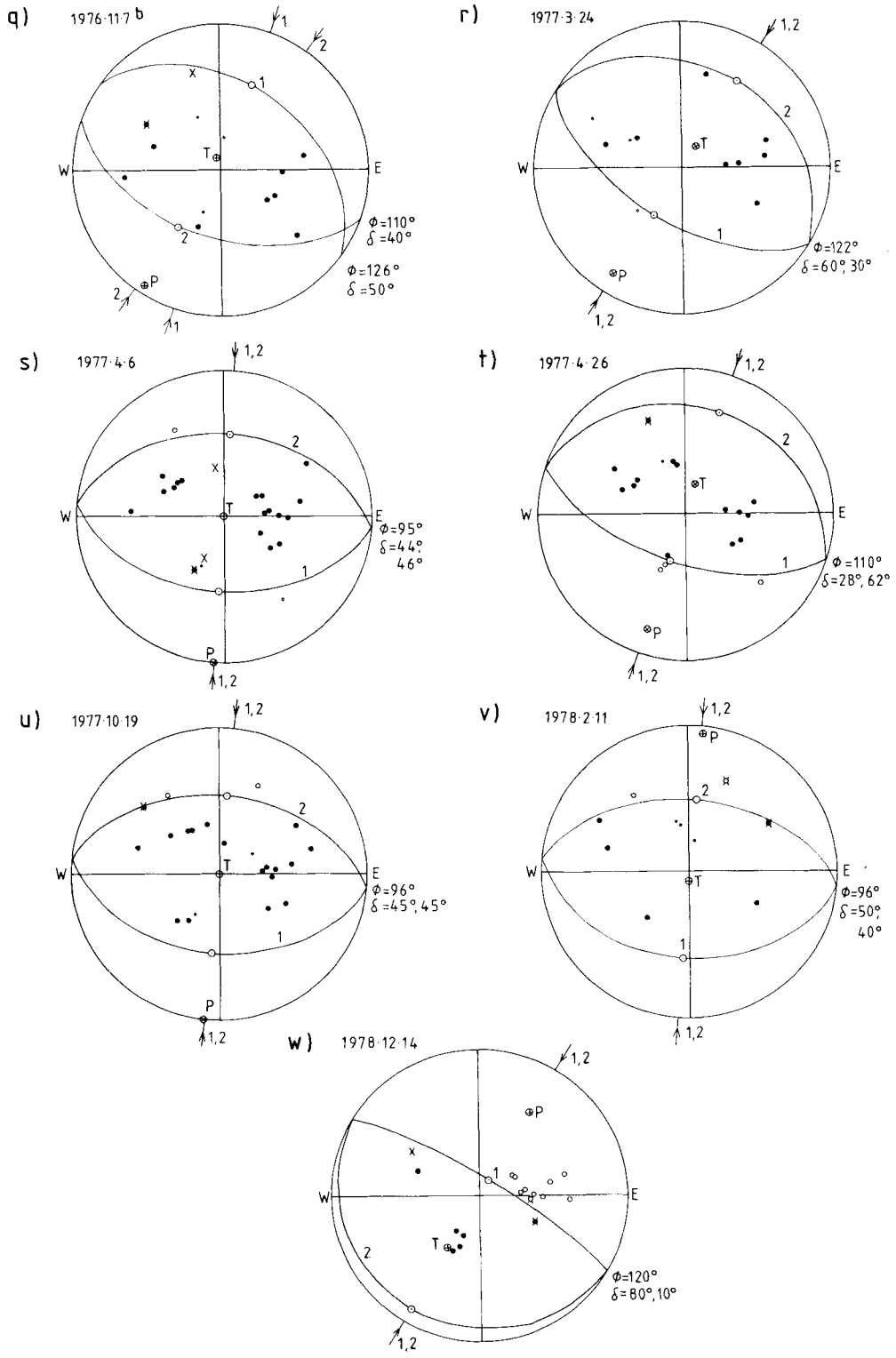

Figure 22 – *continued*

Thrust Line' of Stöcklin (1968) and others) seen in Figs 1 and 20. The Main Zagros Reverse Fault is an old geological feature, whose most recent sense of motion is that of a reverse fault (thrust), but which has been in existence since at least the lower Palaeozoic and controlled the deposition of sediments in the Mesozoic and Cenozoic Zagros basin. It also marks the NE extent of the thick infracambrian Hormuz Salt Formation (see, e.g. Stöcklin 1974; Berberian 1981, for a review). There is no surface evidence of recent thrusting on the Main Zagros Reverse Fault, although, as Berberian (1981) points out, the macroseismic epicentres of some shocks in the NW Zagros, which are too small to obtain fault plane solutions, lie on this structure.

In the NW Zagros a large active fault, called the Main Recent Fault by Tchalenko & Braud (1974), follows the trace of the Main Zagros Reverse Fault SE at least as far as 32°N, although most of the recent seismic activity on this line has been in the NW. It is on this structure that the right lateral strike-slip motion of eastern Turkey continues SE of the Van-Rezaiyeh region (see Figs 12 and 13). Several large earthquakes have been associated with the Main Recent Fault in the area east of Kermanshah (34.3°N 47.0°E), although the only fault plane solution available since the WWSSN was installed is that of 1963.3.24 (Figs 21 and 22a). Although this solution is not well constrained, it is compatible with a mechanism almost identical to those of the 1970.10.25 and 1930 earthquakes further NW (Fig. 13), involving right lateral strike-slip with a component of normal faulting. Three earlier shocks, for which Shirokova (1967) gives fault plane solutions, occurred in the same region in 1957 and 1958. Her solutions show that the earthquake of 1957.12.13 (marked C in Fig. 21) apparently involved thrust faulting with a NW strike, whereas the solution for 1958.8.14 (marked B) and 1958.8.16 (with a similar location) are compatible with right lateral strike-slip motion on a fault trending NW. The 1958 solutions were wrongly plotted in I and Jackson & Fitch (1979) but are correctly presented by Berberian (1981). It is not possible to assess the reliability of these solutions, which have therefore been omitted from Fig. 21. Of this sequence between 1957 and 1963 only the 1958 earthquakes could be unequivocally associated with surface faulting on the Main Recent Fault system, but no strike-slip component of motion could be reliably determined by the several field investigations 15 years after the event (Ambraseys, Moinfar & Peronaci 1973; Ambraseys & Moinfar 1974a, b; Tchalenko & Braud 1974; Ambraseys & Melville 1982). On the basis of the clear en echelon arrangement of fault segments, Tchalenko & Braud (1974) consider the overall late Quaternary motion on this part of the Main Recent Fault to be right lateral, which indeed seems likely. A previous large earthquake in 1909, about 100 km further SE, was associated with at least 45 km of faulting along the trace of the Main Recent Fault. Again there is no conclusive evidence of strike-slip motion, though the NE side was downthrown, in common with the mechanisms of the 1930 Salmas as well as the 1970.10.25 and 1963.3.24 earthquakes (Ambraseys & Moinfar 1973; Ambraseys 1974; Tchalenko & Braud 1974; Ambraseys & Melville 1982). The evidence presented in this discussion, though not compelling, makes it likely that the right lateral strike-slip system of eastern Turkey extends SE, probably with a small normal faulting component, through the Lake Van region and into the north-western Zagros at least as far south as 34°N.

Figs 1 and 20 show that the seismicity of the Zagros extends over most of the width of the Folded Belt; an area of thick Palaeozoic–Mesozoic–Tertiary shelf deposits warped into long gentle linear folds in the Miocene onwards (Falcon 1969). Most of the seismicity in the Folded Belt appears to occur on high angle reverse faults in the basement, with strikes approximately parallel to the SE to ESE trend of the regional fold axes. There is no evidence for subcrustal seismicity in the Zagros. Teleseismic body-wave modelling demonstrates that most of the larger earthquakes nucleate at depths of 10–20 km, below the thickness of sediments estimated from either stratigraphic or aeromagnetic data. Jackson (1980a), Jackson,

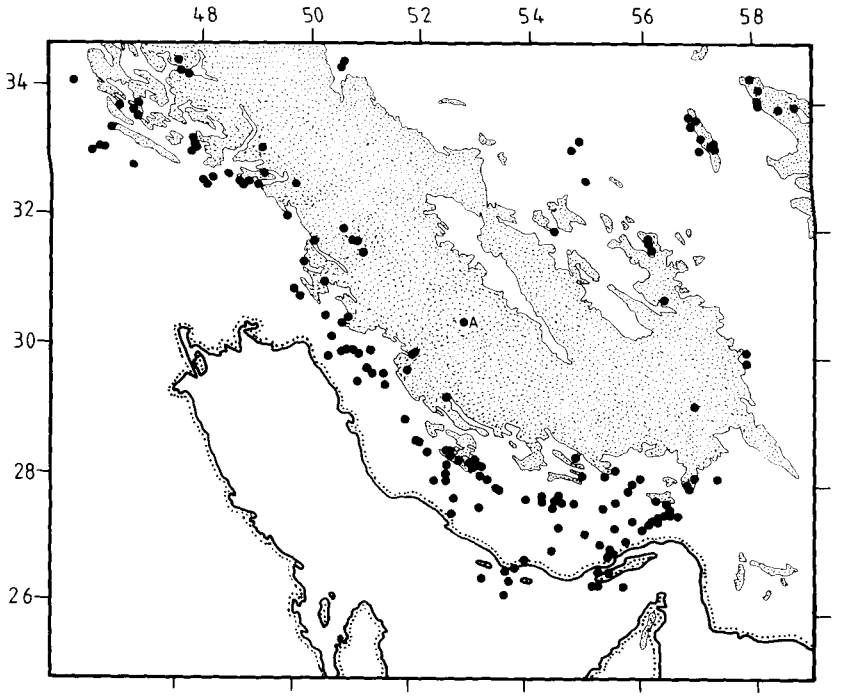

Figure 23. Epicentres of earthquakes in the Zagros with m_b 5.0 or greater, showing their relation to the topography, which is shaded above 1500 m. That marked A is the Deh Bid earthquake of 1973.11.11 (Fig. 21).

Fitch & McKenzie (1981), Jackson & Fitch (1981) and Kadinsky-Cade & Barazangi (1982) summarize this work. Microearthquake surveys by von Dollen *et al.* (1977), Savage *et al.* (1977), Niazi *et al.* (1978) and Nowroozi *et al.* (1977) confirm the lack of subcrustal seismicity and also indicate that microearthquakes do occur within the sedimentary column, presumably in response to movement in the basement underneath. The many extra fault plane solutions obtained since those reported in Jackson *et al.* (1981) do not substantially change this picture. Even though the strikes of nodal planes are not very well constrained the dips are usually required to be steep (40–50°) and so rule out the possibility of a single low angle décollement surface that is seismically active, although such a feature could be present and aseismic.

There is substantial evidence, summarized by Stöcklin (1968, 1974), Haynes & McQuillan (1974), Stoneley (1976), Murris (1980) and Koop & Stoneley (1982), among others, that what is now the Simply Folded Belt of the Zagros was a subsiding passive continental margin in the Mesozoic and Tertiary. The 40–50° dips of the active faults in the Zagros are very similar to those seen in areas of active normal faulting, such as the Aegean and western Turkey. This observation led to the suggestion that much of the seismic activity in the basement of the Zagros Fold Belt occurs as high angle reverse faulting on old, inherited normal fault planes that were responsible for the stretching and subsidence of the region in the early Mesozoic (Jackson 1980a; Jackson *et al.* 1981). The reversal of motion on old normal fault planes has been demonstrated to occur elsewhere, especially in the inverted basins of NW Europe (e.g. Stoneley 1982; Cohen 1982), but in the Zagros it remains only a plausible hypothesis. Although the NW-trending sediment isopachs in the Luristan and Kuhzistan regions of the northern Zagros suggest that subsidence occurred on basement faults of the

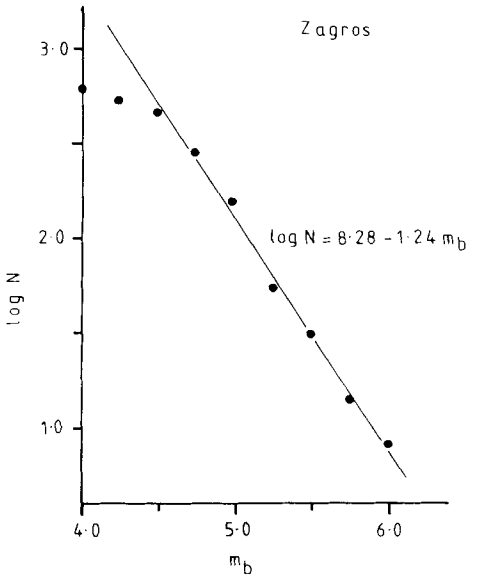

Figure 24. Magnitude–frequency plot for earthquakes in the Zagros Folded Belt between the corners: 36°N 47°E, 27°N 58°E, 25°N 56°E and 33°N 44°E. Magnitudes are m_b values reported by NOAA, USCGS and NEIS, and the time interval taken is from 1963.3.24 to 1980.12.31. *A* and *b* values are given for the straight line drawn. Note the tailing-off below m_b 4.5, indicating that detection is not complete at this level. This figure is included in this paper to emphasize that the Zagros is one of the few areas in the Middle East where the last 20 years of instrumental data are representative of longer periods. Elsewhere in the Middle East this is not the case, and plots such as this one, based on data from short recording periods, should not be used for seismic risk assessment.

same trend (Szabo & Kheradpir 1978; Setudehnia 1978; Koop & Stoneley 1982), the decoupling of the sedimentary layers by evaporite horizons, as well as repetition of sequences caused by thrust faulting in the cores of anticlines (Colmann-Sadd 1978), does not allow a straightforward reconstruction of the subsidence history from borehole stratigraphy, as was possible in extensional environments such as the North Sea (Sclater & Christie 1980). The large thickness of evaporites in the infracambrian, Jurassic and Tertiary makes it unlikely that there is a simple correlation between structures in the basement and those observed at the surface (Lees 1952; Falcon 1969). This is probably the case everywhere in the Zagros as evaporites occur at one level or another over virtually the whole region (see Berberian 1981). It is likely that the stretching which caused subsidence involved normal faults dipping predominantly away from the stable continent, i.e. to the NE, as in the Bay of Biscay (de Charpal *et al.* 1978), but there is generally no way of deciding which of the nodal planes in a fault plane solution is actually the fault plane. In the case of the Ghir earthquake of 1972.4.10 there is weak evidence that the causative fault dips NE (Dewey & Grantz 1973; Jackson & Fitch 1979). This uncertainty in the dip direction of the fault planes, together with the presence of thick evaporites, prevents a reliable association of NE-dipping basement faults with the obvious asymmetry of the Zagros anticlines, most of which have steeper flanks on the SW (Falcon 1969; Colmann-Sadd 1978). Except for the shocks on the Main Recent Fault mentioned earlier, there have been no reports of surface faulting following a Zagros earthquake. This is generally attributed to the evaporate horizons preventing fault propagation from the basement reaching the surface, which deforms by folding instead. However, as pointed out earlier, small earthquakes do occur within the sedi-

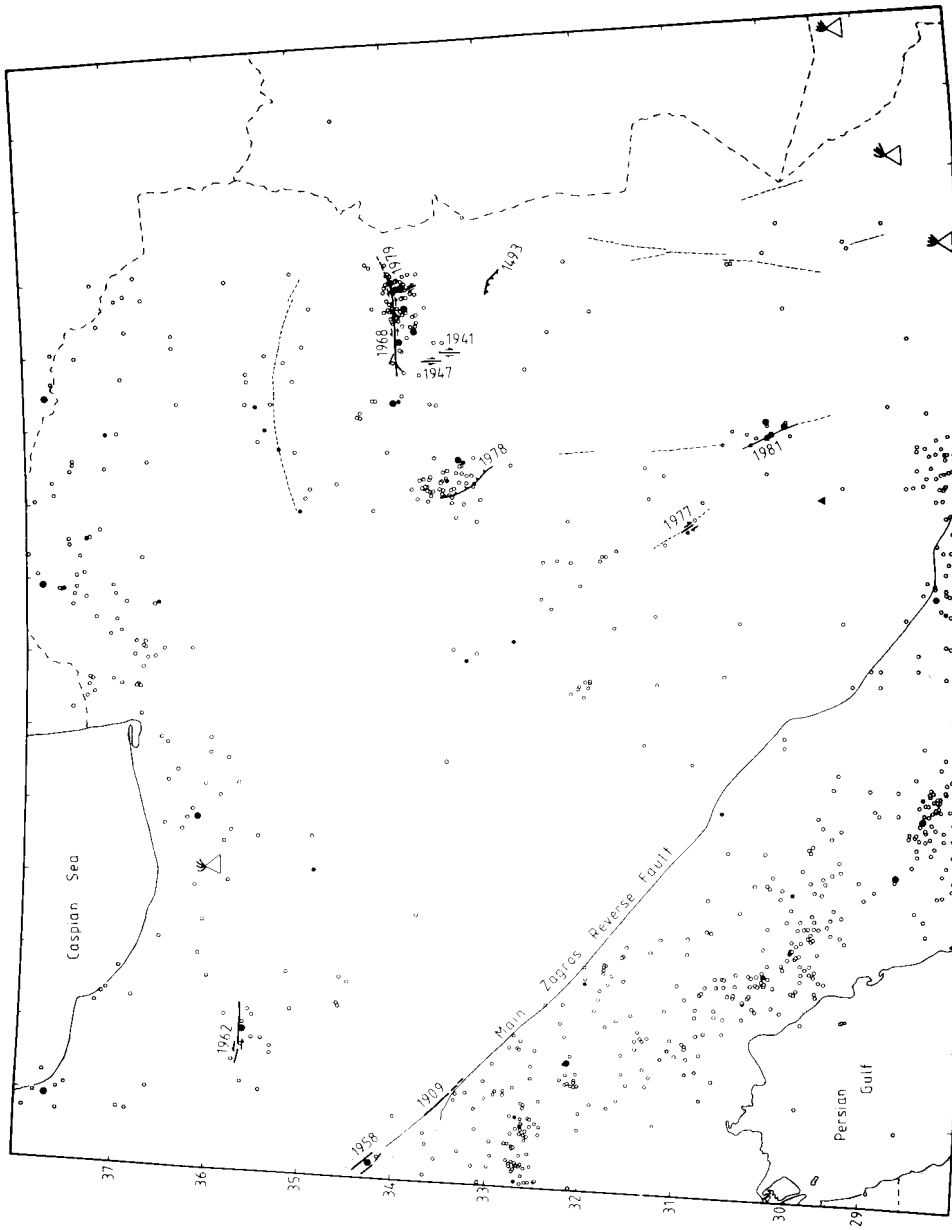

Figure 25. All epicentres reported in central and eastern Iran during the period 1961 January to 1980 December. Symbols as in Fig. 6. Note the filled triangle at 29.5°N 56.9°E marking the 1970.11.9 earthquake at a focal depth of 106 km (see Fig. 26). There is no evidence that the other apparently subcrustal locations in the area (Fig. 3) are genuine and all have been drawn as shallow.

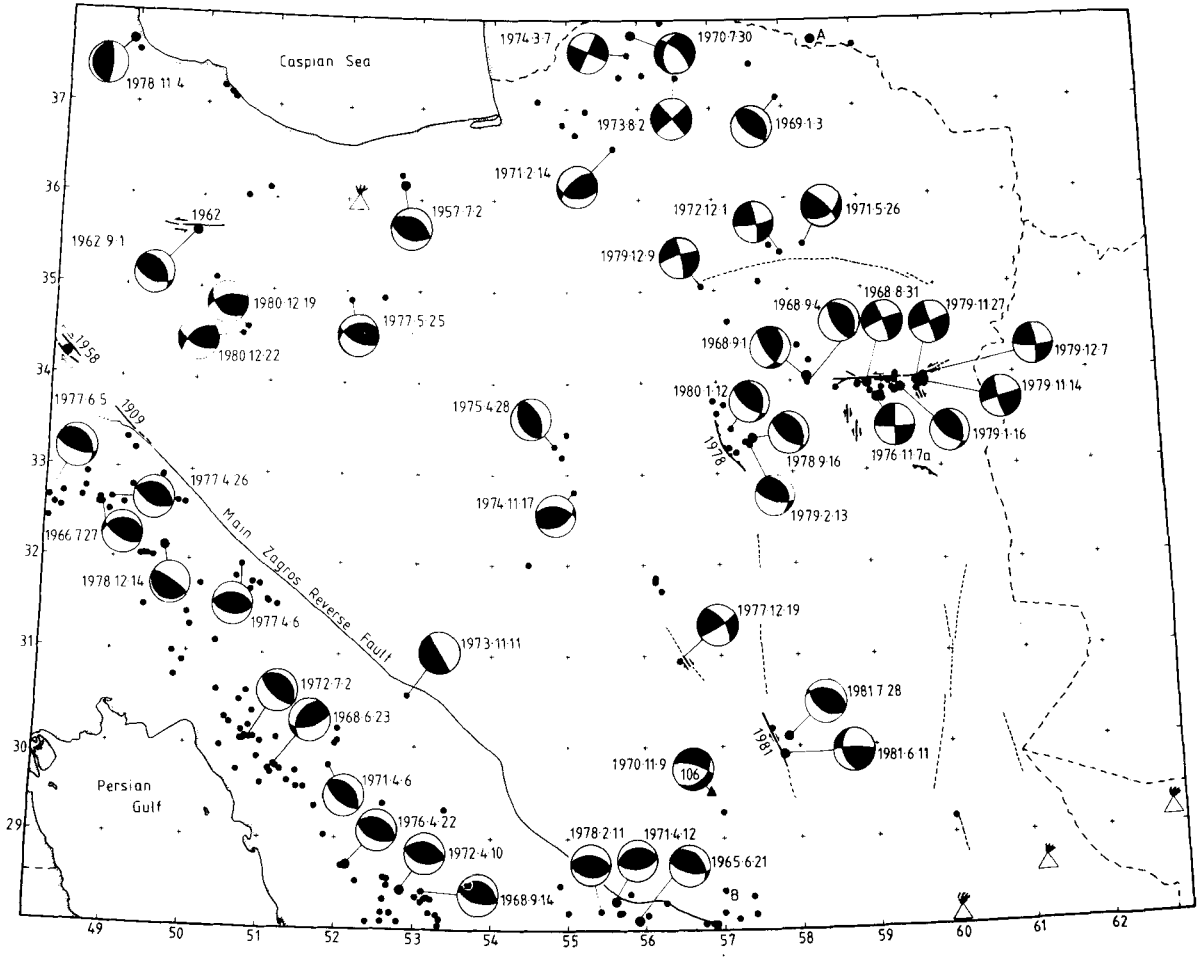

Figure 26. Epicentres of the larger shocks in Fig. 25. Symbols as in Fig. 7. New fault plane solutions are shown in Fig. 28 (see Table 1). The Ashkhabad earthquake of 1948.10.5 is marked A.

mentary column. An escarpment claimed by Berberian (1981) to have formed in the Mishan earthquake of 1972.7.2 is said by Ambraseys & Melville (1982) to have already been there in 1955.

Some of the fault plane solutions in Fig. 21 do not follow the usual pattern of high angle reverse faulting parallel to the regional fold axes. A few, such as 1978.12.14, have one almost vertical nodal plane. Three events, on 1972.6.14, 1968.6.23 and 1974.12.2 show thrusting perpendicular to the strike. These three were not large earthquakes (see Table 1) and presumably are not representative of the overall regional slip vector, which is clearly between north and NE over most of the belt. None the less, because they were unusual, these solutions were checked with great care. At stations controlling the strikes of the nodal planes, particularly those recording dilatations to the west at HLW (Helwan), JER (Jerusalem) and EIL (Eilat), first motions on vertical component instruments were checked for consistency with those on the horizontal instruments. The station polarity was then independently checked by looking at the first motions from thrust events in the western Pacific that occurred near the same date. Middle Eastern stations, being in the middle of the radiation pattern for these thrusts, should all show compressional first motions. These tests confirm the anomalous mechanisms of these three events in the Zagros. Our solution for 1968.6.23 is incompatible with that of Nowroozi (1972) which shows an east–west thrust. Body-wave modelling (Jackson & Fitch 1981) confirms a shallow depth of about 8 km for this shock, incompatible with that of 30–70 km deduced by Bird (1978) from surface waves. The ISC location for 1968.6.23 places it east of its USGS location in Fig. 21, on an important structure called the Kazerun Line (marked KL in Figs 20 and 21), which crosses the Zagros with the north–south trend common in Oman (e.g. Stöcklin 1974; Haynes & McQuillan 1974). This location is supported by macroseismic evidence (Berberian 1976). There is little doubt that the Kazerun Line is an important basement structure as it has strongly influenced sedimentation in the Zagros since at least the Middle Cretaceous (Koop & Stoneley 1982). Fold axes do not cross this line and are generally thought to be offset in a right lateral sense, partly because that is to be expected from a structure oblique, in the way that the Kazerun Line is, to the direction of shortening (Falcon 1969; Haynes & McQuillan 1974; Colmann-Sadd 1978). However, the fault plane solution of 1968.6.23 requires predominantly thrusting, and although there are several other such north–south lines crossing the Zagros and apparently offsetting fold axes, such as one NW of the Ghir (1972.4.10) area (see Dewey & Grantz 1973), there is not yet any seismic evidence of significant strike-slip faulting anywhere in the Zagros except on the Main Recent Fault. One obvious explanation for shortening parallel to the strike is that it is a geometrical consequence of radially compressing a curved arc, though this is hardly adequate for the straight part of the belt in the NW.

To the NW the Zagros structures continue into Iraq and curve westwards into northern Syria, where buried anticlines are responsible for oil fields. Some anticlines similar to those in the Zagros are visible on *Landsat* images (Plates 4 and 5), and scattered seismicity (Fig.12) suggests that they too may cover basement reverse faults at depth. In the SE Zagros the fold axes and the strikes of the nodal planes in the fault plane solutions curve to the east and the seismicity extends offshore. This end of the Zagros appears to be the most active and may be moving more quickly, though there is little knowledge of the rates of motion. Vita-Finzi (1982) claims that Holocene uplift rates of 1.8–6.6 mm yr^{-1} in the Strait of Hormuz indicate a shortening, by folding, of about 29 mm yr^{-1}.

There is an abrupt change of seismicity and structure at the SE end of the Zagros along a line, called the Oman Line (Falcon 1976; Stöcklin 1974; Haynes & McQuillan 1974; Kadinsky-Cade & Barazangi 1982), that separates the Zagros from the Makran and marks the projected continuation of the Mussandam peninsular into Iran. Here the seismicity

extends NE of the Main Zagros Reverse Fault along what Kadinsky-Cade & Barazangi (1982) claim is a NE seismic lineament (see Figs 20, 21 and 25). A poorly controlled solution for an earthquake on 1964.12.22 on this supposed lineament is given in I and has been omitted from Fig. 21, on which its epicentre is marked A. Kadinsky-Cade & Barazangi also give a solution for this shock showing thrusting with an east–west strike, and a focal depth, constrained by waveform modelling, of about 18 km. They claim that the depth of seismicity increases to the NE along this lineation from about 10 to 18 km over a distance of about 100 km, but the steep dips of the nodal planes in the fault plane solutions preclude this seismicity occurring on a single shallow dipping surface. Such a small increase in focal depth, if real, is difficult to interpret, as other factors such as heat flow (Sibson 1982; Chen & Molnar 1983) are known to have an important effect. Kadinsky-Cade & Barazangi show several other fault plane solutions for shocks in Fig. 21, which are in good agreement with ours.

One striking feature of the seismicity in Figs 20 and 21 is how the epicentres of the larger shocks sweep round in an arc from 1977.10.19 to about 1972.7.2. This arc parallels the change in strike of the fold axes and approximately coincides with the position of the 1500 m contour (Fig. 23) separating the peaks of the High Zagros (about 3000 m in the south and 4000 m in the north) from the lesser topography of the Simple Folded Belt. Indeed, the ground higher than 1500 m is remarkably free of earthquakes larger than m_b 5.0 (Fig. 23) and the only fault plane solution in the High Zagros, that of 1973.11.11 at Deh Bid, has a curious mechanism (Figs 21 and 22k). The effect of topography on crustal stresses is known to be important (Dalmayrac & Molnar 1981; England & McKenzie 1982) and may cause seismicity to concentrate in regions of steep topographic gradient rather than the high mountains themselves, which may remain relatively aseismic. A similar pattern is seen in the Karakoram (Jackson & Yielding 1983). A topographic contrast of 1500 m will cause a differential shear stress in the crust of about 100 bar (England & McKenzie 1982), which is roughly the size of the stress drop observed in earthquakes. For the earthquake of 1973.11.11 two types of mechanism are possible within the first motion constraints (Fig. 22k). Neither mechanism is obviously compatible with motion on the Main Zagros Reverse Fault, near which the shock occurred. That shown in Fig. 21 may indicate a collapse mechanism caused by the high topography in the region (about 3000 m), similar to that thought to be responsible for the normal faulting found in Tibet (Molnar & Tapponnier 1978).

Whether the occurrence of several shocks along strike, such as 1972.4.10, 1968.9.14, 1966.9.18 and 1970.2.23, implies continuity of individual basement faults over hundreds of kilometres, as suggested by Berberian (1981), must remain conjectural. The lack of earthquakes larger than about M_S 7.0 with source regions larger than 30–40 km, as well as the observation that individual anticlines plunge along strike with wavelengths smaller than 100 km, perhaps make such large-scale continuity of faults doubtful. Ambraseys & Melville's (1982) study shows no evidence of historical events in the Zagros Fold Belt larger than that at Ghir (1972.4.10). Hence the period since 1963, when magnitudes were first regularly reported by NOAA, seems to be long enough to estimate seismic risk (Fig. 24). This is almost certainly not true for the rest of Iran, where Ambraseys & Melville show that the last 20 years of data are definitely not representative of longer periods.

7 Central and eastern Iran

The seismicity and fault plane solutions in central and eastern Iran are shown in Figs 25 and 26. Unlike those in the Zagros, several earthquakes in this region are associated with

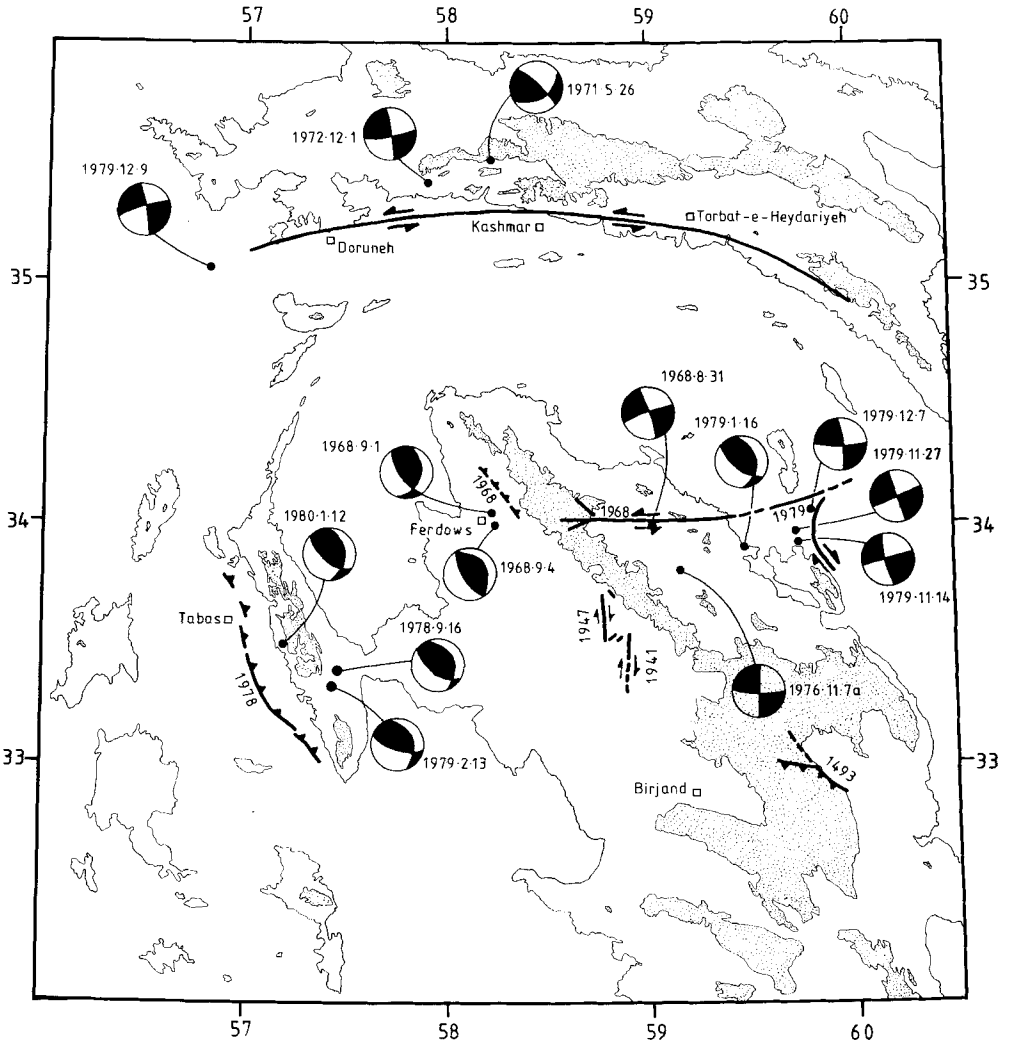

Figure 27. Fault plane solutions, faults and topography in NE Iran. Contours are at 4000 to 6000 ft and are shaded above 6000 ft (from Operational Navigation Chart G5). Except for the Doruneh Fault, whose trace is marked from satellite images, all the faults shown moved during earthquakes in the year written adjacent to them, and are taken from Berberian (1979b), Haghipour & Amadi (1980) and Ambraseys & Melville (1982).

surface faulting. The Buyin Zara earthquake of 1962.9.1 has already been discussed, and had a mechanism involving thrusting and left lateral strike-slip with a NE slip vector. South of Buyin Zara, two smaller earthquakes on 1980.12.19 and 1980.12.22 affected the area of Giv, 60 km west of Qom, and were not associated with any obvious surface faulting (Akashah *et al.* 1980). They have mechanisms that require thrust faulting (Fig. 28q, r). The fault plane solution for 1980.12.22 is well constrained and, if plane 1 is the auxiliary plane, has a north-eastern slip vector, similar to that of 1962.9.1. The north-eastern elongation of isoseismals in the epicentral region of these earthquakes (Akashah *et al.* 1980) makes such a choice reasonable; but this could have been caused by the relative locations of the two shocks.

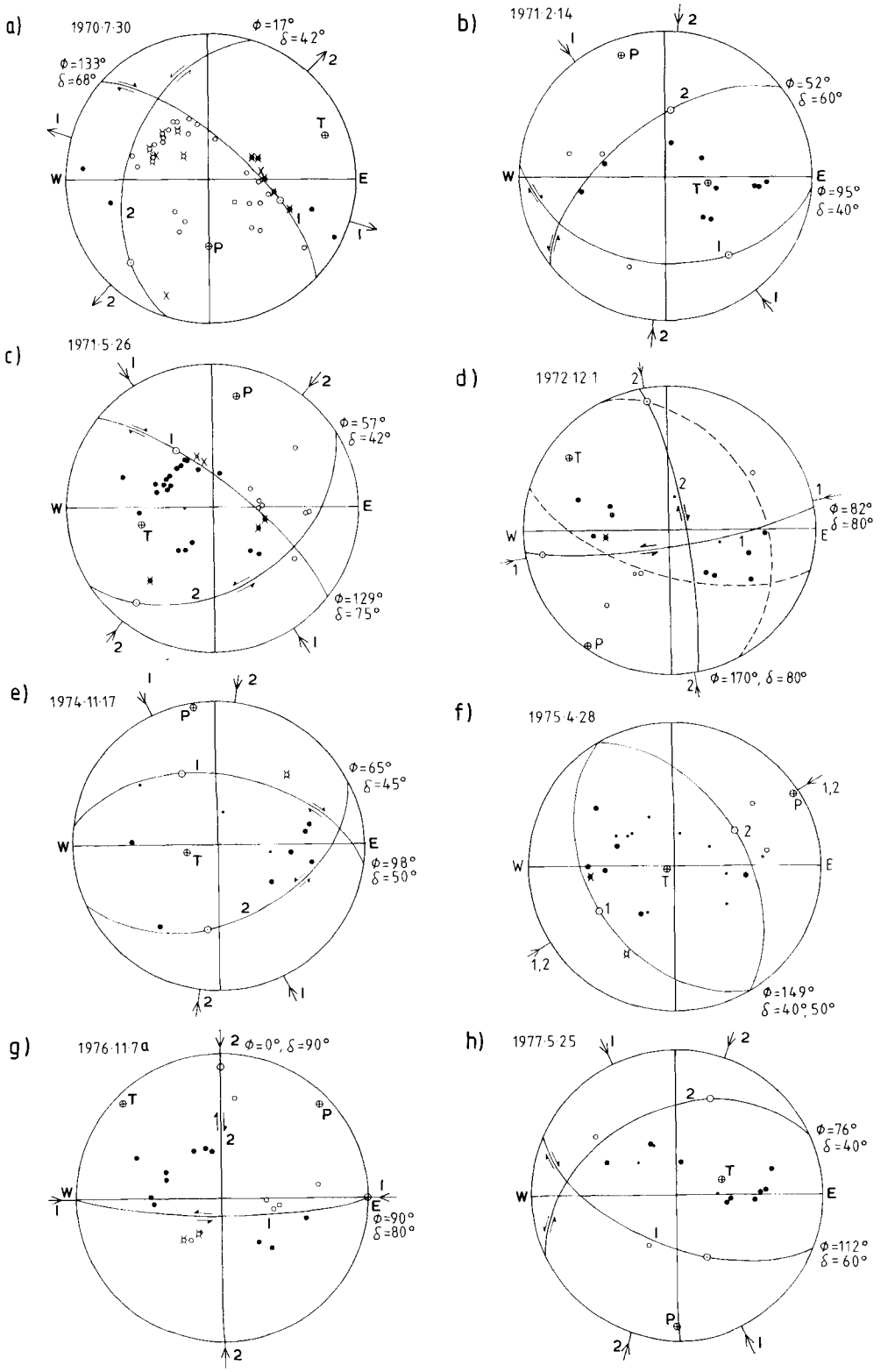

Figure 28. New fault plane solutions in Central Iran, the Alborz and Kopet Dag. Symbols as in Fig. 2. All except (a) are plotted with a crustal velocity at the focus. All polarities are consistent with the nodal planes drawn.

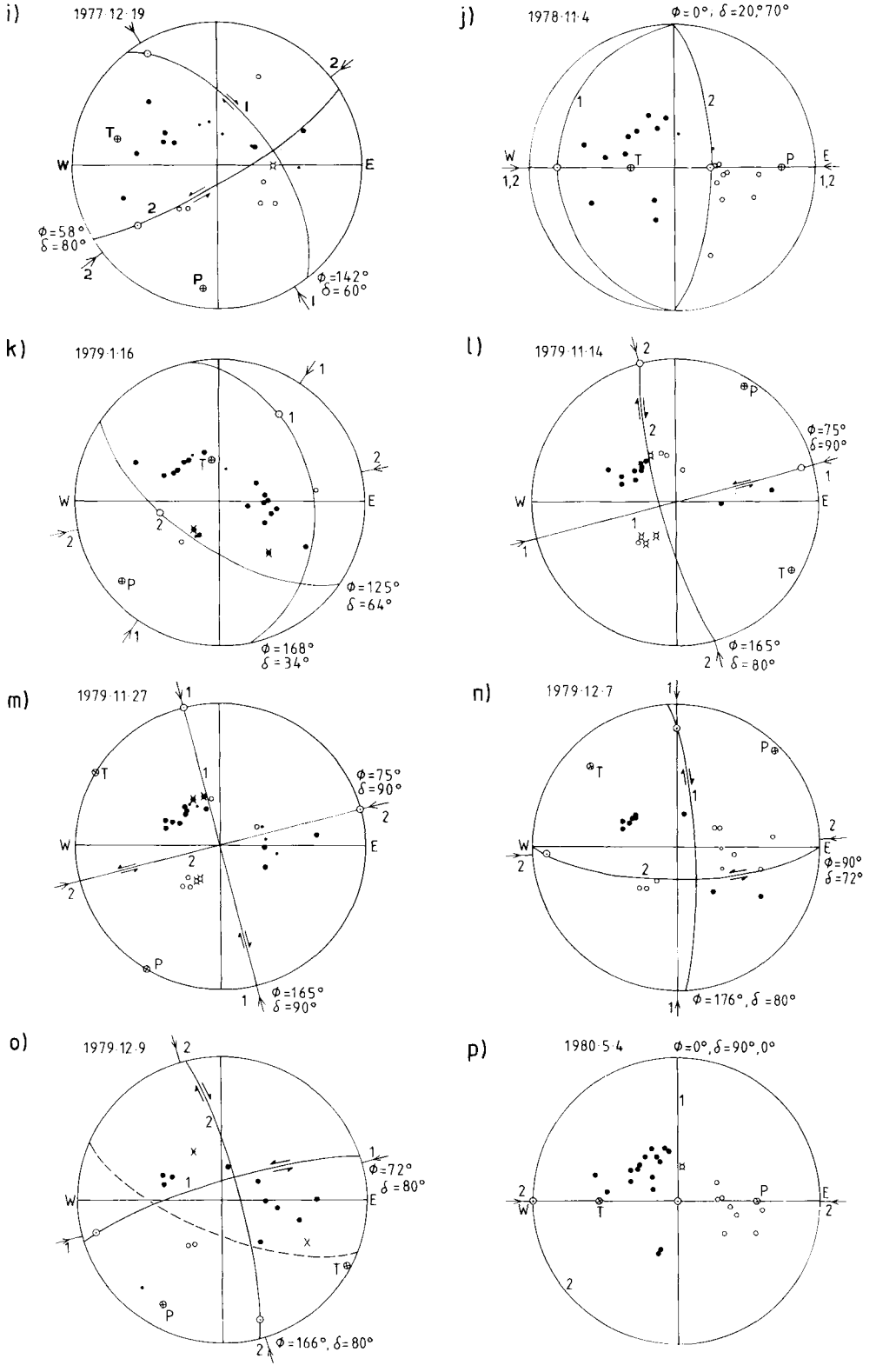

Figure 28 – *continued*

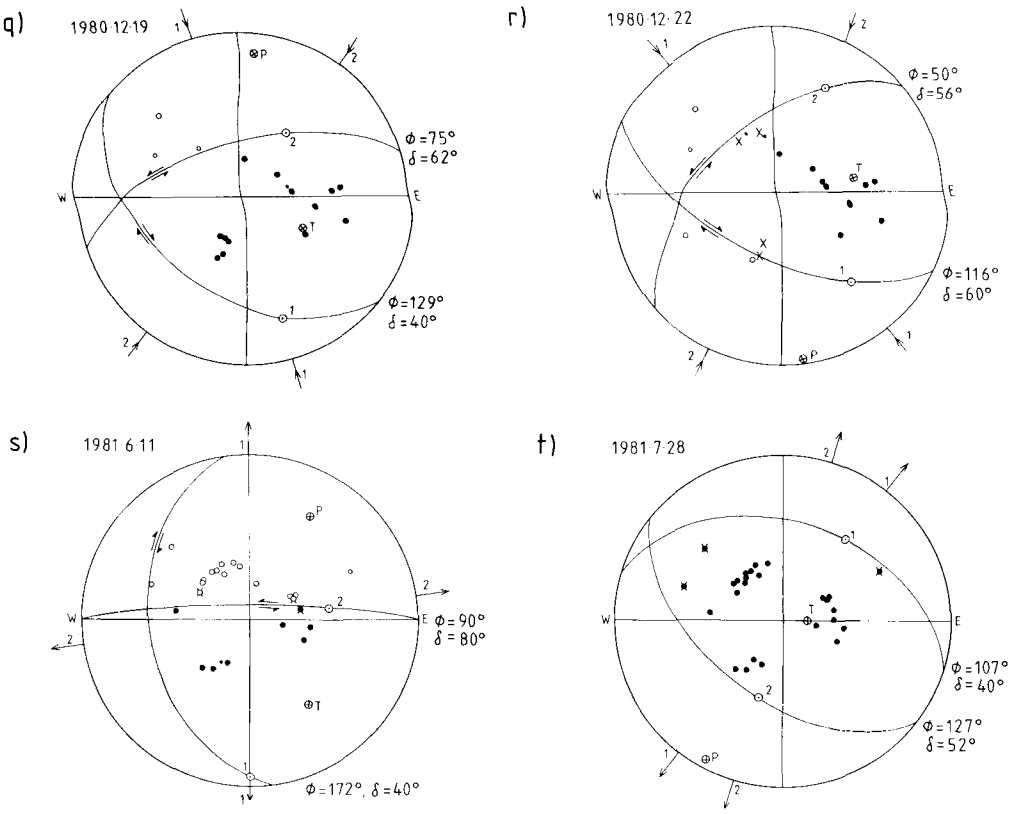

Figure 28 – *continued*

Further east, three shocks, on 1979.12.9, 1972.12.1 and 1971.5.26 occurred near the Doruneh (Great Kavir) Fault (Figs 26 and 27). This is a prominent structure on *Landsat* and aerial photographs as well as on the ground (Wellman 1966; Mohajer-Ashjai, Behzadi & Berberian 1975). Although several historical earthquakes have been located on or near this fault, there are no accounts of surface breaks following any of them. Two particularly destructive shocks of 1903 (near Kashmar) and 1923 (near Torbat-e-Heydarieh) are discussed by Tchalenko (1973b), Ambraseys & Moinfar (1975, 1977b) and Ambraseys & Melville (1982). That of 1923 was given an instrumental epicentre by the ISS that was more than 400 km from its macroseismic epicentre, demonstrating the value of historical studies of this sort. Although the sense of motion on the Doruneh fault probably involves a substantial vertical component east of Torbat-e-Heydarieh (Tchalenko, Berberian & Bezhadi 1972), in the west there is geomorphological evidence of left lateral strike-slip (Mohajer-Ashjai *et al.* 1975). Of the three earthquakes near this fault for which fault plane solutions are available only that of 1979.12.9 had an epicentre on the fault trace. Although the solution for this shock shown in Figs 26 and 27 is compatible with left lateral motion on the Doruneh Fault, the first motion data also permit a thrust mechanism (Fig. 28o), though not with a strike parallel to the Doruneh Fault. The event of 1972.12.1 had a macroseismic epicentre about 20 km north of the Doruneh Fault and may not be associated with it (Ambraseys, private communication). Mohajer-Ashjai *et al.* (1975) suggest that the 1971.5.26 earthquake occurred on a fault branching off the Doruneh Fault and running sub-parallel to it, also with left lateral motion. Although the choice of the left lateral

nodal plane as the fault plane in these three earthquakes cannot be proved correct, such a choice implies an approximately ENE slip vector in each case, consistent with many other slip vectors in NE Iran (Fig. 19).

South of the Doruneh Fault is another large east–west fault, the Dasht-e-Bayaz fault, in this case with east–west left lateral motion clearly demonstrated by 80 km of surface faulting in 1968.8.31 (Ambraseys & Tchalenko 1969; Tchalenko & Berberian 1975) and 60 km in 1979.11.27 (Hahgipour & Amadi 1980). This fault is not as obvious or as long as the Doruneh Fault and may well have had less motion on it. Of particular interest are a number of earthquakes south of the east–west Dasht-e-Bayaz fault of 1968.8.31 and 1979.11.27, in which north–south right lateral strike-slip faulting was observed. In the earthquakes of 1941.2.16 and 1947.9.23, such faulting, with lengths of 10 and 20 km respectively, is known from field studies and interviews with the local population (Ambraseys & Melville 1977, 1982). The earthquake of 1979.11.14 is described by Haghipour & Amadi (1980) and apparently involved a curiously shaped fault of 20 km length with predominantly north–south right lateral slip, but curving to the east at each end. The distance of the 1976.11.7a epicentre south of the Dasht-e-Bayaz fault, as well as the inconclusive ground deformations stretching 9 km with an azimuth of about 140° (Gourdazi & Gharderi-Tafreshi 1976; Khoshbakht-Marvi 1977; Ambraseys & Melville 1982), and the N15°W trend of the locally recorded aftershocks (Niazi, private communication), suggest that this shock also involved right lateral strike-slip, on the north–south nodal plane in the fault plane solution (Fig. 28g). It is not known with which strike-slip system to associate 1979.12.7 as it is located near the junction of the fault breaks of 1979.11.14 and 1979.11.27, and there are no reliable field reports to help. The other available fault plane solutions in this part of NE Iran involve predominantly thrusting on faults with a NW strike bordering topography with the same trend. The 1978 Tabas sequence is discussed in detail by Berberian (1979b, 1982) and Berberian *et al.* (1979), who found 80 km of thrust faulting dipping NE. Berberian's (1982) fault plane solutions for 1978.9.16, 1979.2.13 and 1980.1.12 are in complete agreement with our own first motion observations, and, as his are constrained by additional Iranian stations, we have used his solutions in Figs 26 and 27. The long-period radiation from the mainshock of 1978.9.16 is discussed by Niazi & Kanamori (1981) and Silver & Jordan (1983). The Ferdows earthquakes of 1968.9.1 and 1968.9.4 also involved thrust faulting with a NW strike, as shown by their fault plane solutions, aftershock locations (Jackson & Fitch 1979), and tentative reports of ground displacement on a reverse fault dipping east (Berberian 1979b). Indeed, as remarked by Berberian (1981), many of the mountain ranges in central Iran are bordered by active reverse faults (thrusts). A fine demonstration of the use of historical earthquake studies is the discovery of the fault break of the 1493.1.10 Mu'minabad earthquake (Fig. 27) east of Birjand (Ambraseys & Melville 1977, 1982), which is another NW-striking thrust, still visible at the surface and prominent on air photographs (Fig. 27).

The two shocks in central Iran of 1975.4.28 and 1974.11.17 (Fig. 26) are not obviously correlated with any surface structures. Both were small (m_b 5.3 and 5.2). The fault plane solution for 1975.4.28 requires the NE slip vector seen farther north and east. The 1974.11.17 event appears to have a more northerly slip vector, which is also seen farther to the south.

South of the east–west Dasht-e-Bayaz and Doruneh fault systems are several long linear faults striking north–south, visible on air photographs, satellite images and on the ground (Freund 1970, Dimitrijevic 1973, Mohajer-Ashjai *et al.* 1975 and Plate 7). These extend south towards the Makran region (Section 8), dominating the topography of eastern Iran and the borders of the Lut region. Several are known to be active. The Kuhbanan Fault

moved in the Gisk earthquake of 1977.12.19 (Berberian, Asudeh & Arshadi 1979; Ambraseys, Arsovski & Moinfar 1979; Ambraseys & Melville 1982) with a combination of right lateral and reverse slip consistent with motion on plane 1 of the fault plane solution (Fig. 28i). In the two earthquakes of 1981.6.11 and 1981.7.28 surface movement occurred along about 80 km of the Gowk Fault (the southern part of the Sarvestan and Nayband fault zones), showing both right lateral and reverse slip on north–south faults. These shocks had very complicated multiple rupture processes, and the first motion solutions shown in Fig. 28(s, t) are not representative of the overall fault motions, though the slip vectors in this multiple sequence were all oriented between north and NE (Berberian *et al.* 1984). Both the teleseismic and field observations of Berberian *et al.* (1984) completely disagree with the interpretation of Adeli (1982), who apparently mistook fissuring above a thrust plane for normal faulting. Such fissuring is a common feature of the surface breaks accompanying thrust faulting and is not indicative of major normal faulting at depth (see, e.g. Ambraseys 1981; King & Vita-Finzi 1981; Yielding *et al.* 1981). There is little modern seismicity on the other north–south structures further east. However, the geomorphology of these structures (Plates 6, 7 and Mohajer-Ashjai *et al.* 1975) and historical reports of north–south faulting (Ambraseys & Melville 1982), strongly suggest they are active. In some places recent right lateral displacement can be demonstrated on these faults (Freund 1970; Camp & Griffis 1982; Tirrul *et al.* 1983). Shirokova (1977) reports a fault plane solution for a shock of m_b 5.2 on 1970.8.9, which had an epicentre on the easternmost of the north–south fault systems. Although her solution shows the expected north–south right lateral motion, the arrivals at WWSSN stations for this event were severely contaminated by waves from another, larger shock elsewhere, and we were not able to determine a reliable solution ourselves.

Apart from the Karnaveh earthquake of 1970.7.30 in NE Iran, only one earthquake in Fig. 26, on 1970.11.9, shows normal faulting (Fig. 31c). The large number of recording stations and consistent *pP* and *sP* reports for 1970.11.9 suggest that it probably has a focal depth close to the 106 km at which it was located by the USGS (Jackson 1980b). Kadinsky-Cade & Barazangi (1982) agree with this conclusion but publish a fault plane solution completely different from ours. Theirs is based on short-period polarities published in the *ISC Bulletin* and has many inconsistencies. Ours is based on short- and long-period polarities that we read ourselves, though, admittedly, it is really controlled only by one long-period dilatation in the SE (at CHG). Except for this event, which is discussed in the next section, there is no reliable evidence for other intermediate depth earthquakes in the area contained within Figs 25 and 26.

The seismic activity of eastern Iran decreases abruptly east of about 61°E (Figs 1 and 24). Most of the active structures in eastern Iran south of 34°N run north–south and truncate older structures in western Afghanistan (Plate 6). The quiescence in western Afghanistan probably represents genuinely little active deformation, as the structures in Iran appear to be directed south towards the Makran rather than continue further east (see Section 9). There are very few reports of historical seismicity east of 61°E. Fig. 25 shows only a single small shock in western Afghanistan, close to Herat, although Byron (1937) and Ambraseys & Melville (1982) refer to the loss of minarets in Herat during earthquakes in 1931 and 1950. The apparently feeble seismicity along the south-eastern border of Iran is almost certainly misleading, as catastrophic earthquakes have occurred all along this zone in the past (Ambraseys & Melville 1982). The same is true of the north–south fault zones in the western Lut, though the central Lut may have genuinely little seismicity. Assessing the intensity of active deformation in the central Kavir (between the Zagros, Alborz and Doruneh regions), which has scattered and weak seismicity in Figs 1 and 25, presents more

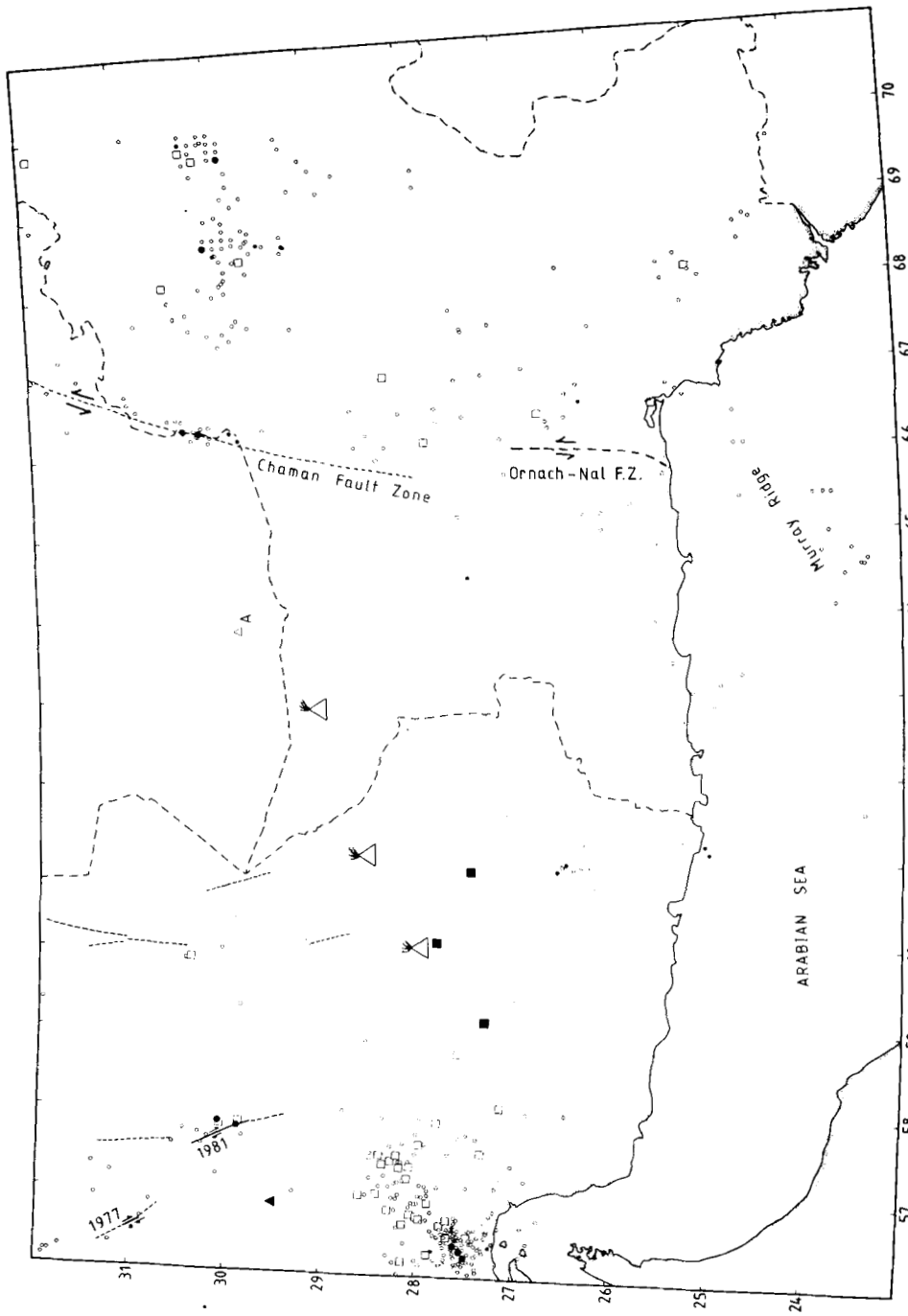

Figure 29. Epicentres of all earthquakes reported in the Makran and West Pakistan during the period 1961 January to 1980 December. Symbols as in Fig. 6. In this figure, because genuinely subcrustal shocks are known to occur, all hypocentres reported deeper than 50 km are shown by squares and those deeper than 100 km by triangles. The position of the small earthquake of 1979.1.31 at 183 km depth is marked A.

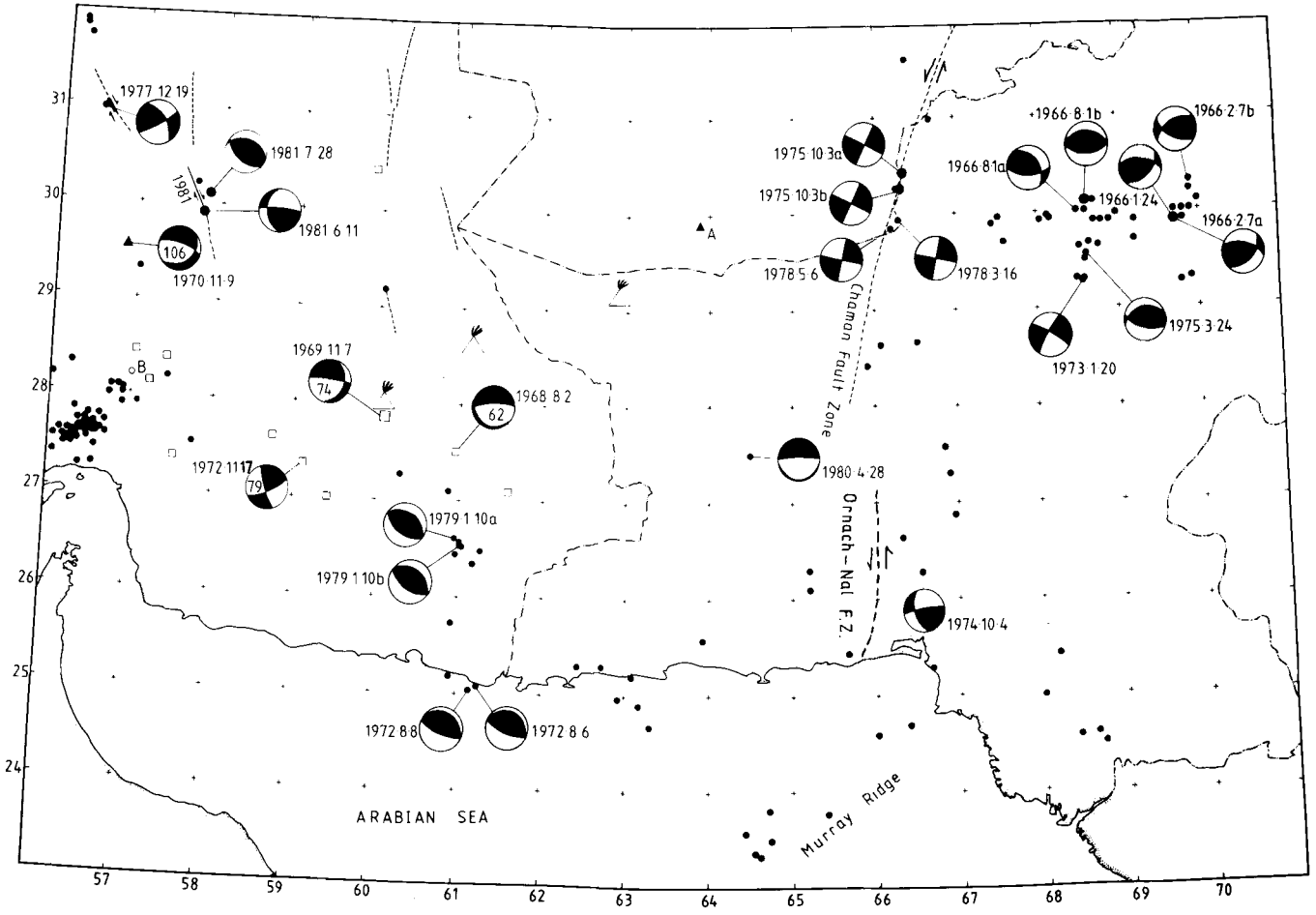

Figure 30. Epicentres of the larger shocks in Fig. 29. New fault plane solutions are shown in Figures 31 and 32 (see Table 1). Symbols as in Fig. 7. The epicentre of 1979.1.31 is marked A, and that of 1964.12.22 is marked B (see Fig. 21).

of a problem. Although there has been little documented historical seismicity, young faults are claimed to exist in this region (e.g. Berberian 1981). Certainly the Doruneh Fault can be seen on satellite images to continue much further west than is drawn in Figs 25, 26 and 27 (e.g. Mohajer-Ashjai *et al.* 1975), though there is no modern or historical seismicity associated with this western part of it. Near Esfahan (32.6°N, 51.6°E), where no significant damage from earthquakes has ever been recorded (Ambraseys & Melville 1982), Tillman *et al.* (1981) report pervasive small faults in Holocene gravels. Although the Dasht-e-Kavir and Lut areas may not be completely aseismic, they certainly appear to be much less active than the regions surrounding them.

8 The Makran and western Pakistan

The simple fold structures of the Zagros are truncated east of the Oman Line. In the region of this line structures trend north–south and there is an abrupt change from the intense seismicity of the Zagros to the relative quiescence of the western Makran (see Figs 29, 30 and Kadinsky-Cade & Barazangi 1983). An abrupt change in basement structure is also seen in seismic reflection profiles near the Oman Line, particularly in the region of the Zendan–Minab Fault zone (Falcon 1976), a structure trending NNW parallel to the western coast of the Makran. The latest motion on the Zendan–Minab system appears to be predominantly thrust faulting (Berberian 1976; Vita-Finzi & Ghorashi 1978; Page, Anttonen & Savage 1978). This change in nature of the active deformation across the Oman Line is presumably related to the change from the shortening of continental basement in the Zagros to the subduction of oceanic crust, probably 70–100 Ma in age (Hutchison *et al.* 1981), under the Makran. We could obtain no fault plane solutions for shocks on the Zendan–Minab system, where all earthquakes reported since the installation of the WWSSN have been small. Chandra (1981) publishes two solutions (without showing individual polarity readings) close together about 20 km east of the Minab fault. His solutions show both normal faulting and thrusting but we were unable to substantiate them, as the two events were small (m_b 5.3 and 4.8) and we could not obtain sufficient reliable polarities on either short- or long-period instruments.

The NE-trending calc-alkali volcanic belt, with the three prominent centres of Bazman (in the SW), Taftan and Sultan (in the NE, see Figs 29 and 30), as well as the sporadic occurrence of intermediate depth earthquakes, have led several authors (e.g. Farhoudi & Karig 1977; Jacob & Quittmeyer 1979) to compare the deformation in the Makran with that in active oceanic island arcs. The differences between the Makran and the Pacific island arc systems are also worth noting: there is no prominent trench in the offshore bathymetry, there are large thicknesses of sediment in the Gulf of Oman, and the east–west fold ranges of Iran, usually considered an accretionary prism, are up to 300 km wide.

Offshore work indicates that a 6–7 km thickness of flat lying sediments resting on normal oceanic crust is being folded and faulted prior to uplift and incorporation into the east–west range of the Makran (White & Klitgord 1976; White 1977, 1979, 1982; White & Ross 1979; White & Louden 1982). This folding is relatively continuous along an east–west strike from the Strait of Hormuz as far east as about 66°E, where the structures turn north into the left lateral Ornach Nal and Chaman fault system (Figs 29 and 30). According to White (1982), folding is initially restricted to the top 2.5 km of the sediment pile, which is then incorporated into the accretionary prism by uplift along thrust faults that flatten out at depth, probably in overpressured shales. Such an interpretation is consistent with the mechanisms of two shallow shocks offshore on 1972.8.6 and 1972.8.8 (Fig. 30), which both show thrust faulting, presumably on shallow planes dipping to the north. If the steep nodal plane

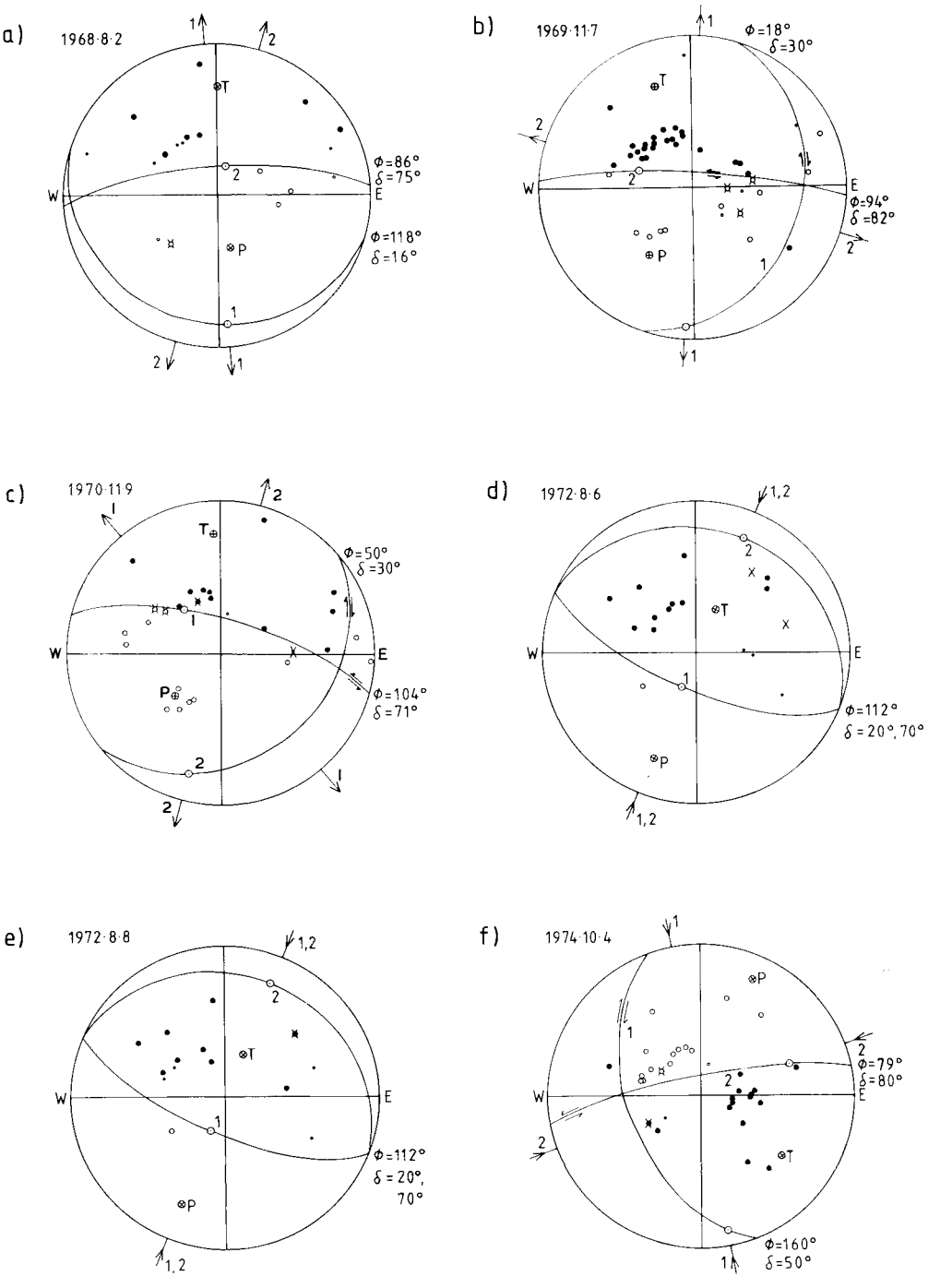

Figure 31. New fault plane solutions in southern Iran. Symbols as in Fig. 2. All except (a), (b), (c) and (n) are plotted with crustal velocities at the focus. The only inconsistent polarity is in (c), where a dilatation (small symbol) at azimuth 005°N is plotted close to nodal plane 1, but in the compressional quadrant.

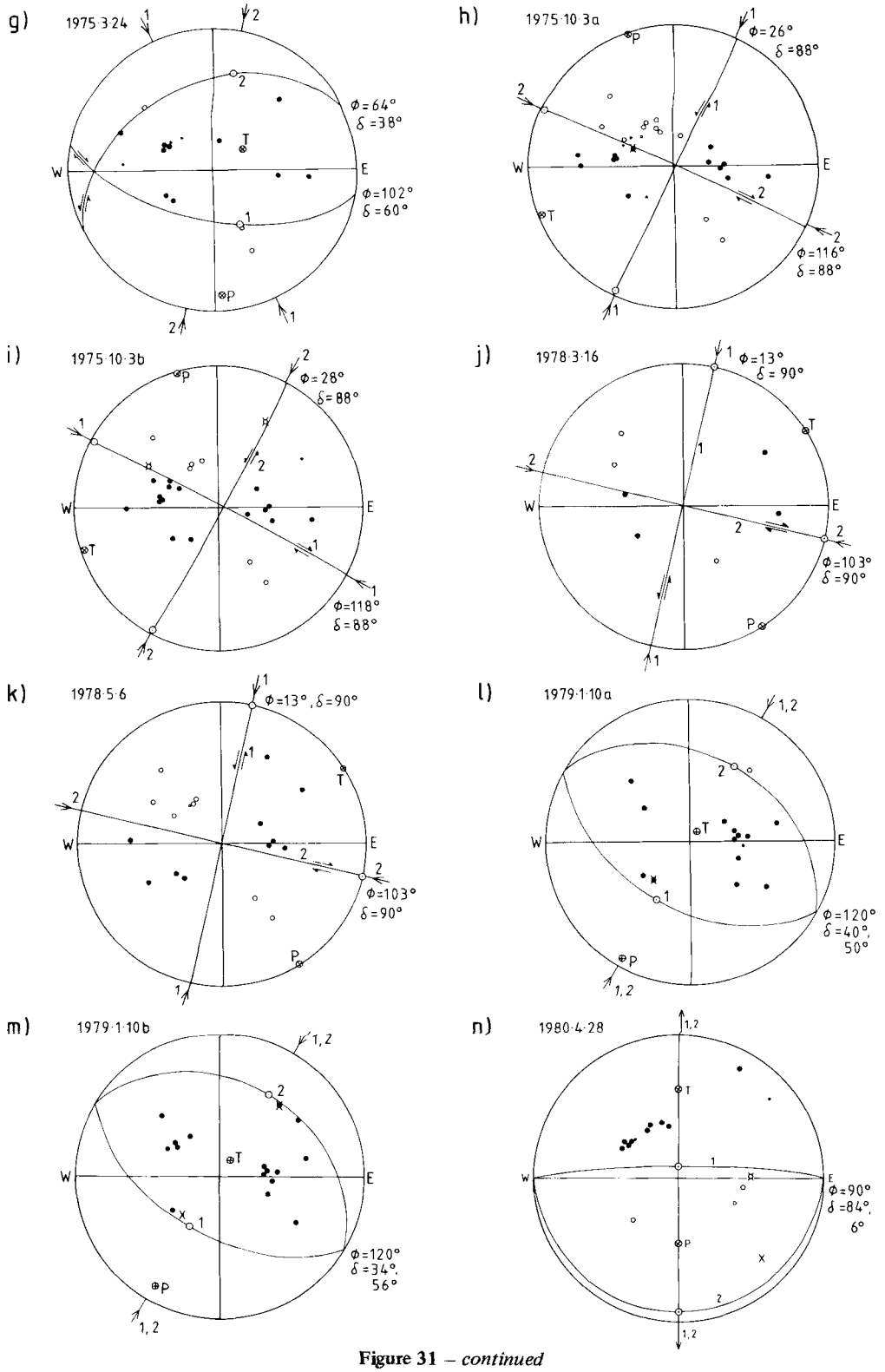

Figure 31 – *continued*

(1 in Fig. 31d, e) really is the auxiliary plane, then the slip vector is constrained to be at least 10–15° east of north. This agrees well with the predicted azimuth of the slip vector between Arabia and Eurasia in the Makran (see Fig. 34 and Jacob & Quittmeyer 1979), the magnitude of which is estimated to be about 4 cm yr^{-1}. Following the large ($Ms > 8.0$) earthquake of 1945.11.27, whose epicentre was in the vicinity of Pasni (approximately 25.2°N, 63.5°E), the coastline was uplifted by about 1–3 m (Page *et al.* 1978, 1979; Ambraseys & Melville 1982). This uplift, together with the large damage area, is consistent with a mechanism in this earthquake similar to those of 1972.8.6 and 1972.8.8 further west; i.e. a shallow thrust dipping northwards. Widespread raised beaches along the Makran coast are evidence of continued uplift and southward propagation of the accretionary prism (Page *et al.* 1979), though the normal faults described in these beaches by Vita-Finzi (1981, 1982) are probably collapse structures in the poorly consolidated marine sediments, rather than indicators of regional extension.

On land, the east–west structures so visible on satellite images (see Plate 8 and Farhoudi & Karig 1977) are folds and thrust faults (Berberian 1981) but there is some disagreement as to whether the oval-shaped depressions within the east–west ranges are eroded synclines (McCall & Kidd 1982) or uplifted basins of flat lying sediments formed between anticline ridges (Farhoudi & Karig 1977), as seen offshore (see, e.g. White 1982). Nevertheless it is clear that shortening is also taking place onshore, as the earthquakes of 1979.1.10a and b (Fig. 30) both show thrust faulting, again with a slip vector east of north, but this time on high angle (40–50°) planes rather than the shallow dips seen on the coast. It is worth noting at this point that the proposed segmentation of the Makran by north–south transverse structures, proposed by Dykstra & Birnie (1979) derives no support from either offshore work (White 1982) or the focal mechanisms in Fig. 30. This suggestion arose because of the NE rather than easterly trend of the calc-alkaline volcanoes and would predict strike-slip motion on the north–south line through the epicentres of 1979.1.10a, b and 1972.8.6 and 1972.8.8.

Like Antalya Bay, this is one of the few areas between Turkey and Pakistan where genuine intermediate depth earthquakes can be demonstrated to occur. Jacob & Quittmeyer (1979) give fault plane solutions for 1968.8.2 and 1969.11.7 which are in good agreement with ours, and in addition show short-period waveforms on which arrivals corresponding in time to *pP* and *sP* can be seen. These confirm the subcrustal depths of about 74 and 62 km given for these shocks by the ISC and USCGS. The event of 1972.11.17 also appears to be genuinely subcrustal (Fig. 32). A normal faulting solution for this shock, given by Chandra (1981), can be ruled out by the clear compressional onset in the form of the impulse response observed on the short-period instrument at COL. The strike-slip mechanism drawn in Fig. 32 also predicts the observed small (nodal) onset at BAG, rather than the large amplitude predicted by a normal faulting solution. The various later phases observed in the seismograms of Fig. 32 have the correct relative amplitudes for the strike-slip mechanism and clearly indicate a depth of 60–80 km, even though the timing of the arrivals at BAG and BUL is not consistent (perhaps not surprising since *pP* and *sP* ray paths to BAG go along the strike of the Makran whereas those to BUL cross it). Further east the earthquake of 1980.4.28 was located at a depth of 34 km by the NEIS. However, its anomalous fault plane solution, lack of aftershocks and poor generation of surface waves suggests that this too may be a subcrustal event; especially since its location is roughly the same distance from the coast as those of 1968.8.2 and 1969.11.7, both of which have mechanisms similar to that of 1980.4.28. Although the ISC located the shock of 1980.4.28 at 22 km depth, they also give an alternative depth of 53 km based on reported *pP* and *sP* arrivals.

Fig. 30 shows several shocks with hypocentres located deeper than 50 km by the NEIS

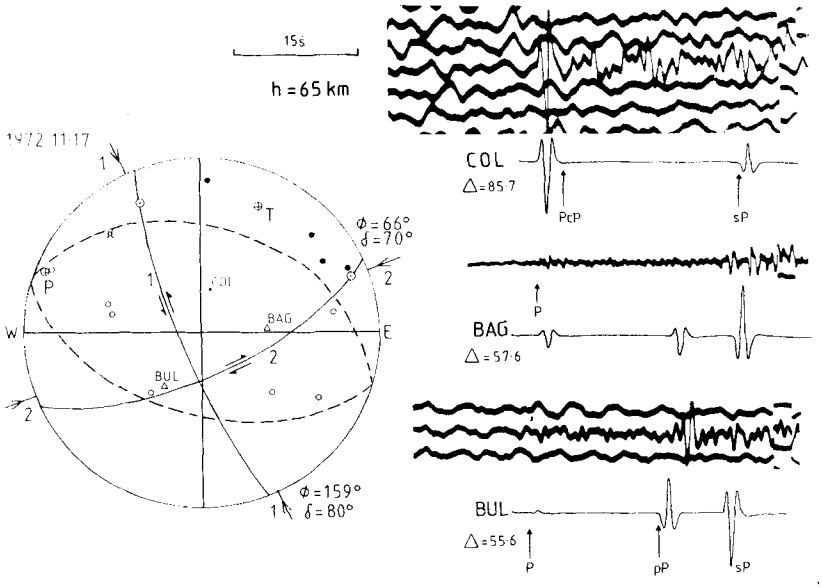

Figure 32. Fault plane solution for 1972.11.17 in southern Iran (see Fig. 30). Symbols as in Fig. 2. The long-period polarities alone allow both normal (dashed lines) and strike-slip (solid) solutions. The clear impulsive onset at COL favours the strike-slip mechanism. Also shown are short-period seismograms at BAG and BUL, whose positions on the focal sphere are marked as open triangles, as well as synthetic short-period seismograms for a depth of 65 km and a triangular time function of 0.8 s, discussed in the text. The amplitude of the synthetic seismogram at BAG has been deliberately exaggerated to emphasize the *relative* amplitudes of *P*, *pP* and *sP*.

and which are either of m_b 5.0 or greater or have at least 50 recording stations. In Fig. 29 all shocks located deeper than 50 km are shown. In spite of the known inaccuracies in these depths, it is interesting that they form a distinct set, apparently existing only north of 27°N and separate from the shallow shocks to the south. Only two of these apparently subcrustal shocks were located at depths greater than 100 km. One was that of 1970.11.9 in the west, located at 106 km (see previous section). The other was a small shock of m_b 4.8 on 1979.1.31 at 30°N 64°E, marked A in Figs 29 and 30, that was located at 183 km by NEIS and 173 km by the ISC. In spite of the lack of observed or reported surface reflections, which may be simply because the earthquake was small, the large number of recording stations (98 for NEIS, 122 for ISC) makes it probable that their depth estimates are approximately correct (see Jackson 1980b). An intermediate depth is also consistent with the observed lack of 20 s surface waves from this event, even at WWSSN stations within 30° of the epicentre. The location of this earthquake is the same as that given by Gutenberg & Richter (1954) for an event on 1914.2.6, which they located at a depth of 60–100 km (see also Quittmeyer, Farah & Jacob 1979; Quittmeyer & Jacob 1979), and to which they assigned a magnitude of 7.0 that is probably an overestimate (Ambraseys, private communication). As pointed out by Jacob & Quittmeyer (1979), the *T*-axes of 1968.8.2 and 1969.11.7, which have a shallow dip to the north, are consistent with those expected from intermediate depth shocks within a subducting plate dipping north. The same is true for the *T*-axes of 1980.4.28 and 1972.11.17, even though all four earthquakes are rather shallower than the seismicity beneath the volcanic arcs of the Pacific, which is generally at about 100 km. In the light of this discussion, and especially since the subducting plate probably

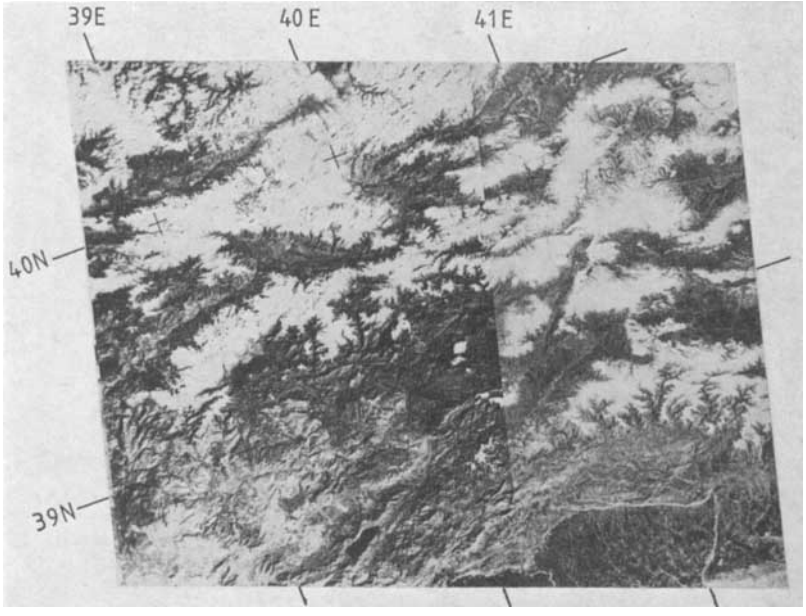

Plate 1. Junction of the North and East Anatolian Fault Zones. Note the splay faults west of the East Anatolian Fault and parallel to it. See Fig. 5 and Plate 9 for location.

[*facing page* 240]

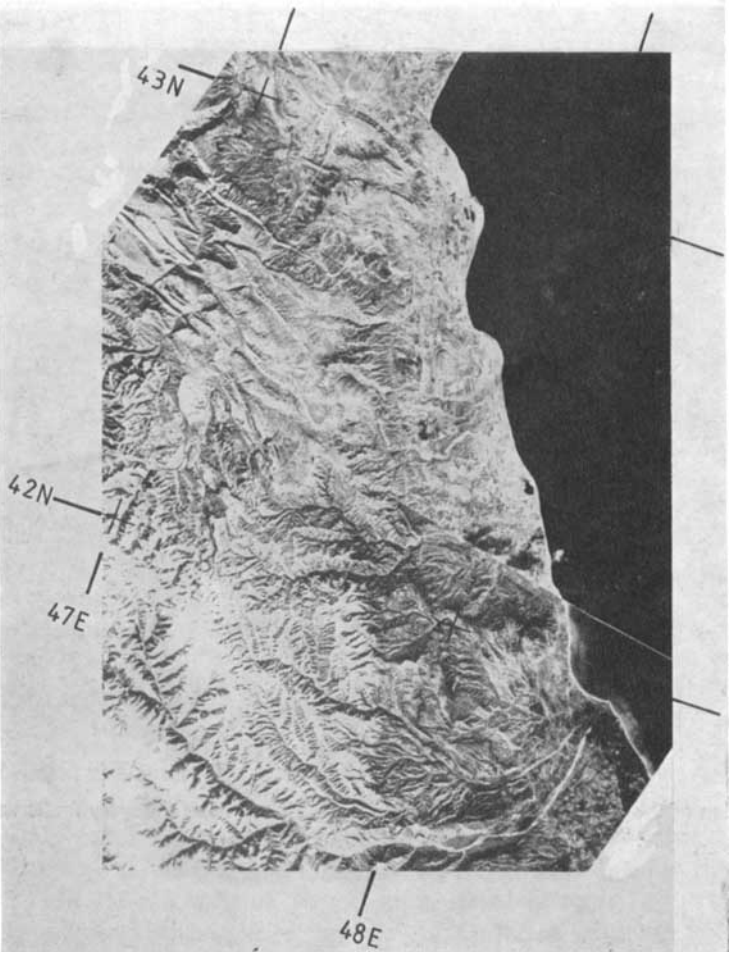

Plate 2. Fold and thrust structures in the Caucasus. Note especially the break in alluvial slope near 42.4°N 47.7°E, which is probably a thrust, and the folds near 42.5°N 47°E. See Fig. 5 and Plate 9 for location.

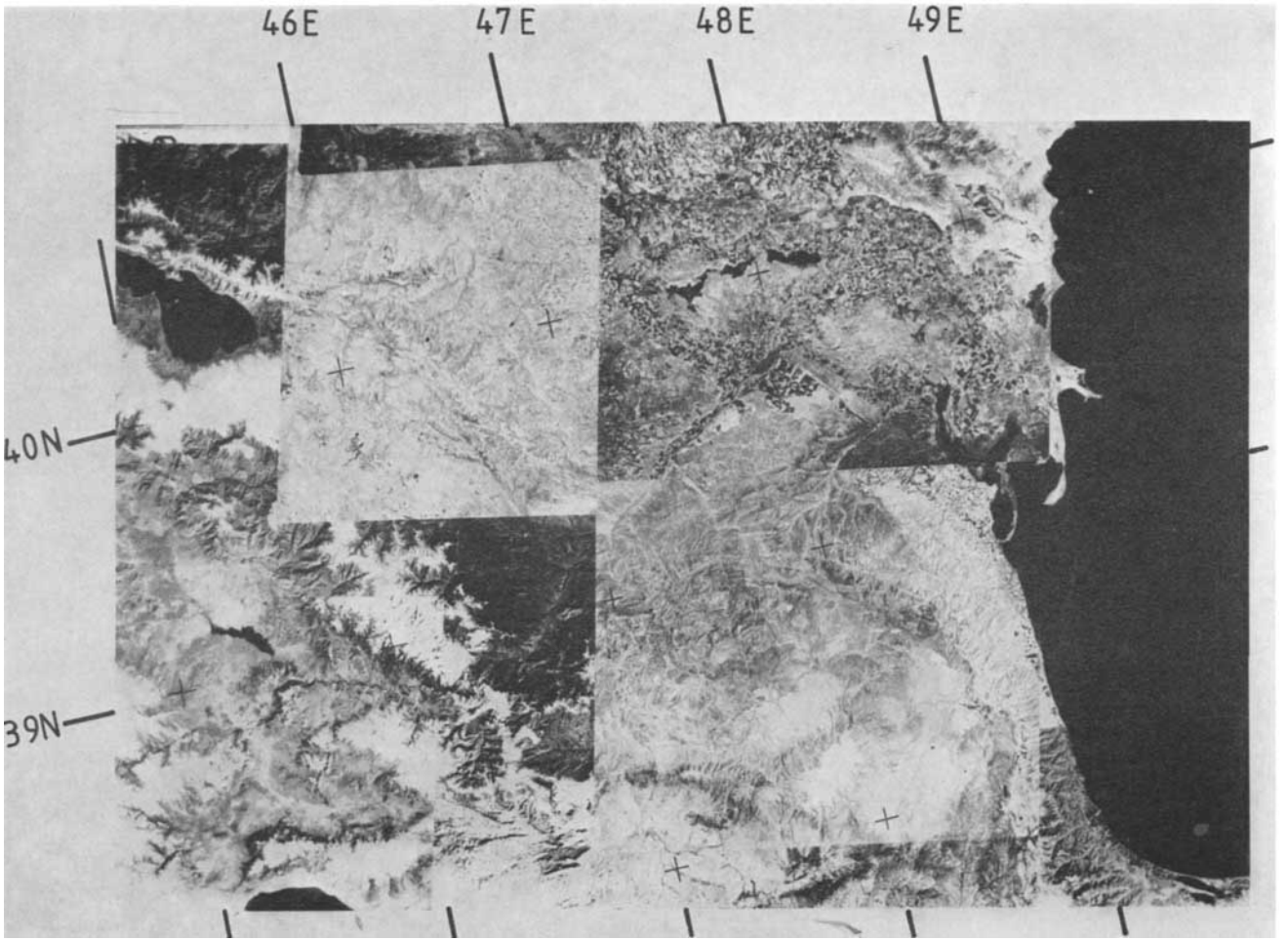

Plate 3. Mosaic to show the lineations following the Araxes (NE) and Akera (NW) rivers, which meet near 39.1°N 46.8°E. See Fig. 5 and Plate 9 for location.

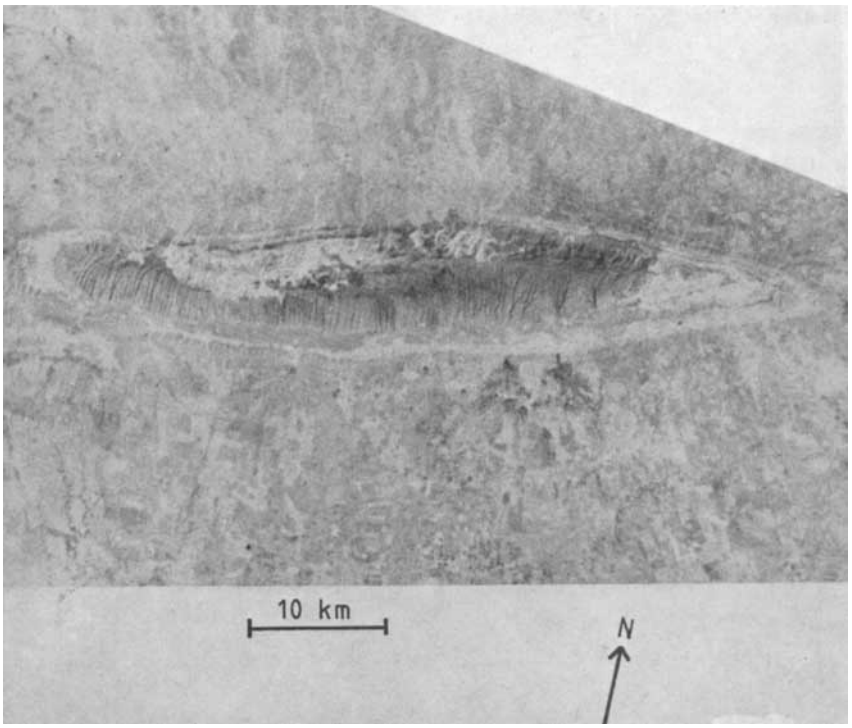

Plate 4. Anticline in northern Iraq. Note the similarity in appearance and scale to those in the Zagros (Plate 5). See Fig. 5 for location.

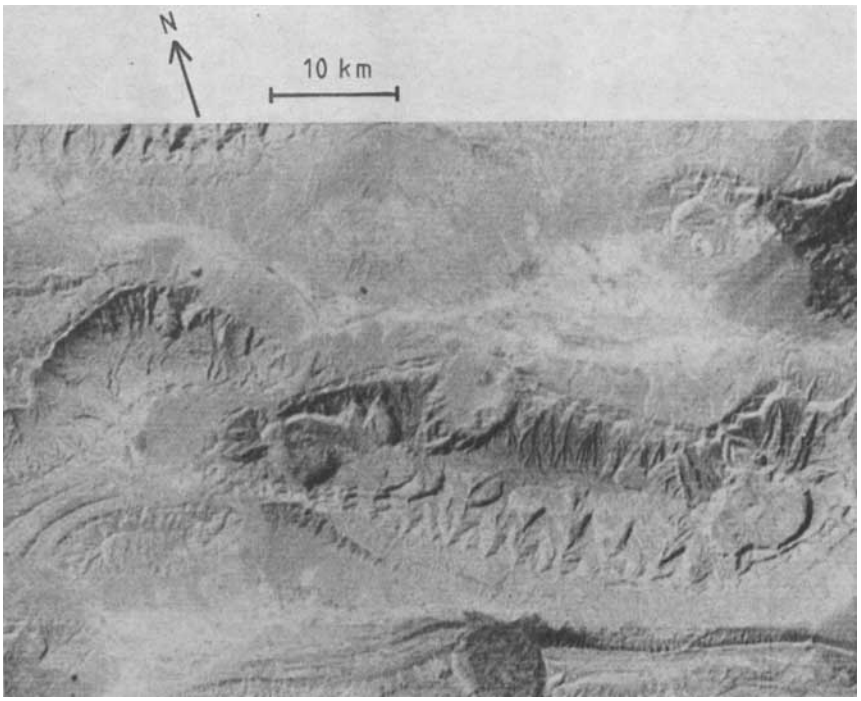

Plate 5. Anticlines in the southern Zagros. See Fig. 5 for location. The dark circular patch in the southern part of the image is an emergent dome of Hormuz salt.

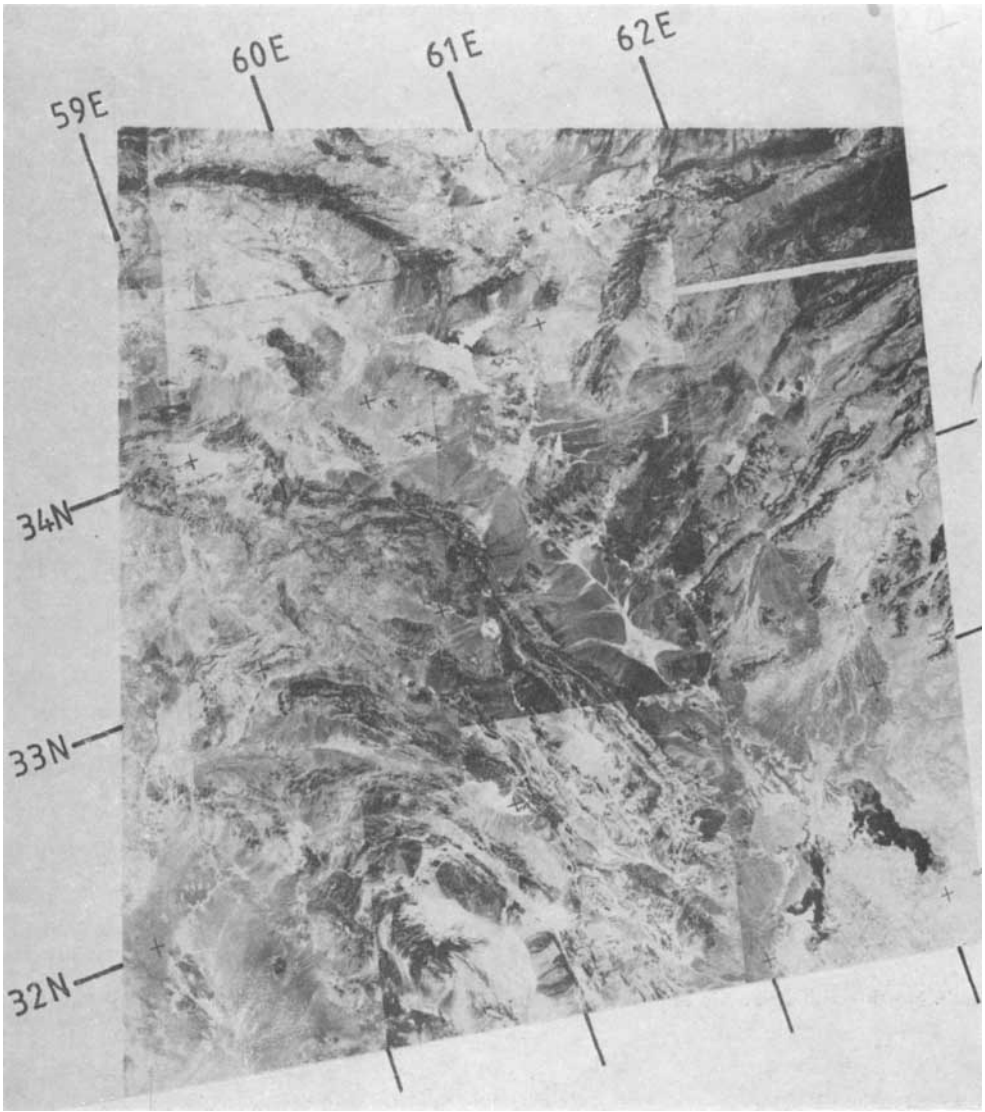

Plate 6. Mosaic showing the truncation of the east–west ranges of western Afghanistan by the north–south ranges of eastern Iran. Note the differences in erosion patterns between the two ranges and the large strike-slip fault running roughly parallel to 60.2°E. See Fig. 5 and Plate 9 for location.

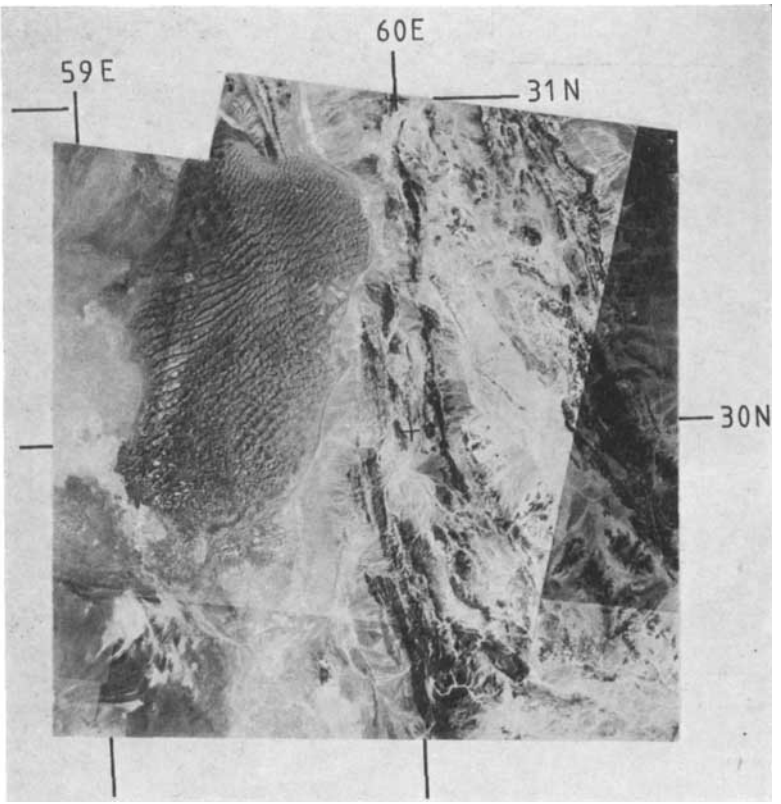

Plate 7. North–south strike-slip fault in the eastern Dasht-e-Lut. See Fig. 5 and Plate 9 for location.

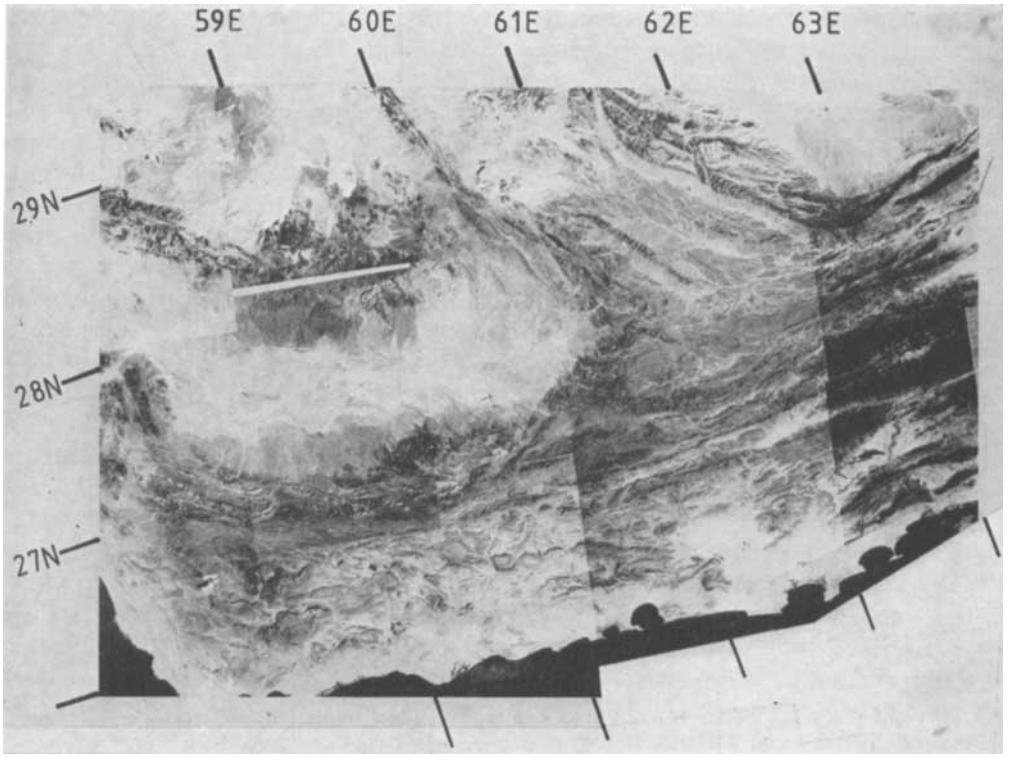

Plate 8. Mosaic showing that the east–west Makran ranges are not cut by the north–south ranges of eastern Iran. Note the prominent volcano of Kuh-e-Bazman at 28°N 60°E. See Fig. 5 and Plate 9 for location.

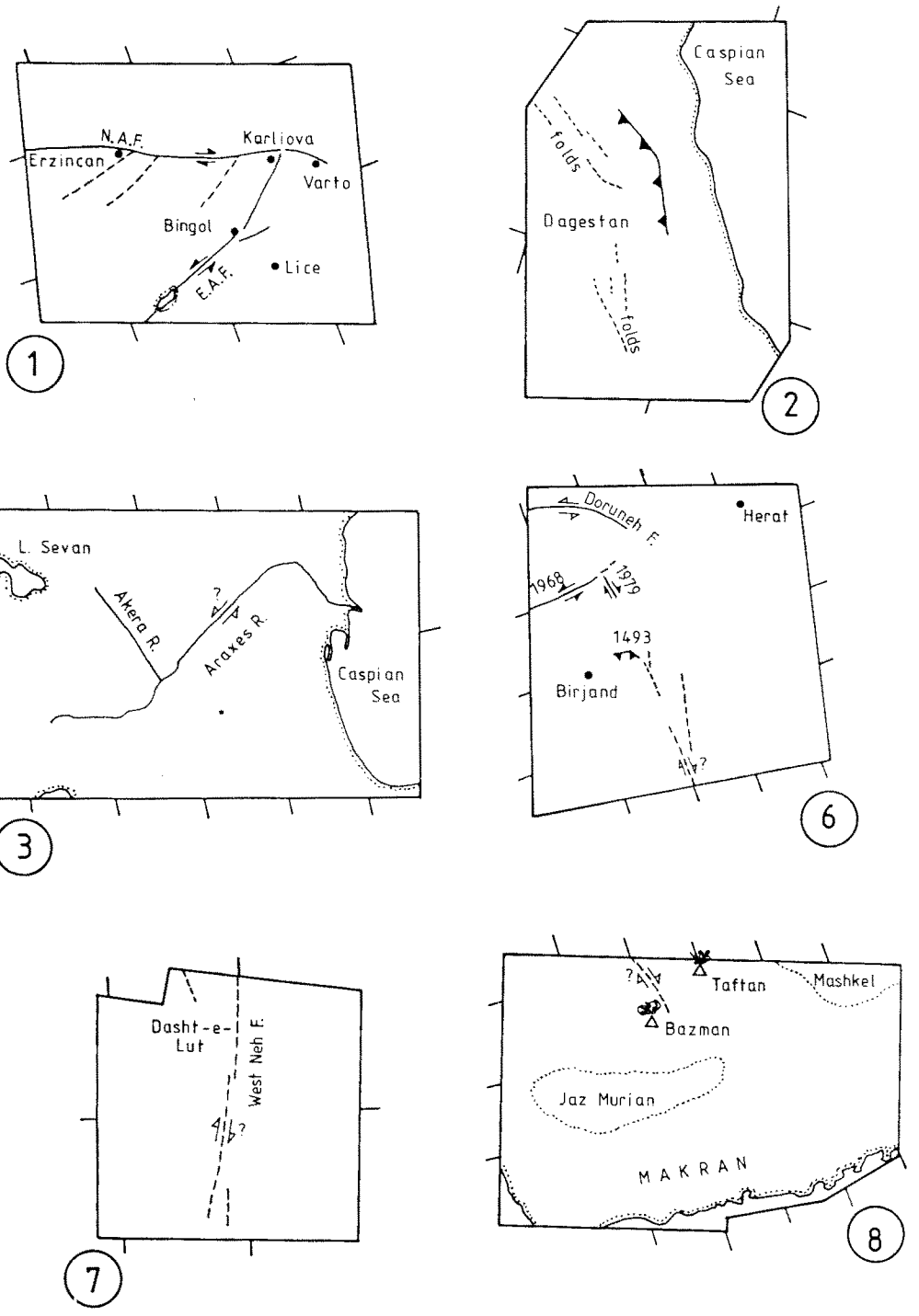

Plate 9. Sketch maps of the areas in Plates 1, 2, 3, 6, 7 and 8, to show the major features and geographical names mentioned in the text.

extends as far north as A (30°N) in Figs 29 and 30, the significance of the earthquake in the west on 1970.11.9 at 106 km depth, whose *T*-axis also dips north, is mysterious. Does it belong to a remnant of the Zagros–Central Iran closure, as suggested by Kadinsky-Cade & Barazangi (1982), or is it a part of the Makran system? The fact that the present-day slip vector in the Makran is slightly east of north perhaps supports the former. There is clearly not enough recorded subcrustal seismicity in this region to define the geometry of any subducting slab, though it is at least now possible to believe in its existence.

The confirmed presence of subcrustal seismicity, together with the Bazman-Taftan-Sultan volcanic chain and its Quaternary calc-alkali andesitic magmas (Berberian *et al.* 1982) obviously tend to confirm the view of Farhoudi & Karig (1977) and Jacob & Quittmeyer (1979) that subduction of the Arabian Sea is occurring under southern Iran and western Pakistan, and that the Makran coast ranges are an accretionary wedge or prism. It is not our purpose to pursue detailed analogies with oceanic arc systems. However, the Jaz Murian and Mashkel depressions, immediately south of the volcanic belt and popularly regarded as subsiding 'upper slope' or 'fore-arc' basins in the oceanic analogy, do not appear to be bounded by normal faults. Indeed, as Berberian (1981) points out, the most recent motion on the faults bounding the Jaz Murian and Makran ranges has been of a high angle reverse nature. Until accurate focal depths are known for the crustal shocks in the Makran, it will not be possible to define the basement geometry. The shocks of 1979.1.10a and b were located at depths of 4 and 3 km by the ISC. They are unlikely to be deeper than 20–30 km, in which case there must be a rather sudden increase in the depth of seismicity near 27°N, and if the slab extends as far as north as A (Figs 29 and 30), it would have a dip of about 30°. This geometry would confirm the notion of Farhoudi & Karig (1977) that the entire width of the Makran coast ranges, as far north as the Jaz Murian, is a sedimentary accretionary prism, formed of sediments scraped off the Arabian Sea and moving over oceanic basement.

The eastern boundary of the Makran system is at about 66°E where the structures bend north along the Chaman and Ornach Nal fault zones, which are prominent on satellite and aerial photographs (Abdel-Gawad 1971; Hunting Survey Corporation 1960). At this point the weak seismicity of the Murray Ridge, an apparently tensional feature (White 1982), continues on land. In spite of the seismicity associated with the north–south Chaman system, some activity does continue eastward along the coastal region, as demonstrated by the 1819 earthquake in the Rann of Kutch, close to the modern India–Pakistan border at about 24°N, 69°E (Richter 1958). The earthquake of 1974.10.4 is apparently not on the north–south Ornach Nal fault system, and its mechanism is incompatible with the north–south left lateral offsets of alluvial deposits observed there in aerial photographs by the Hunting Survey Corporation (1960) and Kazmi (1979). Quittmeyer *et al.* (1979) show a fault plane solution similar to ours, but as theirs was plotted with a mantle source velocity, it has a smaller strike-slip component.

Farther north, four new fault plane solutions show the left lateral strike-slip motion deduced for the Chaman Fault from satellite and aerial photographs (Abdel-Gawad 1971; Hunting Survey Corporation 1960; Wellman 1966). None of these were large shocks, but those of 1975.10.3a and b were associated with a 5 km fault break showing 4 cm of left lateral motion striking NNE (Farah 1976). The Chaman Fault is clearly a major structure with an offset of more than 100 km (Lawrence & Yeats 1979; Lawrence *et al.* 1981) and extends north into Afghanistan. Surface breaks are known on this fault from earthquakes in 1505 and 1892 (Oldham 1882; Griesbach 1893; Quittmeyer & Jacob 1979).

About 70 km east of the Chaman Fault, at a latitude of about 30°N, is another north–south fault, responsible for the catastrophic earthquake at Quetta (West 1935). Composite fault plane solutions from a local network indicate that motion on this too is left lateral

(Armbruster *et al.* 1979). Still farther east, fault plane solutions in a diffuse east–west band of seismicity show thrusting in the Zhob and Loralai ranges; again consistent with a slip vector slightly east of north. The seismicity then continues north and east on the Chaman Fault and in the Sulaiman Range eventually to join the activity in the Karakoram, Pamir and Himalaya.

Two obvious gaps in the shallow seismicity of the Makran region exist both west and east of the Iran–Pakistan border. To the east the lack of seismicity may be due to strain release following the earthquake of 1945. The low level of seismicity in the eastern Makran makes it difficult to investigate the connection between the east–west ranges and the north–south structures of Chaman and Ornach Nal. Satellite images show that the east–west structures curve gently into the north–south strike-slip faults, apparently acquiring an oblique component of motion as they do so (Lawrence *et al.* 1981). To the west of the Iranian border there is very little seismicity. Niazi, Shimamura & Matsu'ura (1980) operated a local seismic network in the western Makran for two weeks and detected no microearthquakes at all. It is not known whether this lack of seismicity represents temporary quiescence following a large earthquake or is permanent. The only likely candidate for a large event in the past is one in 1483, which apparently affected the Strait of Hormuz and NE Oman, and which Ambraseys & Melville (1982) think may have had an epicentre in the western Makran. However, information regarding this event is scarce and inconclusive.

9 The deformation of Iran

The information presented in Sections 5 to 8 supports the general outline of the regional motions presented in I and by Nowroozi (1972), though certain modifications are required. Nowroozi believed that the southern part of the Caspian sea is moving north-westward relative to Eurasia, but the thrust solutions in the eastern Caucasus and the similarity of the slip vectors in the Alborz south of the Caspian and in the Kopet Dag, where the two bands of seismicity have joined, strongly support the view that the southern Caspian is moving north-eastwards relative to Eurasia, though less rapidly than Iran.

The expulsion of NW Iran eastwards away from the collision zone in the Lake Van region, which marks the northernmost penetration of the Arabian promontory, is indicated by: (1) the NW-trending right lateral strike-slip system between Van and the Zagros; (2) the small normal faulting component in the earthquakes of 1930.5.6, 1970.10.25 and 1963.3.24; (3) the NE-trending fault zone along the Araxes river, which the fault plane solution of 1976.2.3 suggests is associated with left lateral strike-slip motion; (4) the thrust faulting solutions for 1978.11.4 and 1980.5.4 in the south-western Caspian. The volcanoes of the Van region are presumably related to the collision between Arabia and Eurasia, but whether they are a consequence of tension perpendicular to the shortening, as their apparent NE alignment might suggest, or of substantial crustal thickening, is not yet known. The low level of seismicity in the large area immediately SE of Lake Rezaiyeh allows a further test of this proposed eastward expulsion of material. The slip vectors on the SW side of this block, along the Main Recent Fault and Salmas (1930) Fault, have a greater westerly component than those predicted by the motion between Arabia and Eurasia (see fig. 4 in I). If this block is moving eastwards relative to Eurasia, the slip vectors on the northern side should have a more easterly component (see fig. 33b in I), which, judging by the fault plane solutions on the SW Caspian shore, they do. The slip vectors in the central Caucasus seem more representative of the predicted relative motion between Eurasia and Arabia. In Figs 5 and 13 there is an indication that the slip vectors are directed outwards at the eastern and western ends of the Caucasus. This implies that some shortening is taken up by elongation along strike as the Caucasus overthrusts the Caspian and Black Seas.

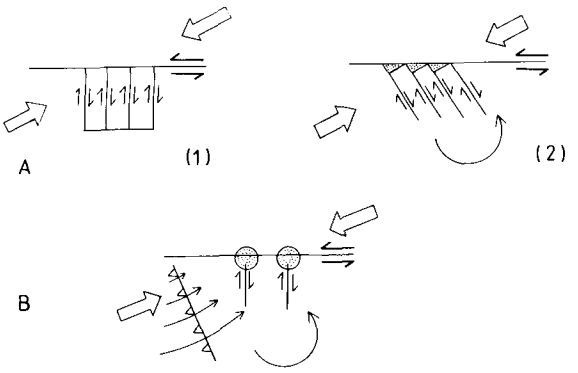

Figure 33. Cartoons to illustrate rotation as a result of combined strike-slip and thrust faulting. Plan views are shown and large arrows mark the direction of overall shortening (*P*-axis). If the major through-going strike-slip fault is unchanged in shape, rotation can occur as in A (1 and 2). The stippled region of apparent extension near the main left lateral fault is a consequence of surface area being conserved from stage 1 to 2. In reality, the presence of thrusting indicates that area is not conserved, and it is likely that some complicated form of deformation, on many minor faults, occurs at the junction of the conjugate sets. An alternative visualization is shown in B, where displacement on the thrust faults(s) varies along strike (indicated by the length of the arrows on the thrust). This too will lead to a rotation in the same sense and also require complicated multiple fracturing in the stippled areas. Note, however, that there is no particular reason why the through-going left lateral fault should keep its geometry unchanged, and that these cartoons are, of course, gross simplifications.

An unsatisfactory feature of both McKenzie's (1972) and Nowroozi's (1972) work was that neither offered any explanation for the lack of seismicity between 60° and 65°E north of the Makran coast. The gap must be a temporary feature because the motion between the Arabian Sea and Eurasia must be taken up somewhere within the Alpine–Himalayan Belt. The information presented in Sections 7 and 8 suggests that the active structures in NE Iran do not continue eastward through Afghanistan, as Nowroozi (1972) and Wellman (1966) thought, but are connected through a series of north–south structures with the Makran coast, as Gutenberg & Richter (1954) appeared to believe. The satellite images of eastern Iran (see Mohajer-Ashjai *et al.* 1975 and Plate 6) clearly show a system of north–south structures between 59° and 61°E that truncate the older NE trending structures east of Birjand. The satellite images of Afghanistan show that there is no clear eastward continuation of the Kopet Dag structures that is now active, although there are apparent dextral offsets of drainage on the Hari Rud Fault further east at about 65°E (Wellman 1966; Auden 1974; Sborshchikov *et al.* 1981).

The fault plane solutions in NE Iran show that the region is dominated by strike-slip and thrust faulting. The slip vectors in Fig. 19, together with the lack of seismicity north of the Kopet Dag and in Afghanistan, show that the NE compression seen in the folds and thrusts of the Zagros mountains to the SW persists farther NE as Iran is pushed against its stable north-eastern and eastern borders. The compression of NE Iran against its borders is also evident in the topography (Fig. 19). In Section 7 it was shown that both east–west left lateral and north–south right lateral strike-slip faulting are present in NE Iran, as well as thrust faulting with a north-westerly strike. This complete system of thrust and conjugate strike-slip faults is consistent with a north-easterly direction of shortening. Fig. 27 shows that the NW-trending ranges are bordered by thrusts and that the dominant strike-slip system is left lateral with an easterly strike. It is not possible for two intersecting strike-slip

systems to be active simultaneously, and it appears that the north–south right lateral set is subordinate to, and does not intersect, the major east–west faults of Dasht-e-Bayaz and Doruneh. This combination of one dominant strike-slip fault with an accompanying mixture of subsidiary conjugate strike-slip faults and thrusts will inevitably lead to major structural rotations in the areas either side of the main fault, as has been noticed in the western USA (e.g. Garfunkel 1974; Bohannon & Howell 1982). There are numerous ways in which the rotation may be accomplished, one of the easiest to visualize being when the shape of the through-going major fault remains unaltered (Fig. 33). In practice it is not really helpful to visualize these motions in terms of blocks because the presence of thrust faulting indicates that surface area is not conserved, and some sort of pseudo-continuous deformation, probably involving multiple fracturing on numerous small faults, must occur where the faults meet. The same effect may also be achieved if the magnitude of thrusting varies along strike (Fig. 33b). Unfortunately it is not possible to predict that the dominant east–west strike-slip system in Fig. 27 will necessarily lead to an overall clockwise rotation in the area, as is implied in Fig. 33. If the stable western edge of Afghanistan is constrained to keep its shape, the east–west left lateral set will cause a shear in a clockwise sense, with local anticlockwise rotations caused by the subsidiary right lateral set. Moreover, there is no particular reason why the dominant strike-slip set should retain its original shape. The San Andreas Fault in the region of the Big Bend does not (see Garfunkel 1974; Bohannon & Howell 1982), and east of Torbat-e-Heydarieh the Doruneh fault curves dramatically to the south (Fig. 27), where it probably acquires a component of thrust motion. This combination of strike-slip and thrust faulting must eventually lead to shortening and crustal thickening in the Kopet Dag, though by that stage the various units making up the folded belt will have suffered considerable rotations and relative displacements along strike. It is likely that structures such as the Doruneh Fault are responsible for large lateral displacements during their early history as strike-slip faults and then, as a result of progressive horizontal rotation, become thrusts. By this mechanism, the original juxtaposition of adjacent units in a thrust belt is obscured, and it cannot be assumed that palinspastic restoration perpendicular to the regional strike is justified. Without detailed palaeomagnetic information, as well as a knowledge of the history of movement on the major strike-slip faults involved, reconstructions of such a fold belt will be speculative at best.

South of the Dasht-e-Bayaz region, in the central Lut, the north–south fault system predominates, with a mixture of thrusting and right lateral strike-slip. Left lateral conjugate faulting on east–west planes, where it is visible, is definitely subsidiary and does not cut the major north–south faults (Freund 1970).

The effect of these motions is to take up the north-eastern compression of Iran against the Turan shield, partly by crustal thickening and partly by the lateral motion of SE Iran on north–south faults towards the Makran, where it can override the oceanic crust of the Arabian Sea. The mixture of thrust and strike-slip fault motion by which this is accomplished is certain to lead to massive horizontal rotations, as the slowly accumulating palaeomagnetic data are starting to confirm. Preliminary measurements on volcanic rocks in eastern Iran have revealed anticlockwise rotations of 90° since the Miocene (Conrad *et al.* 1981) and 135° since the Triassic (Davoudzadeh, Soffell & Schmidt 1981). In the light of such evidence, palaeogeographic reconstructions of Iran based on stratigraphy alone, extending back as far as the Mesozoic (Takin 1972) or even Palaeozoic (Berberian & King 1981), are unlikely to be correct (see also Section 10).

The processes described here are consistent with what is known of the gross velocity and crustal structure of Iran. The careful analysis of Rayleigh-wave phase velocity dispersion and travel times between various stations in Iran by Asudeh (1981, 1982a, b), as well as the gravity analysis by Dehghani (1981), suggest a thickened crust of about 45 km under most of

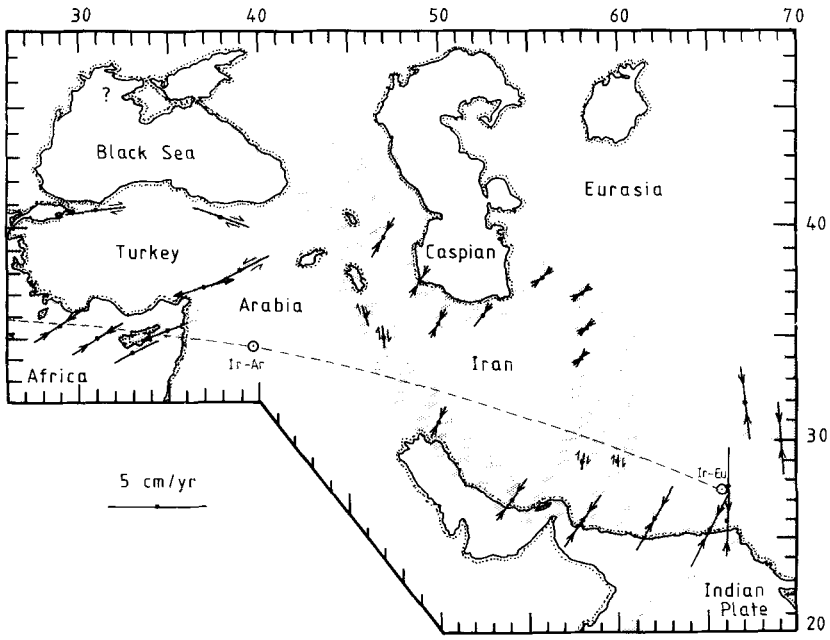

Figure 34. Summary of the active tectonics discussed in this paper. Stippled zones are those in which the present-day deformation is most intense. These surround areas such as central Turkey and central Iran, where, although some seismicity occurs, activity is *relatively* feeble. Slip vectors within these zones have been calculated from the poles and rates in Table 2 and are marked by arrows whose length is proportional to velocity. Directions are those across each belt and *not* relative to Eurasia. Arrows in the Alborz have been drawn assuming all the motion between Iran and Eurasia is taken up there. In reality these must be overestimates as some deformation is taken up in the belt crossing the Caspian. The dashed line is the projection of the great circle joining the Eurasia–Arabia pole with the Iran–Eurasia pole (marked by a circle). The Iran–Arabia pole must lie on this path, which crosses the Zagros (see text).

the Iranian plateau. In the Zagros, where upper mantle velocities are high (Asudeh 1982b) and S_n propagates efficiently (Kadinsky-Cade *et al.* 1981), the crust appears to thicken towards the NE reaching a maximum of about 50 km north of Shiraz, near the Main Zagros Reverse Fault. In NE Iran, upper mantle velocities are low and the propagation of high-frequency S_n inefficient. Both Asudeh (1982a) and Kadinsky-Cade *et al.* (1981) point out that this could be related to the widespread Quaternary alkali volcanism in NE Iran (see, e.g. Berberian & King 1981). Beneath the Black Sea and southern Caspian, the efficient propagation of S_n and poor propagation of L_g are consistent with an oceanic basement. The underthrusting of this material beneath the Alborz is presumably responsible for the large positive Bouger gravity anomaly south of the Caspian Sea (Dehghani 1981). The oceanic character of the basement in the Black Sea and southern Caspian probably accounts for the accommodation of some shortening in the Caucasus by elongation along strike (see Section 4). In the Zagros and eastern Kopet Dag elongation along strike is not seen, as sideways expulsion of material over oceanic-type basement is not possible. These motions will presumably lead to the eventual destruction of the southern Caspian and possible production of a slab dipping west or south in the interior of the continent, similar to that seen in the Hindu Kush. Neither the upper mantle velocity nor the observed gravity supports the existence of any significant amount of subducted continental crust in the Zagros, as envis-

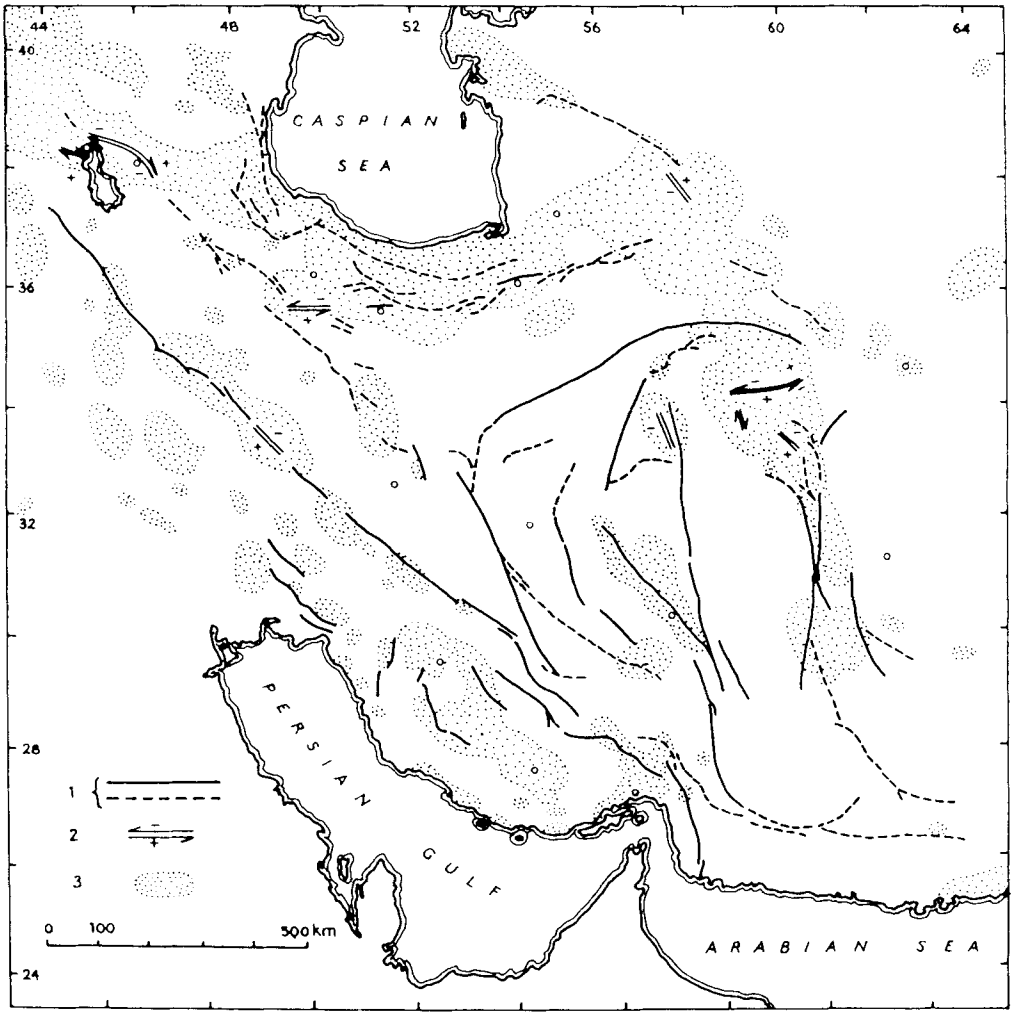

Figure 35. Historical seismicity of Iran, taken from Ambraseys & Melville (1982), with permission of the authors and publishers. (1) Solid lines show major faults of Quaternary age, dashed lines show faults of late Tertiary age. (2) Location, extent and sense of displacement of faulting associated with events since AD 700, superimposed on (3): areas affected by destructive earthquakes since AD 700.

aged by Bird, Toksöz & Sleep (1975) and Toksöz & Bird (1977). Finally, it should be noted that examination of the cumulative seismic moment from earthquakes recorded this century, reported by North (1974) and updated by Shoja-Taheri & Niazi (1981), indicates that less than 10 per cent of the predicted total motion between Arabia and Eurasia takes place seismically. As Ambraseys & Melville (1982) have emphasized, the same result holds for the historical record.

10 Discussion

It is clear from the preceding sections that the deformation is not distributed uniformly over the whole width of the active zone, but is concentrated in belts. The geometry of these belts is shown in Fig. 34, together with the type of movement involved in each. Fig. 35 is taken

Table 2. Poles marked (1) are from Chase (1978), those marked (2) were obtained by addition. If the first plate listed is taken to be fixed, the rotation rate is positive.

	Poles and angular velocities		
	Lat.	Long.	Rate °/10^7 yr
Eurasia–Turkey	14.6	34.0	6.43
Eurasia–Africa (1)	29.2	−23.5	1.42
Eurasia–Arabia (1)	34.9	7.2	4.93
Africa–Turkey (2)	9.3	44.7	5.73
Arabia–Turkey (2)	−20.6	68.9	3.40
Iran–Eurasia	27.5	65.8	5.60
Arabia–Iran (2)	34.5	39.8	9.55
Eurasia–India (1)	24.2	37.4	7.17

from Ambraseys & Melville (1982) and shows their summary of the seismic activity in Iran since AD 700. The similarity between the distribution of recent and historical seismicity is striking. The active belts are thus regions in which the deformation is taken up over long periods, and are not an artefact of the limited duration of the instrumental record. Since the relatively aseismic regions of central Turkey, central Iran and the southern Caspian are deforming slowly compared with the belts surrounding them, it should be possible to represent their motion with respect to Africa, Arabia and Eurasia by rotations about poles. Such a representation will obviously only be approximate, because the interior regions are undergoing slow deformation. However, as we shall see, the variation in the slip vector directions and in the levels of seismic activity corresponds very well with the predictions of this simple model. The belts which bound the relatively aseismic regions are not single faults, but contain distributed deformation over a width of up to 400 km. We therefore need continuum mechanics to describe the instantaneous deformation and to obtain a relationship between the present motions, the crustal thickness, palaeomagnetic and other rotations within these belts. We then use these ideas and the observations discussed above to suggest how some of the features in the area may have been produced.

10.1 MOTIONS OF THE MAJOR BLOCKS

In Turkey, the North Anatolian Fault is strongly arcuate and shows strike-slip motion between its eastern end and 31°E. This geometry was used in I to obtain the pole of rotation of Turkey with respect to Eurasia. We repeated the fit using the slip vectors of the events in Fig. 7 and obtained the pole position in Table 2. The angular velocity about this pole is less easy to determine because there are no spreading ridges on the boundary. We therefore used the construction outlined in I, which assumes that all the motion between Arabia and Eurasia is taken up on the North and East Anatolian Faults. Events such as 1975.9.6 show that this assumption is not strictly correct, and that the angular velocity obtained in this way will only provide an upper bound. Throughout this section the poles used to obtain the plate velocities are those given by Chase (1978). Use of those presented by Minster & Jordan (1978) gives essentially the same pole positions, but the angular velocities are all about 10 per cent smaller. The Africa–Turkey and Arabia–Turkey poles were then obtained by addition (Table 2).

The motion between Iran and Eurasia is less easy to determine than that between Turkey and Eurasia. Many of the earthquakes are caused by thrust faulting and a number of them produced no known surface breaks. In such cases we chose from the fault plane solution the

Table 3. Epicentres and observed slip vectors for earthquakes in north and east Iran, as well as slip vectors predicted from the poles in Table 2. Because it was not obvious which nodal plane to choose in 1981.8.28, a value of 027° was taken as the observed slip vector; being the mean of the two possible (017° and 037°).

Earthquake	Latitude	Longitude	Observed Az.	Calculated Az.
1957.7.2	36.14	52.70	030	034
1962.9.1	35.63	49.87	055	026
1968.8.31	33.97	59.02	072	046
1968.9.1	34.04	58.22	058	043
1968.9.4	33.99	58.24	057	043
1969.1.3	37.13	57.90	042	053
1978.9.16	33.39	57.43	038	037
1979.2.13	33.32	57.43	013	037
1980.1.12	33.49	57.19	035	037
1974.3.7	37.60	55.83	023	047
1970.7.30	37.82	55.88	042	048
1971.2.14	36.56	55.63	004	044
1971.5.26	35.51	58.22	039	049
1972.12.1	35.42	57.91	079	047
1973.8.2	37.35	56.51	048	049
1977.5.25	34.89	52.06	019	028
1979.1.16	33.90	59.47	035	047
1979.11.14	33.92	59.74	162	049
1979.11.27	33.96	59.73	075	049
1979.12.9	35.05	56.82	074	042
1981.6.11	29.91	57.72	000	017
1981.7.28	30.17	57.84	027	019

slip vector whose trend was closest to that of nearby earthquakes with surface breaks. The resulting azimuths and locations are given in Table 3. We first tried to obtain the pole position without using the slip vectors from 1981.6.11 and 1981.7.28. Though this data set accurately determined the direction in which the pole lay, it did not determine the distance. Inclusion of these two events resolved this uncertainty and gave the pole in Table 2. The angular velocity about the Iran–Eurasia pole is also somewhat difficult to determine. The difficulty arises because it is not obvious how much of the motion between Arabia and Eurasia is taken up in the Zagros, the boundary between Arabia and Iran, and how much on the boundary between Iran and Eurasia. This problem can be overcome by using the slip vectors in the Zagros. Since the position of the Iran–Eurasia pole is known, the value of the angular velocity about this pole determines the position of the Iran–Arabia pole if the Arabia–Eurasia pole and rotation rate are both known. The position of the Iran–Arabia pole must be compatible with the seismic observations in the Zagros. These show a mixture of thrusting and strike-slip movement in the NW. Moving SE, the seismicity increases but strike-slip motion is not seen. The Iran–Eurasia angular velocity in Table 2 gives a position for the Iran–Arabia pole which satisfies these conditions, but cannot be regarded as well determined.

There are still no reliable fault plane solutions in the belt of seismicity that extends from the Caucasus to the Kopet Dag. Therefore the motion of the southern Caspian with respect to Eurasia is still unknown. The absence of earthquakes with magnitude (m_b) greater than 5.3 on this boundary probably indicates that the relative motion is slow. For the reasons

discussed in Section 9, the direction of motion is probably similar to that of Iran with respect to Eurasia.

The direction and magnitudes of the slip vectors obtained from the poles in Table 2 are plotted in Fig. 34. Those in northern Turkey are parallel to the North Anatolian Fault because its motions were used to locate the pole. Slip vectors in south-eastern Turkey are parallel to the East Anatolian Fault because of the choice of the angular velocity between Turkey and Eurasia. However, west of the junction between Africa and Arabia the motion on the East Anatolian Fault must contain a normal faulting component. It is presumably this component that produced the Gulf of Iskenderun by extension. South of Cyprus the movement is strike-slip, changing to thrust faulting on the Florence Rise further west. The velocity is surprisingly large considering the low level of seismic activity in this region. A similar remark applies to the Makran, where there is also a great thickness of sediment overlying the plate which is being subducted. Both the direction and magnitude of the motion are, however, consistent with the presence of intermediate depth earthquakes beneath Antalya Bay. Such events would be expected to occur only within a slab dipping NE, produced by subduction west of Cyprus. The observed distribution of seismicity in Fig. 6 is therefore in excellent agreement with the predicted motions.

The predicted motions in the Zagros change from a combination of thrusting and right lateral strike-slip in the NW, with a slip rate of about 1 cm yr^{-1}, to pure thrusting with no strike-slip at a rate of 2.6 cm yr^{-1} in the SE (Fig. 34). The increase in rate can account for the increase in seismicity towards the SE, and the absence of strike-slip movement is compatible with the sinuosity of the southern part of the Main Zagros Reverse Fault (Fig. 20). The agreement between the slip vector directions and the strike of the nodal planes is good everywhere except near the Strait of Hormuz. Here both the earthquake mechanisms and the trend of the fold axes show that there is a larger component of movement towards the NW than is predicted by the slip vectors from the poles. This difference could be caused by the Musandam peninsular acting as a wedge driving material westward, in the same manner, but on a smaller scale, as Arabia itself is doing. Such westward movement could also contribute to the observed minor thrusting perpendicular to the regional strike (Fig. 21). Farther east, the predicted motion on the Oman Line is a combination of strike-slip and thrusting, and the thrusting component will be increased by any eastwards wedging driven by the Musandam peninsular. The velocity between Iran and Arabia increases eastwards, and beyond 63°E is little different in either magnitude or direction from that between Eurasia and Arabia. This behaviour is in agreement with the observed absence of variations in the structure of the Makran (Section 8). The direction of the slip vector obtained from the Iran–Arabia pole agrees well with those of 1972.8.6 and 1972.8.8 (Fig. 30).

The movement between Iran and Eurasia in NW Iran has a slightly different direction from that of the Araxes fault (Plate 3, Fig. 13). This difference is compatible with an eastward movement of the Azarbaijan block with respect to both Iran and Eurasia, which is also shown by 1980.5.4 and 1978.11.4 (Fig. 13). Farther to the SE, the slip vector of 1962.9.1 agrees well with that predicted, as do most of the mechanisms in north and east Iran. In the eastern Alborz the motion contains a component of left lateral strike-slip, and changes to pure thrusting in the north-eastern part of the boundary. The slip rate decreases continuously from the NW to the SE, as the position of the pole is approached, and the motion in eastern Iran changes from a combination of strike-slip and thrusting in the north to pure strike-slip in the south. Because the location of the pole is so close to the junction between this belt and the Makran no major structure is required to take up the motion. This geometry can thus explain why the east–west coastal ranges of the Makran appear absolutely unaffected by any north–south structures both on satellite images (Plate 8)

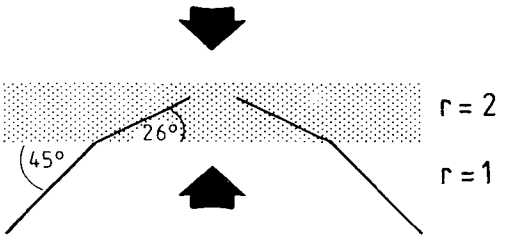

Figure 36. Cartoon to illustrate fault rotation as a result of shortening. The stippled band marks a region where uniaxial shortening by a factor (r) of 2 in the direction shown by the arrows has occurred. The shortening has rotated a fault initially at 45° to the zone to a new angle of 26°.

and offshore (White 1982). Throughout this region the agreement, in both direction (see Table 3) and rate, between the motion calculated from the pole positions and the observations is surprisingly good.

The motion across the eastern part of the Makran is between Arabia and Eurasia and changes to India–Eurasia where the active belt joins that from the Murray Ridge. The motion predicted from the India–Eurasia pole is in good agreement with the strike of the Ornach Nal Fault and the slip vector of 1974.10.4, if plane 1 is the fault plane (Figs 30 and 31f). Further north, the Chaman Fault Zone is not parallel to the India–Eurasia slip vector, probably because of the deformation inthe Zhob and Loralai ranges.

The movement of Turkey and Iran away from the Caucasus dominates the deformation of the whole region. The agreement between the slip vectors calculated from the poles in Table 2 and the observed motions is striking, and suggests that the rate of internal deformation of both Iran and Turkey is much smaller than that of the belts between these regions and the plates on either side. In this sense both Turkey and Iran can be described as plates.

10.2 DEFORMATION WITHIN THE ACTIVE BELTS

The strain rate and not the stress must control the deformation within the active belts between the plates, because the observed slip vectors agree well with those calculated from the poles. We should therefore seek a description of this deformation in terms of velocities and displacements, not stresses. Although, ultimately, a description in terms of stresses may be desirable, we have, at present, no way of measuring such stresses.

In the western part of the region the main motion occurs on strike-slip faults, and is eventually taken up by the movement of the Aegean. These strike-slip faults are vertical and the deformation is restricted to zones no more than a few kilometres wide. Such zones can therefore be described as plate boundaries. In contrast, the thrusting in the Caucasus, Zagros and northern Iran is distributed over a zone several hundred kilometres wide. In northern and eastern Iran there is some shearing between the two sides of the active belt, whereas in the Zagros and NE Iran there is little movement parallel to the boundaries of the belt. In the Caucasus the active region appears to have a small component of elongation along its strike. The deformation associated with these types of strain is discussed in McKenzie & Jackson (1983). Since shortening is occurring in all these belts, there will be rotation of any vectors attached to the material within them. This rotation will tend to align all vectors parallel to the strike of the belt. The most obvious and prominent markers in the material are the strike-slip faults such as the Dasht-e-Bayaz and Doruneh faults in NE Iran. These faults probably start as straight lines, and are presumably formed by the initial deformation on the SW margin of the deforming belt. As they move NE into the belt of shortening they must be

rotated in the way shown in Fig. 36. We can use the shape of the Doruneh Fault and the expressions given by McKenzie & Jackson (1983) to estimate some of the parameters which control this deformation. They consider a velocity field

$$u = (S-T)x + Wy \tag{1}$$
$$v = -(S+T)y$$

where u is in the x-direction, v in the y-direction, and S, T and W are constants. The long axis of the deforming belt is taken to be in the x-direction. $S = T = 0$, $W > 0$ corresponds to progressive simple shear (Hobbs, Means & Williams 1976). $W = T = 0$, $S > 0$ corresponds to progressive pure shear, with shortening in the y-direction and extension in the x-direction without any crustal thickening. $W = S = 0$, $T > 0$ produces crustal thickening by uniform contraction in the x- and y-directions. As McKenzie & Jackson (1983) point out, homogeneous strain within the belt is only possible if $S = T$. They also show that, if a vector initially makes an angle θ with the x-axis, then after deformation the same vector will make an angle θ', where

$$\tan\theta' = \frac{\tan\theta \exp(-2St)}{(1 + W\tan\theta/2S)} \tag{2}$$

and t is the duration of the deformation. The two constants T and W can be estimated from the crustal thickening and palaeomagnetic rotation respectively, but S is in general difficult to obtain. Only when markers are present can S be estimated. We can illustrate these remarks by using the geometry of the Doruneh Fault to estimate St. If we assume that $W = 0$ in north-eastern Iran and take the normal to the slip vector to be the x-axis, then the Doruneh Fault in Fig. 27 makes an angle of 59° with the x-axis at its western end, changing to 14° at its eastern end. Substitution in (2) gives

$$St = 0.95. \tag{3}$$

If we now assume that $S = T$ we can use (1), the width of the belt and the slip rate to estimate t. The velocity between the sides of the belt is given by the pole of rotation between Iran and Eurasia and is about 1 cm yr^{-1} (Fig. 34). If the width of the belt is 100 km, (1) gives

$$s = 5 \times 10^{-8}\ yr^{-1}$$

and

$$t = 19\ Ma.$$

This attempt to relate the shape of the Doruneh Fault to a continuum description of the deformation should not be regarded as more than an illustration. The assumption that $W = 0$ has not been tested using palaeomagnetic observations, and it seems improbable that the deformation has continued at a constant rate for 20 Ma.

The principal geometric effect of the deformation is the large rotations which strike-slip faults undergo in such belts. Under such conditions the faults will cease to be strike-slip faults as they become sub-parallel to the shortening direction. If they are to remain active they must therefore become thrusts. Such behaviour is illustrated by the eastern end of the Doruneh Fault in Fig. 27. Once the nature of the faulting has changed from strike-slip faulting to thrusting, the amount, or even the existence of strike-slip faulting will be difficult

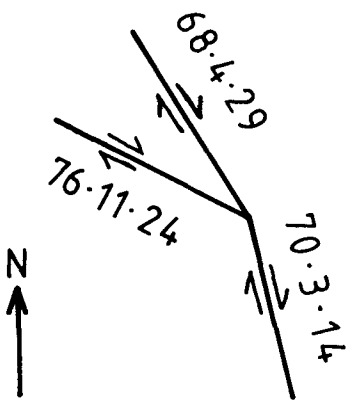

Figure 37. Orientation of the three active dextral strike-slip faults on the Turkey–Iran border (see Figs 12 and 13). This geometry cannot persist for long periods, and perhaps indicates that a new generation of strike-slip faults is cutting an older generation that had been rotated by shortening (see text).

to detect geologically. If strike-slip motions are to continue, new faults must form at a greater inclination to the deforming belt than the original faults. A fault system of this kind probably exists on the Turkey–Iran border, sketched in Fig. 37, and in the Markansu valley of Tadjikistan (Jackson *et al.* 1979). Both areas have undergone considerable shortening, which could have produced the necessary rotation.

The northern and eastern belts of Iran are not only undergoing shortening, but are also being sheared. Therefore, in these regions, not only should fault rotations occur but also palaeomagnetic rotations. As McKenzie & Jackson (1983) demonstrate, there is in general no simple relationship between the two rotations. In the simplest kinematic model of a deforming belt in which the velocity is given by (1), the palaeomagnetic rotation, Ψ, is given by

$$\Psi = \frac{-Wt}{2} .$$

It is clear that palaeomagnetic observations can provide important constraints on the deformation within the active belts. Though large rotations have been observed in eastern Iran (Conrad *et al.* 1981) the observations are as yet restricted in time and space, and cannot yet be used to investigate the history of the deformation in the region.

10.3 VULCANISM

Our last remark concerns vulcanism rather than kinematic questions. We have argued that the fault plane solutions, epicentral depths and the location of volcanoes in south-eastern Iran and western Afghanistan support earlier suggestions that a shallow thrust fault underlies the whole region south of the volcanoes. The argument that these features are connected depends on the existence of a few genuine sub-crustal earthquakes, which we believe are associated with subduction beneath the Makran. If this subduction ceased, the volcanoes would probably continue to be active for several million years, but their connection with subduction would no longer be apparent, both because of their distance from the Makran coast, and because their trend is at an oblique angle to the site of subduction. Exactly this problem arises with the volcanoes in central Turkey, which are not obviously related to any

subduction zone, though their chemistry suggests that they could be (Innocenti *et al.* 1975; Brinkmann 1976; Keller *et al.* 1977; Schleicher & Schwarz 1977). The geometry of the Makran shows that the surface expression of any associated subduction need not be nearby. In the case of central Turkey, the most obvious location for such subduction is in the active belt south of Cyprus. This belt is still subducting the Mediterranean west of Cyprus, and, if the westward motion of Turkey was less pronounced in the past, subduction would have been required along the whole belt. Alternatively, the subduction could have occurred along the Black Sea coast, though we feel that this possibility is less likely. But, wherever the site of subduction may have been, huge areas of southern or northern Turkey may be underlain by a thrust of shallow dip. The possibility that the thrusts in the Taurus mountains are splays from such a fault should be carefully examined.

It is even less clear whether the volcanoes in eastern Turkey are related to a previous subduction zone (Gülen 1982). If they are, it is also likely to have been several hundred kilometres away to the north or south, and again large parts of the area may be underlain by shallow thrusts.

The Hellenic Arc, the Florence Rise and the Makran all differ from the Pacific Island Arcs because there is a great thickness of sediment on the plate that is being subducted. The isotopic composition of the Aegean volcanics suggests that most of the sediments entering the Hellenic Trench are scraped off the subducting plate before the associated magma is generated (e.g. Barton, Salters & Huijsmans 1983). If the thrusts related to this subduction cut the surface in the Hellenic Trench, there is nowhere to put the sediment which is scraped off (McKenzie 1978a). For this reason a number of authors have suggested that the Mediterranean Ridge is underlain by a thrust, and contains the sediments scraped off the subducting plate (e.g. Kenyon, Belderson & Stride 1982). As in the Makran, there is little seismicity associated with this movement, and the geometry of the area is complicated. Furthermore, the Hellenic Trench is still a deep trough, presumably because some thrust faulting emerges on its inner wall (Fig. 38a). The Makran probably represents a later stage of the process, when none of the movement at the surface is taken up near the bend in the sinking slab, and the accumulated sediment pile is thicker and therefore exposed. As the sediment pile becomes thicker, the stresses on the basal thrust will increase, and so the transition from (a) to (b) in Fig. 38 will result from sediment accumulation alone. Once the sinking slab is beneath a pile of sediment it can peel back in the manner discussed by Jacoby (1973, 1976). This type of behaviour is especially likely if the consumption rate is increased. As the sinking slab moves towards the site of subduction it will leave behind the volcanoes, and may also have sufficient negative buoyancy to produce extension in the sediment wedge. These processes could account for the present geometry of the region between the Florence Rise and central Turkey as well as the basins north of Cyprus. The peeling back may have resulted from an increase in subduction rate when Turkey started moving rapidly westward.

11 Conclusions

This study demonstrates that in the Middle East, as elsewhere in the Alpine–Himalayan Belt, there are large blocks in which the seismicity is relatively feeble. These blocks, such as central Turkey, the Iranian Plateau and the southern Caspian, can usefully be regarded as rigid, and their motions can be described by rotations about poles. This description in terms of poles accounts very well for the general slip vector directions and levels of seismicity throughout the region.

The new set of fault plane solutions presented here strongly supports previous suggestions that continental material is moving laterally away from the Caucasus to avoid crustal thickening. The new data also outline another relatively aseismic region, the Azarbaijan

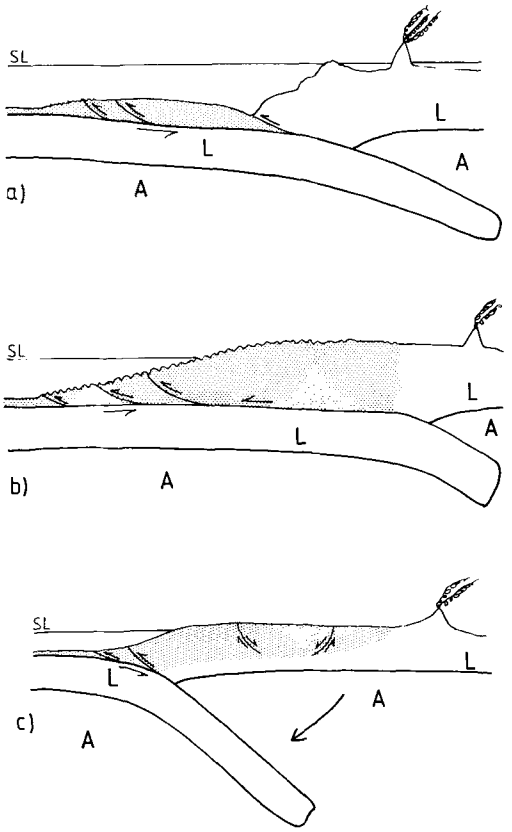

Figure 38. Three stages in the evolution of a subduction zone in which oceanic crust covered with a thick sedimentary section (shown dotted) is subducted. The first stage (a) shows the sediment pile decoupled from the lithosphere, but with a major part of the motion still taken up on the thrust which emerges in the trench. The geometry of the Hellenic Arc and Mediterranean Ridge resembles (a). The thickening of the sedimentary pile by thrusting eventually chokes the trench, (b), and gravitational forces transfer all the thrusting to the foot of the pile. The geometry of the subducted lithosphere remains unchanged, as does the location of the volcanoes. The geometry of the Makran resembles (b). Finally, in (c) the subducted lithosphere sinks into the asthenosphere A, and the gravitational energy released is sufficient to produce extension and normal faulting in the fore-arc region, which will probably occur on reactivated thrusts. The volcanoes are no longer above the sinking slab and will gradually become extinct, being replaced by new volcanoes in the extending region. The geometry NE of the Florence Rise resembles (c).

Block, which forms a NW protuberence to central Iran. Movement of material away from the Caucasus is made possible by low-angle thrusting over the basements of southern Caspian and Black Seas, which will lead to the eventual consumption and disappearance of these basins. The compression of the north-eastern borders of Iran against the stable shields of Turkmenistan and Afghanistan is accomplished by shortening in a belt up to 200–300 km wide and helped by the lateral movement of material southwards towards the Makran on strike-slip faults. The Makran accretionary wedge itself must extend about 200 km inland.

The relatively aseismic blocks are surrounded by active belts in which the seismicity is distributed over 200–300 km width. Within these deforming regions continuum theory is needed for a description of the kinematics, even though much of the motion is concen-

trated on faults. Interaction between faults within the mobile belts is controlled by geometric constraints, particularly the requirement that voids do not form and that conjugate strike-slip faults do not intersect. These constraints lead to the dominance of one strike-slip direction, which, combined with the thrusting, will lead to considerable structural rotations. The shearing accompanying the shortening in north and east Iran is responsible for large palaeomagnetic as well as fault rotations. The original relative juxtaposition of units within a deformed orogenic belt is obscured by these processes, and may bear no obvious relation to the present arrangement of units, especially since strike-slip faults, which in the early stages of collision can be responsible for considerable lateral movement, may change their orientation through rotation and become thrusts. The common geological assumption that such belts may be palispastically restored perpendicular to their strike is therefore probably not justified.

Most large shallow continental earthquakes appear to nucleate at depths of 8–15 km, and thus the deformation in these regions involves the basement even when, as in the Zagros, the sediments are known to be decoupled from the basement by horizons of evaporites or shale. As seen in the Makran and Mediterranean Ridge, the basement and sedimentary cover need not deform in the same place. This too may obscure the geological record and in particular remove any obvious association between vulcanism and subduction.

Although the processes described in this paper are complicated, they appear to be the consequence of rather simple notions; the relative strength of old shield areas, the difficulty of subducting continental crust, and the ease with which oceanic-type basement may be overridden. Compression against a stable shield, as is observed in NE Iran, is known to have occurred many times in the geological record. In general the direction of motion will not be perpendicular to the edge of the shield and compression will thus involve both shortening and shearing, as is seen in the Middle East. The processes described here should therefore be looked for in the older geological record and their effects, which are considerable, accounted for; otherwise detailed reconstructions of continental orogenic belts are unlikely to be correct.

Acknowledgments

We would like to thank N. N. Ambraseys for many helpful discussions and for introducing us to much unpublished data. Peter Molnar generously made available some unpublished fault plane solutions in western Pakistan, which are shown in Fig. 30 and Table 1. Peter Molnar, Muawia Barazangi, Celal Şengör and Graham Yielding suggested several improvements to this manuscript. Mansour Niazi kindly provided us with the results of his unpublished aftershock survey of the 1976.11.7a earthquake in eastern Iran. The skill of D. Bursill in producing clear photographs from appalling original drawings is also much appreciated. This work was supported by the Natural Environment Research Council and is contribution number 471 of the Department of Earth Sciences, Cambridge University.

References

Abdel-Gawad, M., 1971. Wrench movements in the Baluchistan arc and relation to Himalayan–Indian Ocean tectonics, *Bull. geol. Soc. Am.*, **82**, 1235–1250.

Adeli, H., 1982. The Sirch (Kerman, Iran) earthquake of 28 July 1981: a field investigation, *Bull. seism. Soc. Am.*, **72**, 841–861.

Akashah, B., Javahari, J. H., Ishki, I. & Islami, A. A., 1980. The Giv earthquake of 19 December 1980, *J. Earth Space Phys. Teheran Univ.*, **9**, 23–26.

Allen, C. R., 1965. Transcurrent faults in continental areas, *Phil. Trans. R. Soc.*, **258**, 82–89.

Allen, C. R., 1969. Active faulting in northern Turkey, *Div. geol. Sci., Contr. No. 1577,* California Institute of Technology, Pasadena.

Allen, C. R., 1975. Geological criteria for evaluating seismicity, *Bull. geol. Soc. Am.,* **86,** 1041–1057.

Alptekin, O., 1973. Focal mechanisms of earthquakes in western Turkey and their tectonic implication, *PhD thesis,* Faculty of New Mexico Institute for Mining and Technology.

Alptekin, O. & Ezen, U., 1978. Focal mechanisms of some earthquakes in the region surrounding the Akkuyu nuclear power plant site, *Rep. Tech. Univ. Istanbul, TEK-77-02/3.*

Ambraseys, N. N., 1963. The Buyin-Zara (Iran) earthquake of September, 1962: a field report, *Bull. seism. Soc. Am.,* **53,** 705–740.

Ambraseys, N. N., 1965. The seismic history of Cyprus, *Revue Un. int. Secours, no. 3,* 25–48.

Ambraseys, N. N., 1970. Some characteristic features of the North Anatolian Fault zone, *Tectonophys.,* **9,** 143–165.

Ambraseys, N. N., 1971. Value of historical records of earthquakes, *Nature,* **232,** 375–379.

Ambraseys, N. N., 1974. The seismicity of Iran: the Silakhor, Lurestan, earthquake of 23rd January 1909; part II, *Annali Geofis.,* **27,** 399–427.

Ambraseys, N. N., 1975. Studies in historical seismicity and tectonics, in *Geodynamics Today; a review of the Earth's dynamic processes,* pp. 7–16, Royal Society, London.

Ambraseys, N. N., 1978. The relocation of epicentres in Iran, *Geophys. J. R. astr. Soc.,* **53,** 117–121.

Ambraseys, N. N., 1981. The El Asnam (Algeria) earthquake of 10 October 1980: conclusions drawn from a field study. *Q. J. eng. Geol.,* **14,** 143–148.

Ambraseys, N. N., Arsovski, M. & Moinfar, A., 1979. The Gisk earthquake of 19 December 1977 and the seismicity of the Kuhbanan fault zone, *UNESCO Publ. No. FMR/SC/GEO/79/192,* Paris.

Ambraseys, N. N. & Jackson, J. A., 1982. Earthquake hazard and vulnerability in the northeastern Mediterranean, *Disasters,* **5,** 355–368.

Ambraseys, N. N. & Melville, C. P., 1977. The seismicity of Kuhistan, Iran, *Geogrl J.,* **14,** 179–199.

Ambraseys, N. N. & Melville, C. P., 1982. *A History of Persian Earthquakes,* Cambridge University Press, 219 pp.

Ambraseys, N. N. & Moinfar, A., 1973. The seismicity of Iran: the Silakhor, Lurestan earthquake of 23rd January 1909, *Annali Geofis.,* **26,** 659–678.

Ambraseys, N. N. & Moinfar, A., 1974a. The seismicity of Iran: the Firuzabad, Nehavend, earthquake of 16th August 1958, *Annali Geofis.,* **27,** 1–21.

Ambraseys, N. N. & Moinfar, A., 1974b. The seismicity of Iran: the Karkhaneh, Kangavar, earthquake of 24th March 1963, *Annali Geofis.,* **27,** 23–36.

Ambraseys, N. N. & Moinfar, A., 1975. The seismicity of Iran: the Turshiz, Kashmar-Khorsan earthquake of 25th September 1903, *Annali Geofis.,* **28,** 253–269.

Ambraseys, N. N. & Moinfar, A., 1977a. The Torud earthquake of 12th February 1953, *Annali Geofis.,* **30,** 185–200.

Ambraseys, N. N. & Moinfar, A., 1977b. The Kaj Darakht, Torbat-e-Haidariyyeh earthquake in Iran of 25th May 1923, *Annali Geofis.,* **30,** 3–18.

Ambraseys, N. N., Moinfar, A. & Peronaci, F., 1973. The seismicity of Iran: the Farsinaj, Kermanshah, earthquake of 13th December 1957, *Annali Geofis.,* **26,** 679–692.

Ambraseys, N. N., Moinfar, A. & Tchalenko, J. S., 1971. The Karnaveh (Northeast Iran) earthquake of 30 July, 1970, *Annali Geofis.,* **24,** 475–495.

Ambraseys, N. N. & Tchalenko, J. S., 1969. The Dasht-e-Bayaz (Iran) earthquake of August 31, 1968: A field report, *Bull. seism. Soc. Am.,* **59,** 1751–1792.

Ambraseys, N. N. & Tchalenko, J., 1972. Seismotectonic aspects of the Gediz, Turkey, earthquake of March 1970, *Geophys. J. R. astr. Soc.,* **30,** 229–252.

Ambraseys, N. N. & Zatopek, A., 1968. The Varto, Ustukran (Anatolia) earthquake of 1966 August 19: a summary of a field report, *Bull. seism. Soc. Am.,* **58,** 47–102.

Ambraseys, N. N. & Zatopek, A., 1969. The Mudurnu, west Anatolia, Turkey, earthquake of 1967, July 22, *Bull. seism. Soc. Am.,* **59,** 521.

Armbruster, J., Seeber, L., Quittmeyer, R. & Farah, A., 1979. Seismic network data from Quetta, Pakistan, *Rec. geol. Surv. Pakist.,* **49,** 1–5.

Arni, P., 1938. Zum Erdbeben zwischen Kirşehir, Keskin und Yerköy, *Veröff. Int. Lagerstättenforsch. der Türkei, Serie B: Abhandlungen no. 1,* 38 pp.

Arpat, E., 1977a. 1975. Lice depremi *Yeryuvari ve insan,* **2,** 15–28.

Arpat, E., 1977b. 1976 Çaldiran depremi *Yeryuvari ve insan,* **2,** 29–41.

Arpat, E. & Şaroğlu, F., 1972. The East Anatolian Fault system: thoughts on its development, *Bull. Miner. Res. Explor. Inst., Turkey,* **78,** 33–39.

Arpat, E. & Şaroğlu, F., 1975. Türkiye deki Bazi Önemli Genç Tektonik Olaylar, *Tür. Jel. Kür. Bül.*, **18**, 91–101.

Asudeh, I., 1981. The crust and upper mantle structure of Iran, *PhD thesis*, University of Cambridge, 113 pp.

Asudeh, I., 1982a. P_n velocities beneath Iran, *Earth planet. Sic. Lett.*, **61**, 136–142.

Asudeh, I., 1982b. Seismic structure of Iran from surface and body wave data, *Geophys. J. R. astr. Soc.*, **71**, 715–730.

Ateş, R. & Bayulki, N., 1977. *26 Mart 1977 Palu (Elazig) Depremi*, Deprem Araştirma Enstitüsü, Ankara.

Auden, J. B., 1974. Afghanistan–West Pakistan, in *Mesozoic-Cenozoic Orogenic Belts*, ed. Spencer, A. M. *Spec. Publs geol. Soc. London, No. 4*, 235–253, Geological Society, London.

Aytun, A., 1971. Experience gained from recent earthquakes in Turkey, *Cento Conf. Working Pap. No. 7*, Istanbul.

Barton, M., Salters, V. & Huijsmans, J., 1983. Sr-isotope and trace element evidence for the role of continental crust in calc-alkaline volcanism on Santorini and Milos, Aegean Sea, Greece, *Earth planet. Sci. Lett.*, **63**, 273–291.

Ben-Menahem, A., Nur, A. & Vered, M., 1976. Tectonics, seismicity and structure of the Afro-Eurasia junction – the breaking of an incoherent plate, *Phys. Earth planet. Int.*, **12**, 1–50.

Berberian, M., 1976. Contributions to the seismotectonics of Iran (Part 2), *Rep. geol. Surv. Iran, No. 39.*

Berberian, M., 1977. Contributions to the seismotectonics of Iran (Part 3), *Rep. geol. Surv. Iran, No. 40.*

Berberian, M., 1979a. Evaluation of the instrumental and relocated epicentres of Iranian earthquakes, *Geophys. J. R. astr. Soc.*, **58**, 625–630.

Berberian, M., 1979b. Earthquake faulting and bedding thrusts associated with the Tabas-e-Golshan (Iran) earthquake of 16 September 1978, *Bull. seism. Soc. Am.*, **69**, 1861–1887.

Berberian, M., 1981. Active faulting and tectonics of Iran, in *Zagros, Hindu Kush, Himalaya Geodynamic Evolution*, eds Gupta, H. K. & Delany, F. M., *Geodyn. Ser. Am. geophys. Un.*, **3**, 33–69.

Berberian, M., 1982. Aftershock tectonics of the Tabas-e-Golshan (Iran) earthquake sequence: a documented active 'thick and thin skinned tectonic' case, *Geophys. J. R. astr. Soc.*, **68**, 499–530.

Berberian, M. & Arshadi, S., 1976. On the evidence of the youngest activity of the North Tabriz fault and the seismicity of Tabriz city, *Rep. geol. surv. Iran. No. 39*, 397–418.

Berberian, M., Asudeh, I. & Arshadi, S., 1979. The surface rupture and mechanism of the Bob-Tangol (south-eastern Iran) earthquake of 19 December 1977, *Earth planet. Sci. Lett.*, **42**, 456–462.

Berberian, M., Asudeh, I., Bilham, R. G., Scholz, C. H. & Soufleris, C., 1979. Mechanism of the main-shock and the aftershock study of the Tabas-e-Golshan (Iran) earthquake of September 16, 1978: a preliminary field report, *Bull. seism. Soc. Am.*, **69**, 1851–1859.

Berberian, M., Jackson, J. A., Ghorashi, M. & Kajar, M. H., 1984. Field and teleseismic observations of the 1981 Golbaf-Sirch (SE Iran) earthquakes, *Geophys. J. R. astr. Soc.*, **77**, in press.

Berberian, M. & King, G., 1981. Towards a palaeogeography and tectonic evolution of Iran, *Can. J. Earth. Sci.*, **18**, 210–265.

Berberian, F., Muir, I. D., Pankhurst, R. J. & Berberian, M., 1982. Late Cretaceous and early Miocene Andean-type plutonic activity in northern Makran and central Iran, *J. geol. Soc. Lond.*, **139**, 605–614.

Bird, P., 1978. Finite element modelling of lithosphere deformation: the Zagros collision orogeny, Tectonophys., **50**, 307–336.

Bird, P., Toksöz, M. & Sleep, N., 1975. Thermal and mechanical models of continent–continent convergence zones, *J. geophys. Res.*, **80**, 4405–4416.

Bohannon, R. G. & Howell, D. G., 1982. Kinematic evolution of the junction of the San Andreas, Garlock and Big Pine faults, California, *Geology*, **10**, 358–363.

Brinkmann, R., 1976. *The Geology of Turkey* (F. E. Verlag, Stuttgart), Elsevier, Amsterdam.

Butler, R., 1982. The 1973 Hawaii earthquake: a double earthquake beneath the volcano of Mauna Kea, *Geophys. J. R. astr. Soc.*, **69**, 173–186.

Byron, R., 1937. *The Road to Oxiana*, London.

Camp, V. E. & Griffis, R. J., 1982. Character, genesis and tectonic setting of igneous rocks in the Sistan suture zone, eastern Iran, *Lithos*, **15**, 221–239.

Chandra, U., 1981. Focal mechanism solutions and their tectonic implications for the eastern Alpine–Himalayan region, in *Zagros, Hindu Kush, Himalaya Geodynamic Evolution*, eds Gupta, H. K. & Delaney, F. M., *Geodyn. Ser. Am. geophys. Un.*, **3**, 243–271.

de Charpal, O., Montadert, L., Guennoc, P. & Roberts, D. G., 1978. Rifting, crustal attenuation and subsidence in the Bay of Biscay, *Nature*, **275**, 706–711.

Chase, C. G., 1978. Plate kinematics: the Americas, East Africa, and the rest of the world, *Earth planet. Sci. Lett.*, **37**, 355–368.

Chen, W.-P. & Molnar, P., 1983. Focal depths of intracontinental and intraplate earthquakes and their implications for the thermal and mechanical properties of the lithosphere, *J. geophys. Res.*, **88**, 4183–4214.

Cohen, C. R., 1982. Model for a passive to active continental margin transition: implications for hydrocarbon exploration, *Bull. Am. Ass. Petrol. Geol.*, **66**, 708–718.

Colmann-Sadd, S. P., 1978. Fold development in the Zagros simply folded belt, south-west Iran, *Bull. Am. Ass. Petrol. Geol.*, **62**, 984–1003.

Cominiakis, P. E. & Papazachos, B. C., 1972. Seismicity and some tectonic features of the Mediterranean Ridge, *Bull. geol. Soc. Am.*, **83**, 1093–1102.

Conrad, G., Montigny, R., Thuizat, R. & Westphal, M., 1981. Tertiary and Quaternary geodynamics of the southern Lut (Iran) as deduced from paleomagnetic, isotopic and structural data, *Tectonophys.*, **75**, T11–T17.

Dalmayrac, B. & Molnar, P., 1981. Parallel thrust and normal faulting in Peru and constraints on the state of stress, *Earth planet. Sci. Lett.*, **55**, 473–481.

Davoudzadeh, M., Soffel, H. & Schmidt, K., 1981. On the rotation of the Central-East-Iran microplate, *Neves Jb. Miner. Geol. Paläont. Mh.*, **1981**(3), 180–192.

Dehghani, G., 1981. Schwerfeld und Krustenaufbau im Iran, *Hamburger Geophys. Einzelschr. 54, Reihe A*, 74 pp.

Dewey, J. W., 1976. Seismicity of northern Anatolia, *Bull. seism. Soc. Am.*, **66**, 843–868.

Dewey, J. W. & Grantz, A., 1973. The Ghir earthquake of April 10, 1972 in the Zagros mountains of southern Iran: seismotectonic aspects and some results of a field reconnaissance, *Bull. seism. Soc. Am.*, **63**, 2071–2090.

Dimitrijevic, M. D., 1973. Geology of the Kerman region, *Rep. geol. Surv. Iran, No. Yu/52–1973.*

von Dollen, F. J., Alt, J. N., Tocher, D. & Nowroozi, A., 1977. Seismological and geologic investigations near Bandar Abbas, Iran, *Abstr. geol. Soc. Am.*, **9**, 521.

Dykstra, J. D. & Birnie, R. W., 1979. Segmentation of the Quaternary subduction zone under the Baluchistan region of Iran and Pakistan, in *Geodynamics of Pakistan*, eds Farah, A. & DeJong, K. A., Geological Survey of Pakistan, Quetta.

England, P. C., 1983. Constraints on the extension of continental lithosphere, *J. geophys. Res.*, **88**, 1145–1152.

England, P. C. & McKenzie, D. P., 1982. A thin viscous sheet model for continental deformation, *Geophys. J. R. astr. Soc.*, **70**, 295–321.

Eos, 1980. Frontpiece: *Landsat* image of the Chaman Fault, Pakistan, *Eos, Trans. Am. geophys. Un.*, **61**, 1182.

Erinç, S., Bener, M., Sungur, K. & Göcmen, K., 1971. 12 Mayis 1971 Burdur Depremi, *IU Edebiyet Fakultesi Yayinlari, No. 1707.*

Evans, R., Asudeh, I., Crampin, S. & Üçer, B., 1984. Microtectonics in the Marmara Sea region, in preparation.

Evans, G., Morgan, P., Evans, W. E., Evans, T. R. & Woodside, J. M., 1978. Faulting and halokinetics in the north-eastern Mediterranean between Cyprus and Turkey, *Geology*, **6**, 392–396.

Eyidoğan, H., 1980. The source parameters of the Lice, Turkey earthquake, in *Individual Studies by Participants at the IISEE, Tokyo*, **16**, 107–130.

Falcon, N. L., 1969. Problems of the relationship between surface structure and deep displacements illustrated by the Zagros Range, in *Time and Place in Orogeny, Spec. Publs geol. Soc. Lond.*, **3**, 9–22, Geological Society, London.

Falcon, N. L., 1976. The Minab anticline, in *The Geological Evolution of Southern Iran: the report of the Iranian Makran expedition*, ed. Sherman, D. J., *Geogrl J.*, **142**, 409–410.

Farah, A., 1976. Study of recent seismotectonics in Pakistan, *Proc. 4th meeting of CENTO working group on recent tectonics*, Istanbul.

Farhoudi, G. & Karig, D., 1977. Makran of Iran and Pakistan as an active arc system, *Geology*, **5**, 664–668.

Fitch, T. J., 1981. Correction and addition to 'Estimation of the seismic moment tensor from teleseismic body wave data with applications to intraplate and mantle earthquakes' by T. J. Fitch, D. W. McCowan & M. W. Shields, *J. geophys. Res.*, **86**, 9375–9376.

Freund, R., 1965. A model of the structural development of Israel and adjacent areas since Upper Cretaceous times, *Geol. Mag.*, **102**, 189–205.

Freund, R., 1970. Rotation of strike-slip faults in Sistan, south-east Iran, *J. Geol.*, **78**, 188–200.

Garfunkel, Z., 1974. Model for the late Cenozoic tectonic history of the Mojave Desert, California, and its relation to adjacent regions, *Bull. geol. Soc. Am.*, **85**, 1931–1944.

Garfunkel, Z., Zak, I. & Freund, R., 1981. Active faulting in the Dead Sea Rift, *Tectonophys.*, **80**, 1–26.

Gourdazi, K. M. & Ghaderi-Tafreshi, M., 1976. The Qaen, Khorassan earthquake of November 7, 1976, *Proc. CENTO Semin. Earthq. Hazard Minimization*, Teheran.

Griesbach, C. L., 1893. Notes on the earthquake in Baluchistan on 20th December 1892, *Rec. geol. Surv. India*, **26**(2), 57–61.

Gülen, L., 1982. Sr, Nd and Pb isotrope systematics of Ararat and Suphan volcanoes, eastern Turkey (Abstr.), *Eos Trans. Am. geophys. Un.*, **63**, 1145.

Gutenberg, B. & Richter, C. F., 1954. *Seismicity of the Earth and Associated Phenomena*, Princeton University Press, Princeton, New Jersey.

Haghipour, A. & Amadi, M., 1980. The November 14 to December 25, 1979 Ghaenat earthquakes of northeast Iran and their tectonic implications, *Bull. seism. Soc. Am.*, **70**, 1751–1757.

Halbouty, M. T., 1980. Geologic significance of Landsat data for 15 giant oil and gas fields, *Bull. Am. Ass. Petrol. Geol.*, **64**, 8–36.

Haynes, S. J. & McQuillan, H., 1974. Evolution of the Zagros suture zone, southern Iran, *Bull. geol. Soc. Am.*, **85**, 739–744.

Helwig, J., 1976. Shortening of continental crust in orogenic belts and plate tectonics, *Nature*, **290**, 768–770.

Hobbs, B. E., Means, W. D. & Williams, P. F., 1976. *An Outline of Structural Geology*, Wiley, London.

Hunting Survey Corporation, 1960. *Reconnaissance Geology of part of West Pakistan*, Government of Canada, Toronto, 550 pp.

Hutchison, I., Louden, K. E., White, R. S. & von Herzen, R. P., 1981. Heat flow and the age of the Gulf of Oman, *Earth planet. Sci. Lett.*, **56**, 252–262.

Innocenti, F., Mazzuoli, R., Pasquare, G., Radicati di Brozlo, F. & Villari, L., 1975. The Neogene calc-alkali volcanism of central Anatolia: geochronological data on Kayseri-Niğde area, *Geol. Mag.*, **112**, 349–360.

Innocenti, F., Mazzuoli, R., Pasquare, G., Radicati di Brozolo, F. & Villari, L., 1976. Evolution of the volcanism in the area of interaction between the Arabian, Anatolian and Iranian plates (Lake Van, E. Turkey), *J. Volcanol. Geotherm. Res.*, **1**, 103–112.

Jackson, J. A., 1980a. Reactivation of basement faults and crustal shortening in orogenic belts, *Nature*, **283**, 343–346.

Jackson, J. A., 1980b. Errors in focal depth determination and the depth of seismicity in Iran and Turkey, *Geophys. J. R. astr. Soc.*, **61**, 285–301.

Jackson, J. A. & Fitch, T. J., 1979. Seismotectonic implications of relocated aftershock sequences in Iran and Turkey, *Geophys. J. R. astr. Soc.*, **57**, 209–229.

Jackson, J. A. & Fitch, T. J., 1981. Basement faulting and the focal depths of the larger earthquakes in the Zagros mountains (Iran), *Geophys. J. R. astr. Soc.*, **64**, 561–586.

Jackson, J. A., Fitch, T. J. & McKenzie, D. P., 1981. Active thrusting and the evolution of the Zagros Fold Belt, in *Thrust and Nappe Tectonics*, eds McClay, K. & Price, N., *Spec. Publ. geol. Soc. London*, **9**, 371–379, Blackwell Scientific Publications, Oxford.

Jackson, J. A., Gagnepian, J., Houseman, G., King, G., Papadimitriou, P., Soufleris, C. & Virieux, J., 1982a. Seismicity, normal faulting and the geomorphological development of the Gulf of Corinth (Greece): the Corinth earthquakes of February and March 1981, *Earth planet. Sci. Lett.*, **57**, 377–397.

Jackson, J. A., King, G. & Vita-Finzi, C., 1982b. The neotectonics of the Aegean: an alternative view, *Earth planet. Sci. Lett.*, **61**, 303–318.

Jackson, J. A. & McKenzie, D. P., 1983. The geometrical evolution of normal fault systems, *J. struct. Geol.*, **5**, 471–482.

Jackson, J. A., Molnar, P., Patton, H. & Fitch, T., 1979. Seismotectonic aspects of the Markansu valley, Tadjikistan earthquake of August 11, 1974, *J. geophys. Res.*, **84**, 6157–6167.

Jackson, J. A. & Yielding, G., 1983. The seismicity of Kohistan: source parameters of the Hamran (1972.9.3), Darel (1981.9.12) and Patan (1974.12.28) earthquakes, *Tectonophys.*, **91**, 15–29.

Jacob, K. & Quittmeyer, R. C., 1979. The Makran region of Pakistan and Iran: trench-arc system with active plate subduction, in *Geodynamics of Pakistan*, eds Farah, A. & DeJong, K. A., Geological Survey of Pakistan, Quetta.

Jacoby, W. R., 1973. Model experiment of plate movements, *Nature*, **242**, 130–134.

Jacoby, W. R., 1976. Paraffin model experiment of plate tectonics, *Tectonophys.*, **35**, 103–113.

Jongsma, D. & Mascle, J., 1981. Evidence for northward thrusting southwest of the Rhodes basin, *Nature*, **293**, 49–51.

Kadinsky-Cade, K. & Barazangi, M., 1982. Seismotectonics of southern Iran: the Oman Line *Tectonics*, **1**, 389–412.

Kadinsky-Cade, K., Barazangi, M., Oliver, J. & Isacks, B., 1981. Lateral variations of high frequency seismic wave propagation at regional distances across the Turkish and Iranian plateaus, *J. geophys. Res.*, **86**, 9377–9396.

Kazmi, A. H. K., 1979. Active fault systems in Pakistan, in *Geodynamics of Pakistan*, eds Farah, A. & DeJong, K. A., Geological Survey of Pakistan, Quetta.

Keller, J., Jung, D., Burgath, K. & Wolff, F., 1977. Geologie und Petrologie des neogene Kalk-alkali vulcanismus von Konya (Ereuler Dag–Alacadag Massiv, zentral Anatolien), *Geol. Jb.*, **B25**, 37–117.

Kenyon, N. H., Belderson, R. H. & Stride, A. H., 1982. Detailed tectonic trends on the central part of the Hellenic Outer Ridge and in the Hellenic Trench System, in *Trench-Forearc Geology: Sedimentation and Tectonics in Modern and Ancient Active Plate Margins*, ed. Leggett, J. K., *Spec. Publ. geol. Soc. Lond.*, **10**, 335–343, Blackwell Scientific Publications, Oxford.

Ketin, I., 1948. Uber die tektonischmechanischen Folgerungen aus den grossen anatolischen Erdbeben des Letzten Dezenniums, *Geol. Rdsch.*, **36**, 77–83.

Ketin I. & Abdüsselamoğlu, S., 1970. Bartin depreminin etkileri, *Türk. Jeol. Kür. Bül.*, **12**, 66–76.

Khoshbakht-Marvi, A., 1977. A brief report of the Qaen earthquake of November 7, 1976. in Khorassan, Iran, *Proc. CENTO Semin. Earthq. Hazard Minimization*, Teheran. *Tech. Res. Stand. Bur. Plan Budget Org., Publ. no. 70*, 280.

King, G. & Vita-Finzi, C., 1981. Active folding in the Algerian earthquake of 10 October 1980, *Nature*, **292**, 22–26.

Kirrillova, I. V., Lyustikh, Ye. N., Rastvorova, V. A., Sorskiy, A. A. & Khain, V. Ye., 1960. *Analysis of the Geotectonic Development and the Seismic Nature of the Caucasus*, Academy of Sciences USSR, Moscow.

Koop, W. J. & Stoneley, R., 1982. Subsidence history of the Middle East Zagros basin, Permian to Recent, *Phil. Trans. R. Soc. A*, **305**, 149–168.

Langston, C. A. & Helmberger, D. V., 1975. A procedure for modelling shallow dislocation sources, *Geophys. J. R. astr. Soc.*, **42**, 117–130.

Lawrence, R. D., Khan, S. H., DeJong, K. A., Farah, A. & Yeats, R. S., 1981. Thrust and strike slip fault interaction along the Chaman transform zone, Pakistan, in *Thrust and Nappe Tectonics*, eds McClay, K. & Price, N., *Spec. Publ. geol. Soc. Lond.*, **9**, 363–370, Blackwell Scientific Publications, Oxford.

Lawrence, R. D. & Yeats, R. S., 1979. Geological reconnaissance of the Chaman Fault in Pakistan, in *Geodynamics of Pakistan*, pp. 351–358, eds Farah, A. & DeJong, K., Geological Survey of Pakistan, Quetta.

Lees, G. M., 1952. Foreland folding, *Q. Jl geol. Soc. Lond.*, **108**, 4–34.

Le Pichon, X. & Angelier, J., 1979. The Hellenic arc and trench system: a key to the neotectonic evolution of the eastern Mediterranean area, *Tectonophys.*, **60**, 1–42.

Letouzey, J., Biju-Duval, B., Dorkel, A., Gonnard, R., Kristchev, K., Montadert, L. & Sungurlu, O., 1977. The Black Sea: a marginal basin. Geophysical and geological data, in *Structural History of the Mediterranean Basins*, pp. 363–376, eds Biju-Duval, B. & Montadert, L., Editions Technip, Paris.

McCall, G. & Kidd, R., 1982. The Makran, south-eastern Iran: the anatomy of a convergent plate margin active from Cretaceous to present, in *Trench–Forearc Geology: Sedimentation and Tectonics in Modern and Ancient Active Plate Margins*, ed. Leggett, J. K., *Spec. Publ. geol. Soc. Lond.*, **10**, 387–397.

McKenzie, D. P., 1972. Active tectonics of the Mediterranean region, *Geophys. J. R. astr. Soc.*, **30**, 109–185.

McKenzie, D. P., 1976. The East Anatolian Fault: a major structure in eastern Turkey, *Earth planet. Sci. Lett.*, **29**, 189–193.

McKenzie, D. P., 1978a. Active tectonics of the Alpine–Himalayan Belt: the Aegean Sea and surrounding regions, *Geophys. J. R. astr. Soc.*, **55**, 217–254.

McKenzie, D. P., 1978b. Some remarks on the development of sedimentary basins, *Earth planet. Sci. Lett.*, **40**, 25–32.

McKenzie, D. P. & Jackson, J. A., 1983. The relationship between strain rates, crustal thickening, palaeomagnetism, finite strain and fault movements within a deforming zone, *Earth planet. Sci. Lett.*, **65**, 182–202.

McKenzie, D. P., Molnar, P. & Davies, D., 1970. Plate tectonics of the Red Sea and East Africa, *Nature*, **226**, 243–248.

Melaart, J., 1967. *Çatal Hüyük: a Neolithic Town in Anatolia*, pp. 59–60, Thames & Hudson, London.

Mercier, J., Vergeley, P. & Delibassis, N., 1973. Comparison between deformation deduced from the analysis of recent faults and from focal mechanisms of earthquakes (an example: the Paphos region, Cyprus), *Tectonophys.*, **19**, 315–332.

Minster, J. B. & Jordan, T. H., 1978. Present-day plate motions, *J. geophys. Res.*, **83**, 5331–5354.

Mohajer-Ashjai, A., Behzadi, H. & Berberian, M., 1975. Reflections on the rigidity of the Lut Block and recent crustal deformation in eastern Iran, *Tectonophys.*, **25**, 281–301.

Molnar, P. & Gray, D., 1979. Subduction of continental lithosphere: some constraints and uncertainties, *Geology*, **7**, 58–62.

Molnar, P. & Tapponnier, P., 1975. Cenozoic tectonics of Asia: effects of a continental collision, *Science*, **189**, 419–426.

Molnar, P. & Tapponnier, P., 1978. Active tectonics of Tibet, *J. geophys. Res.*, **83**, 5361–5375.

Molnar, P. & Tapponnier, P., 1981. A possible dependence of tectonic strength on the age of the crust in Asia, *Earth planet. Sci. Lett.*, **52**, 107–114.

Morelli, C., Pisani, M. & Gantar, C., 1975. Geophysical studies in the Aegean Sea and in the Eastern Mediterranean, *Boll. Geofis. teor. appl.*, **18**, 127.

MTA, 1962. *Geological Map of Turkey, 1:500 000*, MTA, Ankara.

Muehlberger, W. R., 1981. The splintering of the Dead Sea Fault Zone in Turkey, *Yebilimleri (Bull. Inst. Earth Sci., Hacettepe Univ.), Beytape Ankara*, **8**, 123–130.

Murris, R. J., 1980. Middle East: stratigraphic evolution and oil habitat, *Bull. Am. Ass. Petrol. Geol.*, **64**, 597–618.

Neprochnov, Yu. P., 1968. Structure of the Earth's crust of epicontinental seas: Caspian, Black Sea and Mediterranean, *Can. J. Earth Sci.*, **5**, 1037–1043.

Niazi, M., Asudeh, I., Ballard, G., Jackson, J., King, G. & McKenzie, D., 1978. The depth of seismicity in the Kermanshah region of the Zagros mountains (Iran), *Earth planet. Sci. Lett.*, **40**, 270–274.

Niazi, M. & Kanamori, H., 1981. Source parameters of the 1978 Tabas and 1979 Qainat, Iran, earthquakes from long period surface waves, *Bull. seism. Soc. Am.*, **71**, 1201–1213.

Niazi, M., Shimamura, H. & Matsu'ura, M., 1980. Microearthquakes and crustal structure off the Makran coast of Iran, *Geophys. Res. Lett.*, **7**, 297–300.

North, R. G., 1974. Seismic slip rates in the Mediterranean and Middle East, *Nature*, **252**, 560–563.

North, R. G., 1977. Seismic moment, source dimension and stresses associated with earthquakes in the Mediterannean and Middle East, *Geophys. J. R. astr. Soc.*, **48**, 137–161.

Nowroozi, A. A., 1972. Focal mechanism of earthquakes in Persia, Turkey, west Pakistan and Afghanistan and plate tectonics of the Middle East, *Bull. seism. Soc. Am.*, **62**, 832–850.

Nowroozi, A. A., Mohajer-Ashjai, A. M., Rad, M. R. S. & Izadpanah, A. A. Z., 1977. The mainshock and aftershocks of the March 21, 1977 earthquake in the Khurgu region, *Rep. atom. Energy Auth. Iran*, 56 pp.

Oldham, T., 1882. A catalogue of Indian earthquakes from the earliest time to the end of AD 1869, *Mem. geol. Surv. India* **19**(3), 163–215.

Page, W. D., Alt, J. N., Cluff, L. S. & Plafker, G., 1979. Evidence for the recurrence of large magnitude earthquakes along the Makran coast of Iran and Pakistan, *Tectonophys.*, **52**, 533–547.

Page, W. D., Anttonen, G. & Savage, W. U., 1978. The Makran coast of Iran, a possible seismic gap, in *Methodology for Identifying Seismic Gaps and Soon-to-break Gaps, Open File Rep. U.S. geol. Surv., 78–943*, 611–633.

Parejas, E. & Pamir, H. N., 1939. Le tremblement de terre du 19 avril 1938 en Anatolie centrale, *İstanb. Üniv. Fen. Fak. Mecm.*, **4**, 183–193.

Pinar, N., 1953. La geologie du bassin d'Adana (Turquie) et le seisme du 22 Octobre 1952, *İstanb. Üniv. Fen Fak., Mecm. A*, **18**, 231–241.

Quittmeyer, R. C., Farah, A. & Jacob, K., 1979. The seismicity of Pakistan and its relation to surface faults, in *Geodynamics of Pakistan*, eds Farah, A. & DeJong, K., Geological Survey of Pakistan, Quetta.

Quittmeyer, R. C. & Jacob, K., 1979. Historical and modern seismicity of Pakistan, Afghanistan, northwestern India and south-eastern Iran, *Bull. seism. Soc. Am.*, **69**, 773–823.

Rezanov, I. A. & Chano, S. S., 1969. Reasons for the absence of a 'granitic' layer in basins of the south Caspian and Black Sea type, *Can. J. Earth Sci.*, **6**, 671–678.

Richter, C. F., 1958. *Elementary Seismology*, Freeman, San Francisco.

Roecker, S. W., 1982. Velocity structure of the Pamir-Hindu Kush region: possible evidence of subducted crust, *J. geophys. Res.*, **87**, 945–959.

Rotstein, Y. & Kafka, A. L., 1982. Seismotectonics of the southern boundary of Anatolia, eastern Mediterranean region: subduction, collision and arc jumping, *J. geophys. Res.*, **87**, 7694–7706.

Rustanovich, D. N., 1974. The Zangezur earthquake of 1968, *Izv. Earth Phys.*, **11**, 15–29.

Rustanovich, D. N. & Shirakova, E. I., 1964. Some results of a study of the Askhabad earthquake of 1948, *Izv. Akad. Nauk. USSR, Ser. Geophiz.*, 1077–1080.

Sadovski, M. A., 1981. Earthquakes can be forecast, *Science in the USSR, No. 5*, 59–71.

Savage, W. U., Alt, J. N. & Mohajer-Ashjai, A., 1977. Microearthquake investigations of the 1972 Qir, Iran, earthquake zone and adjacent areas, *Abstr. geol. Soc. Am.*, **9**, 496.

Sborshchikov, I. M., Savostin, L. A. & Zonenshain, L. P., 1981. Present plate tectonics between Turkey and Tibet, *Tectonophys.*, **79**, 45–73.

Schleicher, H. & Schwarz, G., 1977. Zur Geologie und Petrographie des Karadağ, Zentralanatolien, *Geol. Jb.*, **B25**, 119–138.

Sclater, J. G. & Christie, P. A. F., 1980. Continental stretching: an explanation for the post-mid-Cretaceous subsidence of the Central North Sea Basin, *J. geophys. Res.*, **85**, 3711–3739.

Şengör, A. M. C., Burke, K. & Dewey, J. F., 1982. Tectonics of the North Anatolian Transform Fault, in *Multidisciplinary Approach to Earthquake Prediction*, pp. 3–22, eds Mete Işkara, A., Vogel, A., Friedr. Vieweg & Sohn, Braunschweig-Wiesbaden.

Şengör, A. M. C., Büyükaşikoğlu, S. & Canitez, N., 1983. Neotectonics of the Pontides: implications for 'incompatible' structures along the North Anatolian Fault, *J. struct. Geol.*, **5**, 211–216.

Setudehnia, A., 1978. The Mesozoic sequence in south-west Iran and adjacent areas, *J. Petrol. Geol.*, **1**, 3–42.

Seymin, I. & Aydin, A., 1972. The Bingöl earthquake fault and its relation to the North Anatolian Fault Zone, *Bull. Min. Res. Exp. Inst. Turkey*, **79**, 1–8.

Sherman, D. J., 1976. The geological evolution of southern Iran: the report of Iranian Makran expedition, *Geogrl J.*, **142**, 393–413.

Shikalibeily, E.Sh. & Grigoriants, B. V., 1980. Principal features of the crustal structure of the south Caspian basin and the conditions of its formation, *Tectonophys.*, **69**, 113–121.

Shirokova, E. I., 1962. Stresses effective in earthquake foci in the Caucasus and adjacent districts, *Izv. Akad. Nauk. USSR, Ser. Geophiz.*, **10**, 809.

Shirokova, E. I., 1967. General features in the orientation of principal stresses in earthquake foci in the Mediterranean–Asia seismic belt, *Izv. Acad. Nauk. USSR, Ser. Geophiz.*, **1**, 12–22.

Shirokova, E. I., 1977. Changes in the focal mechanisms and their relations to revived faults in the Middle and Far East, *Izv. Earth Phys.*, **13**, 621–626.

Shoja-Taheri, J. & Niazi, M., 1981. Seismicity of the Iranian plateau and bordering regions, *Bull. seism. Soc. Am.*, **71**, 477–489.

Shteynberg, V. V., Levshin, A. L., Aptekmian, Z. Y. & Grudeva, N. P., 1974. Mechanism and source parameters of the focus of the Dagestan earthquake of May 14, 1970, *Izv. Acad. Nauk. USSR, Ser. Geophiz.*, **2**, 3–14.

Sibson, R. H., 1982. Fault zone models, heat flow and the depth distribution of earthquakes in the continental crust of the United States, *Bull. seism. Soc. Am.*, **72**, 151–163.

Silver, P. G. & Jordan, T. H., 1983. Total moment spectra of fourteen large earthquakes, *J. geophys. Res.*, **88**, 3273–3294.

Simkin, T., Siebert, L., McDonald, L., Bridge, D., Newhall, C. & Latter, J. H., 1981. *Volcanoes of the World*, Academic Press, London, 232 pp.

Soufleris, C., Jackson, J. A., King, G., Papazachos, B., Scholz, C. & Spencer, C., 1982. The 1978 Thessaloniki earthquake series in northern Greece, *Geophys. J. R. astr. Soc.*, **68**, 429–458.

Stewart, G. S. & Kanamori, H., 1982. Complexity of rupture in large strike-slip earthquakes in Turkey, *Phys. Earth planet. Int.*, **28**, 70–84.

Stöcklin, J., 1968. Structural history and tectonics of Iran – a review, *Bull. Am. Ass. Petrol. Geol.*, **52**, 1229–1258.

Stöcklin, J., 1974. Possible ancient continental margins in Iran, in *The Geology of Continental Margins*, pp. 873–887, eds Burk, C. A. & Drake, C. L., Springer-Verlag, New York.

Stoneley, R., 1976. On the origin of ophiolite complexes in the southern Tethys region, *Tectonophys.*, **25**, 303–322.

Stoneley, R., 1982. On the structural development of the Wessex Basin, *J. geol. Soc. London*, **139**, 543–554.

Sykes, L. R., 1978. Intraplate seismicity, reactivation of pre-existing zones of weakness, alkaline magmatism, and other tectonism post-dating continental fragmentation, *Rev. Geophys. Space Phys.*, **16**, 621–688.

Szabo, F. & Kheradpir, A., 1978. Permian and Triassic stratigraphy, Zagros basin, south-west Iran, *J. Petrol. Geol.*, **1**, 58–82.

Takin, M., 1972. Iranian geology and continental drift in the Middle East, *Nature*, **235**, 147–150.

Tanner, S., 1983. A detailed survey in the Mediterranean Rise and Herodotus Basin area, *Geophys. J. R. astr. Soc.*, **73**, 173–196.

Tapponnier, P. & Molnar, P., 1977. Active faulting and tectonics in China, *J. geophys. Res.*, **82**, 2905–2930.

Tapponnier, P. & Molnar, P., 1979. Active faulting and Cenozoic tectonics of the Tien Shan, Mongolia and Baykal regions, *J. geophys. Res.*, **84**, 3425–3459.

Tchalenko, J. S., 1973a. Recent destructive earthquakes in the central Alborz, *Annali Geofis.*, **26**, 303–325.

Tchalenko, J. S., 1973b. The Kashmar (Turshiz) 1903 and Torbat-e-Heydarieh (south) 1923 earthquakes in central Khorassan (Iran), *Annali Geofis.*, **26**, 29–40.

Tchalenko, J. S., 1975. Seismicity and structure of the Kopet Dagh (Iran, USSR), *Phil. Trans. R. Soc.*, **278**, 1–25.

Tchalenko, J. S., 1977. A reconnaissance of the seismicity and tectonics at the northern border of the Arabian plate; Lake Van region, *Rev. Geogr. Phys. Geol. Dyn.*, **19**, 189–208.

Tchalenko, J. S. & Berberian, M., 1974. The Salmas (Iran) earthquake of May 6th, 1930, *Annali, Geofis.*, **27**, 151–212.

Tchalenko, J. S. & Berberian, M., 1975. Dasht-e-Bayaz fault, Iran: earthquake and earlier related structures in bedrock, *Bull. geol. Soc. Am.*, **86**, 703–709.

Tchalenko, J. S., Berberian, M. & Bezhadi, H., 1973. Geomorphic and seismic evidence for recent activity on the Doruneh Fault, Iran, *Tectonophys.*, **19**, 333–341.

Tchalenko, J. S. & Braud, J., 1974. Seismicity and structure of the Zagros (Iran): the Main Recent Fault between 33 and 35°N, *Phil. Trans. R. Soc. A*, **277**, 1–25.

Tillman, J. E., Poosti, A., Rossello, S. & Eckert, A., 1981. Structural evolution of Sanandaj-Sirjan ranges near Esfahan, Iran, *Bull. Am. Ass. Petrol. Geol.*, **65**, 674–687.

Tirrul, R., Bell, I. R., Griffis, R. J. & Camp, V. E., 1983. The Sistan suture zone of eastern Iran, *Bull. geol. Soc. Am.*, **94**, 134–150.

Toksöz, M. N., Arpat, E. & Şaroğlu, F., 1977. East Anatolian earthquake of 24 November 1976, *Nature*, **270**, 423–425.

Toksöz, M. N. & Bird, P., 1977. Modelling of temperatures in continental convergence zones, *Tectonophys.*, **41**, 181–193.

Toksöz, M. N., Nabelek, J. & Arpat, E., 1978. Source parameters of the 1976 earthquake in east Turkey: a comparison of field data and teleseismic results, *Tectonophys.*, **49**, 199–205.

Trifonov, V. G., 1971. Report in Russian, see Tchalenko (1975).

Trifonov, V. G., 1978. Late Quaternary tectonic movements of western and central Asia, *Bull. geol. Soc. Am.*, **89**, 1059–1072.

Vita-Finzi, C., 1981. Late Quaternary deformation in the Makran coast of Iran, *Z. Geomorph.*, **40**, 213–226.

Vita-Finzi, C., 1982. Recent coastal deformation near the Strait of Hormuz, *Proc. R. Soc. A*, **382**, 441–457.

Vita-Finzi, C. & Ghorashi, M., 1978. A recent faulting episide in the Iranian Makran, *Tectonophys.*, **44**, T21–T25.

Wallace, R. E., 1968. Earthquake of 1966 August 19 Varto area, eastern Turkey, *Bull. seism. Soc. Am.*, **58**, 11–45.

Wellman, H. H., 1966. Active wrench faults of Iran, Afghanistan and Pakistan, *Geol. Rdsch.*, **55**, 716–735.

West, W. D., 1935. Preliminary geological report on the Baluchistan (Quetta) earthquake of May 31st, 1935, *Mem. geol. Surv. India*, **67** (1), 1–82.

White, R. S., 1977. Recent fold development in the Gulf of Oman, *Earth planet. Sci. Lett.*, **36**, 85–91.

White, R. S., 1979. Deformation of the Makran continental margin, in *Geodynamics of Pakistan*, pp. 295–304, eds Farah, A. & DeJong, K. A., Geological Survey of Pakistan, Quetta.

White, R. S., 1982. Deformation of the Makran accretionary prism in the Gulf of Oman (north-west Indian Ocean), in *Trench–Forearc Geology: Sedimentation and Tectonics in Modern and Ancient Active Plate Margins*, ed. Leggett, J. K., *Spec. Publ. geol. Soc. Lond.*, **10**, 357–372, Blackwell Scientific Publications, Oxford.

White, R. S. & Klitgord, K., 1976. Sediment deformation and plate tectonics in the Gulf of Omain, *Earth planet. Sci. Lett.*, **32**, 199–209.

White, R. S. & Louden, K. E., 1982. The Makran continental margin: structure of a thickly sedimented convergent plate boundary, *Mem. Am. Ass. Petrol. Geol.*, **34**, 499–518.

White, R. S. & Ross, D. A., 1979. Tectonics of the western Gulf of Oman, *J. geophys. Res.*, **84**, 3479–3489.

Wickens, A. J. & Hodgson, J. H., 1967. Computer re-evaluation of earthquake mechanism solutions 1922–62, *Publs Dom. Obs.*, **33**, 1–560.

Wong, H. K. & Finckh, P., 1978. Shallow structures in Lake Van, in *The Geology of Lake Van*, eds Degens, E. T. & Kurtman, F., *M.T.A. Rep. No. 169*, 20–28.

Woodside, J. M., 1977. Tectonic elements and crust of the eastern Mediterranean, *Mar. geophys. Res.*, **3**, 317–354.

Yielding, G., Jackson, J. A., King, G., Sinvhal, H., Vita-Finzi, C. & Wood, R., 1981. Relations between surface deformation, fault geometry, seismicity and rupture characteristics during the El Asnam (Algeria) earthquake of 10 October 1980, *Earth planet. Sci. Lett.*, **56**, 287–304.

Appendix

In the synthesis of long-period body waves from earthquakes in the Zagros, Jackson & Fitch (1981) omitted a factor from the calculation of *sP* amplitudes, equal to the ratio of shear to compressional wave vertical slowness (see also Fitch 1981). The correct formulation is given by Langston & Helmberger (1975). This error was pointed out by J. Nabelek of MIT. This factor is close to 0.5 for teleseismic ray paths, which means that the *sP* amplitudes in Jackson & Fitch (1981) were about twice as big as they should have been, relative to *P* and *pP*. On correcting this error little difference was found to the shape (rather than absolute amplitude) of the waveforms, and this was confirmed by comparison with the program of Langston & Helmberger (1975), which has been used in all subsequent work. As Jackson & Fitch did not attempt to compare absolute amplitudes (necessary to obtain moment estimates), but were only concerned with comparison of shapes to obtain focal depth, there is almost no change to their results. The depth estimates found by the corrected program as well as that of Langston & Helmberger (1975) are effectively the same as before, and well within the errors of ±4 km quoted by Jackson & Fitch (1981). This has been confirmed by the independent checking of the same earthquakes in the southern Zagros by Kadinsky-Cade & Barazangi (1982).